SPIRE-QMW-MOM-000210-10

SPIRE Bolometer Array Technology Meeting
QMW January 21, 22 1999

CONTENTS

B

List of attendees

Peter	Ade	QMW
Patrick	Agnese	LETI
Jamie	Bock	JPL
Terry	Cafferty	JPL
James	Caldwell	GSFC
Christophe	Cara	CEA
Colin	Cunningham	UKATC
William	Duncan	UKATC
Fred	Gannaway	QMW
Walter	Gear	MSSL
Bill	Gray	JPL
Matt	Griffin	QMW
Peter	Hargrave	QMW
Paul	Harvey	U. Texas
Raul	Hermoso	QMW
Kent	Irwin	NIST
Ken	King	RAL
Ernst	Kreysa	MPIfR, Bonn
Yannic	Le Pennec	CEA
Bruno	Maffei	QMW
Harvey	Moseley	GSFC
Hien	Nguyen	JPL
Seb	Oliver	IC
Louis	Rodriguez	CEA
Juan	Roman	GSFC
Bruce	Swinyard	RAL
Neal	Todd	IC
Sarah	Unger	IC
Laurent	Vigroux	CEA
Adam	Woodcraft	QMW

C

MINUTES

Draft minutes of 4th SPIRE Bolometer Array Group Meeting
QMW, London, 21, 22 January 1999

Matt Griffin
February 26 1999

Note:

1. These minutes should be read in conjunction with the viewgraph package from the meeting, which contains most of the information - this will be made available shortly.

2. The topics are ordered here as on the original agenda, not necessarily as actually presented at the meeting.

3. Actions are tabulated in Section 13.

List of attendees

Peter	Ade	QMW
Patrick	Agnese	LETI
Jamie	Bock	JPL
Terry	Cafferty	JPL
James	Caldwell	GSFC
Christophe	Cara	CEA
Colin	Cunningham	UKATC
William	Duncan	UKATC
Fred	Gannaway	QMW
Walter	Gear	MSSL
Bill	Gray	JPL
Matt	Griffin	QMW
Peter	Hargrave	QMW
Paul	Harvey	U. Texas
Raul	Hermoso	QMW
Kent	Irwin	NIST
Ken	King	RAL
Ernst	Kreysa	MPIfR, Bonn
Yannic	Le Pennec	CEA
Bruno	Maffei	QMW
Harvey	Moseley	GSFC
Hien	Nguyen	JPL
Seb	Oliver	IC
Louis	Rodriguez	CEA
Juan	Roman	GSFC
Bruce	Swinyard	RAL
Neal	Todd	IC
Sarah	Unger	IC
Laurent	Vigroux	CEA
Adam	Woodcraft	QMW

1 Introduction and aims of the meeting

Matt Griffin presented some introductory viewgraphs on the aims of the meeting and the current status of FIRST and SPIRE – see viewgraphs.

2 Schedule

Ken King presented the current schedule for the detector development programme and the SPIRE instrument, which is driven by the delivery date for the PFM (mid. 2004). Recent discussion between ESA and the instrument teams on the detailed spacecraft-level AIV plan have not revealed anything grossly unreasonable in ESA's AIV planning. There may be scope for shortening the AIV campaign, but certainly not by 9-12 months. It should therefore be regarded as unlikely that ESA will be willing to accept a significantly later PFM delivery date unless the launch date also slips (which nobody wants). So we must still plan for a SPIRE PDR (or something nearly equivalent to the) in the middle of 1999, before detector selection.

A list of detector development milestones was annotated in real time to indicate those that have been met, revealing how some slips in the schedule have already occurred.

Monthly reports from ALL SPIRE institutes will be mandatory from now on as we have to report to ESA every month.

3 Instrument design status

Bruce Swinyard presented an update on the SPIRE instrument design. The following points are important:

The photometer optical design is under review, and the outcome may depend on what happens with the redefinition of how PACS, SPIRE and HIFI share the FIRST focal plane. Kjetil Dohlen has produced a new design which solves the problems of pupil imaging, Strehl ratio and field of view, but has a slightly anamorphic final image. The impact of this on science is TBD.

The intensity beam divider FTS option is looking promising based on preliminary results from the breadboard model that Peter Ade has made. An optical design based on this scheme for SPIRE is now needed.

For the feedhorn option, the FTS detector array baseline is to have a 200-300 μm band and a 300 – 670 μm band. For the latter, 2Fλ 330 μm feedhorns are baselined, but multimoded at the short wavelength to allow propagation of 670 μm. The efficiency of such horns and the number that can be accommodated need to be studied. The option of having an extra dichroic is not ruled out.

The need for a shutter to eliminate excess background from the cryostat during ground testing is being studied. The advantages are viewed as significant. A first-draft specification will be drawn up and given to Gary Davis (Canadian Associate Scientist) as part of an industrial study phase in Canada with a view to this item being provided by Canada.

The issue of stray light control and baffle design and implementation will need to be carefully addressed in the opto-mecahnical system design. The question of who actually delivers the baffles is still TBD.

The telescope design is still not fixed – the latest JPL design has a larger secondary. Terry Cafferty pointed out that the possibility of having a larger focal ratio for the FIRST primary was being examined at JPL (maybe even up to f/1 instead of the present f/0.5). SPIRE must design for the current value, but a slower primary would reduce field curvature and make it easier to optimise the imaging optics. A decision on this is envisaged on a timescale of 3-6 months.

The SPIRE opto-mechanical system design has still to be properly addressed. Work is now underway to examine the basic concept suggested by Bruce in October.

Mass at 2 K may be a problem. It may be feasible and useful to mount the ^{3}He cooler at 4 K rather than 2 K. Bruce is looking into this with Lionel Duband.

The available volume for the detector array modules may be problematic – it would help the array providers greatly if a 3-D CAD model were available for them to use as a design aid.

The nominal budget for warm electronics power is low for some of the array options. The extent to which this is a problem will need to be examined with ESA.

Matt Griffin said that for this issue, and many others, what is required is that the array groups fill out the system design document following the template already given. This should contain a baseline design with options and questions so that cost/benefit analysis can be done and ESA can provide industry with appropriate information and ask the right questions (e.g., about the impact on lifetime, on-board power consumption, etc. of anything we might want to propose).

4 Status of actions from the Goddard meeting

Ken King reviewed the open actions from the Goddard meeting (see viewgraph and updated action list below).

5 CEA arrays

Laurent Vigroux gave a brief introduction to the CEA array development programme and Louis Rodriguez gave a detailed account of the programme and its current status – see viewgraphs.

Some important issues still to be addressed were:

Optical responsivity (optical tests will be started soon on the single-pixel detector already undergoing tests at QMW)
Power load on the ^{3}He fridge
Thermal isolation of the 2-K multiplexer
RC time constant (a 3-dB frequency of around 50 Hz is predicted)

6 GSFC/NIST arrays

This presentation was divided as follows:

Overview; mechanical design and electronics	Harvey Moseley
TES bolometer fabrication	Kent Irwin
Electronic system design	Jim Caldwell
Plans and Schedule	Juan Roman

The detailed contents are as in the viewgraphs. Below are some points raised or emphasised during the presentations

Points raised during Harvey's talk:

The envisaged filling factor is > 95% with > 80% absorption efficiency over the whole wavelength range.

The MK 1.8 readout electronics have been tested with the SQUID multiplexer, and tests with actual TES bolometers will be done in the near future

Magnetic shielding requirements: cylindrical L/D of around 3 will be needed to shield the detector module. The mechanical design will need to take this into account.

A "double TES" concept has been devised that could deal with the thermal background in orbit being higher than designed (i.e., prevent the TES from being driven normal by the high background). This will not be evaluated as part of the array selection process. However, it's viability, if shown convincingly, would remove one of the worries about the TES technology for SPIRE.

The cryoharness definition for the TES option is still not completely worked out – more details will be available soon (in time to present at the March 15 technical meeting with ESA).

RF shielding will be important for the SQUID detectors, and indeed for all of the SPIRE options. There are dangers of RF interference being conducted into the cryostat along cables or through the HIFI LO window. Preferably, all wires going into the cryostat should be filtered. RFI suppression should be raised as an important system issue with ESA at the March 15 meeting.

Points raised during Kent's talk:

A new fabrication technique should eliminate the noise "bump" shown on the viewgraph (which is due to the use of granular aluminium for the electrical leads).

Optical measurements on TES devices are expected soon (weeks).

Different bi-layer options are being studied: Al/Ag (baseline); Mo/Au (attractive as it is very stable wrt high temperature processing); Mo/Cu

T_c can be controlled to a couple of mK

The 4 x 8 element array for the detector selection can be manufactured at NIST or at Goddard (providing some backup in the case of problems at either institute). The basic processes are the same with minor differences (e.g., Pd/Au is used for the absorber at NIST and Bi is used at Goddard).

Points raised during Jim's talk:

The TES option does not require a Buffer Amplifier Unit on the cryostat outer shell (TBC).

The wire count is TBC, but with around 1000 wires for the worst case. Requirements on the wire resistance etc. will be specified soon.

The front-end frame rate should be between10-100 kHz (preferably at the lower end of this range, using 12-bit ADCs).

It is Goddard's preference to specify the warm electronics for procurement by Saclay rather than to supply boards or boxes. Discussions of the detailed electronic system design have taken place at the splinter meeting on Jan. 20).

Points raised during Juan's talk:

Testing of the mechanical prototype will begin soon.

Goddard needs the BACUS unit to be delivered in early March to be able to meet the test schedule.

At present, no major problems are foreseen with delivering the popup arrays on schedule for testing at QMW.

7 JPL/Caltech arrays

Jamie Bock presented the Caltech/JPL feedhorn array option.

Points raised during Jamie's talk:

Caltech are examining an option with up to 600 detectors in total. This is fine provided that the Feedhorn option system design document presents a baseline number as in the SPIRE proposal with options for a larger number also presented with the implications for system parameters (Focal plane mass and volume, cryoharness requirements, warm electronics power, data rate, etc.)

The estimated mass of a typical array is about 170 gm.

It may be preferred to have the electrical interface (connectors) at 4 K.

Estimated heat load is 4.3 μW at 0.3 K for 5 arrays.

An effective 16-bit ADC readout is required.

The low 1/f noise of NTD Ge detectors could make a slow-scan observing mode possible -this may be attractive for deep survey observations.

The main technical challenges for the feedhorn option are: implementation of the JFET module; Implementation of the feedhorns for the FTS option; overall system design.

8 BACUS and the array test plan

Peter Hargrave described the design of BACUS and the test schedule (see viewgraphs and Annex TBD)

Points raised during Pete's talk:

Commissioning of BACUS is envisaged to take place in early March. This is critically dependant on the delivery of the test dewars from Precision Cryogenics.

There is a problem with the first ^{3}He fridge from Simon Chase - it does not prevent the fridge from working but results in a long re-cycle time. It is thought to be due to a problem with that particular unit rather that with the fridge design.

The possible use in BACUS of infrared illuminators from Jeff Beeman should be investigated.

Caltech and GSFC require delivery of their test dewars on or near on schedule to prevent slips in the delivery of their test arrays to QMW.

Given the extreme pressure on the schedule that is almost inevitable towards the end of 1999, it will facilitate the array evaluation if a lot of the tests carried out at QMW are largely to verify performance already measured at in the US groups' labs. This will allow more time for those tests that are planned to be done only at QMW (such as those using an FTS or telescope simulator).

If desired, filters to allow the US groups to configure their systems to be able to look out of the dewar could be provided (on a best efforts basis) by QMW.

The overall schedule is very tight and has already suffered some delays. It would be optimistic to believe that it will not suffer any further delays. Tests most relevant to the key array selection criteria will need to be given highest priority.

If a full SPIRE PDR is to be held in July, then this may divert much needed effort from the array programme. One option is to split the PDR into separate events. Ken King and Matt Griffin agreed to consider the optimum scheme for the SPIRE PDR.

9 Selection criteria and plan

Matt Griffin made a brief presentation on the array selection criteria. His note on this subject circulated. at the Goddard meeting has not yet been updated. He emphasised the need for selection to be based on a mature system design as well as the measured performance of prototype arrays and simulations of SPIRE observations.

10 Simulations

Laurent Vigroux presented an updated version of the note on simulations by Aussel et al. (see Annex TBD).

Points raised during Laurent's presentation:

The telescope emissivity is a critical parameter. The temperature is not likely to depart much from the nominal 70 K, but the overall effective emissivity is very uncertain. This is particularly important for the TES detectors (as noted at the Goddard meeting).

It is important to distinguish between the NEFD (which is the most important parameter affecting mapping speed) and the confusion-limited sensitivity. If they meet their predicted performance levels, any of the detector options should be able to integrate down to the confusion limit for one field in a relatively

short time (well under an hour). But the ability of SPIRE to carry out a confusion-limited survey of a large area of sky depends on the mapping speed and so on how long or short this basic interval happens to be - it will dictate whether or not the proposed large area survey turns out to be feasible in a reasonable amount of telescope time.

Regardless of the details of the array implementation, the pixel beam pattern on the sky (system impulse response) should contain all of the information needed to evaluate the confusion-limited performance. It is therefore important to characterise this as accurately as possible for the filled array and feedhorn array options.

Fine sampling of the image will be very important regardless of the chosen option. This is significant as it affects the specifications for the chopper (more properly called a "beam steering device").

Seb Oliver reported that the Imperial College group have now set up a simulation package which effectively replicates what the Saclay group have done. It was agreed that having these independent capabilities would be beneficial to the programme.

11 Comments from reviewers and discussion of the programme

Comments from Ernst Kreysa (as noted - not necessarily with complete fidelity - by Matt Griffin at the time, and subject to revision by Ernst):

1. The FIRST spacecraft should have a continuous scanning mode to facilitate the optimum operation of the detector arrays. This was not done for ISO and it was a mistake. Such a capability will be essential to carry out the large areas surveys efficiently.

2. Photons collected by FIRST will be very expensive - the available area in the focal plane should be filled with as many detectors as possible. The envisaged array sizes were not as large as one would like to see.

3. There are differences of opinion as to the relative merits of different array options which must be clarified before the selection can be made.

4. It is a matter of concern that the filled array options proposed for SPIRE have not yet been experimentally tested with submillimetre radiation even at this late stage. Ideally, this concept would be tried out on a ground-based telescope before being implemented in a space instrument.

5. The TES bolometer/SQUID multiplexer technology looks very promising for the future, but is perhaps not quite mature yet.

Comments from Paul Harvey (by e-mail after the meeting):

In general I was very impressed with the plan for development and evaluation of the three bolometer technologies. It is obviously ambitious and not forgiving of unforeseen delays, though. It is a bit scary that already there are problems with on-time delivery of the test cryostats, though those delays appear right now to not have significant impact.

As I said at the meeting, I think what scares me the most is the enormous pressures that will be on everyone late this year. Unless everyone is VERY lucky, there will almost certainly be delays in delivery

of some array(s) to QMW and there will be discussions along the lines of, "If I just had another two weeks, this problem could be addressed." Each of the three bolometer groups is under significant pressure to be successful for other reasons than just SPIRE. Your group at QMW is also under a great deal of pressure to develop the proper test environment to lead to making the right decision. Because two of the three technologies have never been used in a working astronomical instrument before, it is critical that they be evaluated with very stringent testing, yet there will be pressure to accept less-than-specified performance because of the improved capability such detectors would bring to SPIRE.

A smaller problem that became apparent more during some of the splinter meetings last week was the differences in system design that result for different bolometer choices. This is already leading to some duplication of effort at QMW that is unavoidable. Clearly your decision to proceed with a PDR before the "downselect" is necessary for you to meet your schedule requirements with ESA. So I encourage you to continue in that direction.

Finally, I'll again second Ernst Kreysa's comments about trying to install the largest array possible, whichever technology is chosen. I think you'll feel pretty silly ten years from now if someone asks why a 1.5 or 2 x larger array wasn't used if the reason turns out to be something of the scale of "number of wires." I know there are a large number of system issues involved in an issue like this, but many of them can be dealt with if addressed early enough. A related issue to this point is the capability to observe un-chopped with a "slow-scan" mode. Although, I personally am not used to thinking about this, coming from the direction of the KAO and SOFIA, it is clearly likely to be a very good idea for SPIRE on FIRST. This puts requirements on the detector technology as well as opening up the focal plane for larger arrays.

12 Summary and actions

12.1 Summary of the meeting and discussion session at the end (Matt Griffin)

1. A lot of progress has been made since the Goddard meeting on the technical development of the arrays and the definition of their implementation in SPIRE. System designs are not yet available in the appropriate form, but it is apparent that most of the information is there and merely needs to be properly documented.

2. Of all the actions generated at this meeting, the most urgent is that on the array groups to provide their System Design documents in time for the information to be used in updating the IID-B and in discussions with ESA at the technical meeting on March 15 (Action 20 in the table below). The important thing is not necessarily to have all parameters pinned down, but to have a reasonably clear idea as to the system aspects of each option, and to be able to present ESA with options/alternatives which may make different demands on spacecraft resources, perhaps justified by improved scientific return. It will be increasingly difficult to do this as time goes on.

   The specification and design of the SPIRE warm electronics is also highly dependent on the array technology, and it is necessary now to examine the requirements for the electronics.

3. The BACUS schedule has already suffered some delays due to cryostat and cryogenic hardware procurement problems. There is now little room for further delay. Items that are on the critical path must be identified and monitored very closely.

4. The array fabrication and programme must be run actively. Excellent communication and clear understanding between QMW and the array groups will be essential. The progress of the programme should be monitored on a weekly time-scale to ensure that Peter Hargrave has up-to-date information

and visibility of any delays or modifications to the plan and that the array groups are aware of any potential delays on the QMW side. However, it is important that this be done in a manner that does not add any extra admin load on the already hard-pressed array groups.

5. The programme is vulnerable to disruption by various factors such as delays in delivery or commissioning of BACUS hardware, mishaps or problems with staff availability. The potential effects should be minimised and staff at the various sites may need to be flexibly deployed to accommodate events as they occur. The deployment of additional staff is not seen as likely, but any extra effort that could be brought in would be beneficial. For instance, more effort on system design work and technical documentation is clearly needed.

6. The QMW BACUS system will be the only test-bed for the CEA arrays, whereas the US arrays will have undergone some characterisation and calibration prior to delivery to QMW. Priority should therefore be given to CEA array testing in the QMW system if there is a schedule conflict.

7. The feedhorn option is the only one based on instrument-proven technology. To ensure that at least one viable choice is available at the time of selection, the feedhorn option must be developed to a sufficient degree of maturity that it can be chosen if necessary. This does not mean that it is favoured in the event of other options being selectable.

12.2 Other comments

Laurent Vigroux: The CEA array fabrication process is time consuming and requires planning and definition well in advance. There will be little flexibility for re-defining the requirements from now on.

Harvey Moseley: If a US option is selected and larger arrays are wanted, this could increase the cost to NASA, and funding would need to be sought. The likelihood of such additional funding would need to be clear by the time of array selection.

13 List of actions

The table below is a list of outstanding actions from the previous meeting plus additional ones from this meeting (some may have been closed since the time of the meeting).

LIST OF DETECTOR ARRAY GROUP OPEN ACTIONS				
No.	**Action**	**Responsible**	**Deadline**	**Status**
Open actions from Goddard meeting, Sept. 17, 18 1998				
8	Specify He-3 cold stage temperature requirements for SPIRE and BACUS.	Rodriguez, Moseley. Bock	21 Jan. 99	Open
20	**Provide Systems Design Documents based on template provided by Bruce Swinyard**	**Bock, Moseley, Rodriguez**	**Feb. 28**	**Open. Information essential for Systems Team meeting on March 4, 5 and March 15 meeting with ESA**
24	Revise array selection criteria document	Griffin	Nov. 13	Open
25	Ask Lionel Duband to provide cooling power vs. temperature curve for baseline He-3 fridge	Swinyard	Feb. 18	Open
27	Define limiting resource dictating maximum permitted number of detectors in the focal plane for feedhorn option	Cunningham	March 20	Open
New actions from this meeting				
28	Seek information from ESA on the parasitic load on the CVV	Griffin	March 15	Open
29	Check validity of warm electronics power dissipation numbers	Cunningham	Feb. 15	Open
30	Raise RF filtering as FIRST system issue	Griffin	March 15	Open
31	Provide array groups with 3-D CAD model of the FPU for use as a design aid	Swinyard	Feb. 1	Open
32	Draw up detailed draft test plan for the in-house and QMW-BACUS	Hargrave (with array groups)	Feb. 15	Open
33	Investigate availability of illuminators from Jeff Beeman	Hargrave	Feb. 15	Open
34	Define the nature of the SPIRE design review in June 1999	King, Griffin	March 7	Open
35	Revise the array selection criteria document	Griffin	Feb. 15	Open
36	Establish scheme for weekly monitoring of array test programme (with minimal additional admin. overhead)	Hargrave	Immediate	Open
37	Provide written comments on the array programme based on this meeting	Kreysa, Harvey	End Feb.	Open

No.	Action	Responsible	Deadline	Status
38	Write minutes of splinter meetings on: Feedhorn Option ---------- Warm electronics ---------- FPU wiring and connectors ----------	MJG/CRC Cara Cunningham	Feb. 15	Open
39	Provide Laurent Vigroux with comments on latest simulations documents	All	Feb. 15	Open
40	Ask ESA about envisaged practical limit on the scan rate	Griffin	March 15	Open
41	Generate nominal beam profiles for 0.5Fλ and 2.0Fλ pixels and provide Laurent Vigroux with input map projected through the photometer optics onto the detector focal plane	Swinyard	Feb. 1	Open
42	Include Co-I level meeting on array selection guidelines at the Caltech meeting in May	Griffin	May meeting	Open
43	Seek advice from Anthony Murphy on feedhorn design for FTS long wavelength channel	Griffin/Ade	March 1	Open

14 Reports on splinter meetings

14.1 Splinter meeting on feed-horns for the FTS on Jan. 20 (Bruce Swinyard)

Present: William Duncan; Jamie Bock; Matt Griffin (part); Colin Cunningham; Bruce Swinyard

Background: The FTS on SPIRE is presently envisaged to have two detection bands – one covering 200-300 μm and the other covering 300-670 μm. The scientific rationale for the extension to 670 μm is to cover the important CI line at 609 μm. It is accepted that the core scientific objectives are to be met using the 200-400 μm range and the performance in this wavelength range must not be compromised in going to the longer wavelengths.

If filled arrays are employed then there should not be a problem in achieving the extension to longer wavelengths; except that the resonant absorber may have limited performance at the very longest wavelengths and the pixel size will not be optimum. In the case of the single mode feed-horns a problem arises because the width of the band would be too large for one size of horn $\sim\lambda/\Delta\lambda\sim1.3$.

The short-wavelength band: At this meeting it was agreed that the nominal division between the bands should be maintained and that single mode feed-horns of size $2f\lambda$ at 250 μm should be employed in the 200-300 μm band.

Size of the field: The nominal field size for the FTS is 2x2 arcmin – the platescale at the detector focal plane is 12.5 arcsec/mm for a final focal ratio of f/5. For the feed-horn option the field size will have to change slightly to accommodate a whole number of pixels in the focal plane. The short-wavelength band could be arranged as shown in Figure 1.

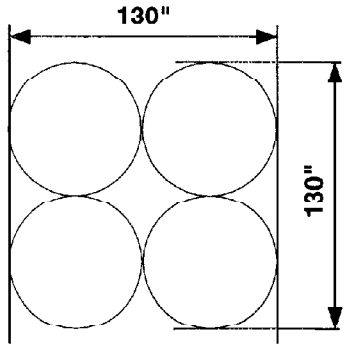

Figure 1: Proposed arrangement for the 200-300 μm band. The pixels here are 2.5 mm in diameter.

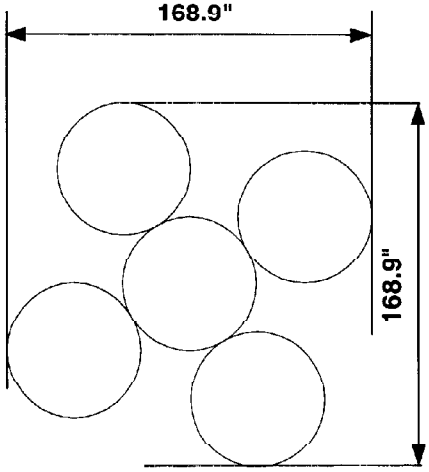

Figure 2: Possible arrangement for the 300-670 μm band using 350 μm $2f\lambda$ horns. These would be undersized towards the longest wavelengths and the efficiency would drop. The dotted circle shows the size of a $2f\lambda$ circle at 550 μm.

The long-wavelength band: The initial decision at the meeting was to adopt 2fλ pixels at 350 μm to cover the whole of the long-wavelength band. These would become essentially 1fλ pixels at the longest wavelengths. The layout of the focal plane would then be as shown in Figure 2.

Note that the field size has now grown to ~2.6x2.6 arcmin. Also shown in figure two is the size of the 2fλ diameter circle at 550 μm. Some calculations are needed to see what response of the horns would be at this and longer wavelengths and what the detection efficiency would be. Another alternative to using the 350 μm horns out to the long wavelengths would be to have a third array centred on 550 μm. This would consist of only a few pixels – possibly only one. Two arrangements for the third array are shown in Figure 3.

Whichever solution is finally adopted, one pixel will need to be co-aligned on each array. This necessitates the arrays looking at slightly different portions of the sky and means that the field mirror will have to be oversized. Figure 4 shows the 250 and 350 μm 2fλ horn arrays laid on top of each other. The total field that will have to be let through the FTS in this case will be ~2.7x2.7 arcmin.

No definitive conclusion was agreed on the need for the third array and further studies on the performance of the 350 μm array at long wavelengths will now be conducted.

Figure 3: Two alternative arrangements for a third array at the output of the FTS to cover the 420-670 μm band. The second has the advantage that the off source position is sampled all around the object of interest although the field is obviously much larger.

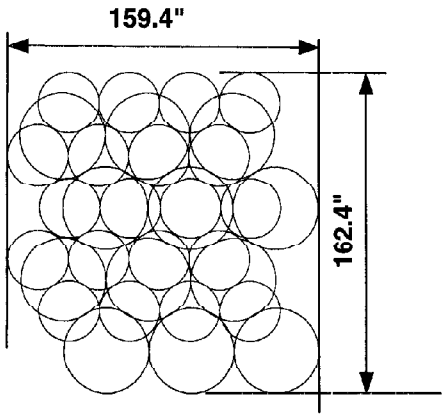

Figure 4: 250 and 350 μm arrays superimposed and aligned on one pixel. The total FOV required for the FTS is thus 2.7x2.7 arcmin assuming any third array is kept within the confines of this field of view.

14.2 Splinter meeting on FPU wiring and connectors on Jan. 21 (Colin Cunningham)

14.2.1 Introduction

The signal wiring within the cold focal plane unit, and between it and the warm electronics provides some of the major engineering challenges for SPIRE. The large number of wires means that tight thermal budgets have to be balanced against requirements to minimise microphonics, EMI, transmitted thermal radiation, and crosstalk. At the same time we need robust structures which can meet vibration loads, and we must have connectors at appropriate points to aid integration and test, while preserving reliability. The late choice of detector technology means that 3 different sets of constraints and trade-off need to be addressed during the period up to array selection . This document attempts to raise the issues, and start the process of coming up with solutions as part of the array and FPU systems design for review at PDR.

14.2.2 Responsibilities for wiring harnesses

As a reminder from the workpackage descriptions, the following table shows who has responsibility for definition, design and manufacture of the various categories of wiring harness. Note that ESA are responsible for procuring the harness between the FPU, BAU and DRC, but we must specify it in detail. While the responsibility for wiring harnesses rests with those responsible for subsystems within the FPU, they cannot be specified and designed in isolation especially from the structure workpackage with regard to ensuring proper support of signal wires to survive launch loads and to avoid microphonics.

Unit	Subsystem	Harness	Cold End Temp (K)	Warm End Temp (K)	Responsibility
FSFPU	Array	Array signals & control	2	4	Array Groups
	Array	Array signals & control	4	15	Array Groups
	FTS Mechanism	Control, position & temperature	4	15	LAS
	Cooler	Control & temperature	2	4	CEA- Grenoble
	Cooler	Control & temperature	4	15	CEA- Grenoble
	Chopper mechanism	Control, position & temperature	4	15	ATC
	FTS Calibrator	Control & temperature	4	15	GSFC
	Photometer Calibrator	Control & temperature	4	15	GSFC
	Shutter Mechanism	Control	4	15	??
	Structure	Temperature	2	4	MSSL
	Structure	Temperature	4	15	MSSL
	FET Box	Control, Signals, Temperature	15	15	JPL/Caltech
Cold Harness	FPU-BAU	Signals	15	80	ESA
	FPU - DRC	Control, Temperature, Positions	15	300	ESA
	BAU-DRC	Signals	80	300	ESA
Warm Electronics	FSWIR DRCU-SPU	Data	300	300	CEA-SAp
	FSWIR DRCU-DPU	Data, Power	300	300	CEA-SAp
	FSWIR SPU-DPU	Data, Power	300	300	CEA-SAp
	DPU – Spacecraft	Data, Power	300	300	ESA

14.2.3 Issues raised

Specification of ESA procured harness: It is urgent that we develop the specification for the harness to link the FPU, BAU and DRC. ESA will include this spec in the ITT, and it will be a technical specification of wire impedances, capacitance to ground & other conductors, shielding, stiffness etc; not a technical prescription as to what technology to use to achieve this spec. They will tend to conservative solutions based on ISO experience (eg stainless steel wires in bundles with epoxy encapsulated heat sinks. We can show them other solutions such as ribbon cables, but will find resistance in getting them to consider such technologies.

The number of signal and screen conductors from the value specified in the IID-B for the CEA option is 430 signal and control lines, with 43 screens. For conventional screened wire bundles, the thermal conductance is dominated by the screens, so we are under pressure to keep the number of screens to a minimum. If we need to increase the number of detectors for the feed-horn option to 600, we would need over 1200 signal and bias lines, plus screens. The TES/SQUID option may need up to 1000 conductors.

Twisted pairs may be needed, depending on detailed EMC design. This could be especially important for the low impedance SQUID option.

Connectors: ESA prefer 37-way MDM connectors with two rows of pins. both for their harness and for our cold harness. We may prefer 51 way MDMs (with 3 rows of conductors), 100 way MDMs (with 4 rows) or even Nanonics high-density connectors, if we are to conserve mass & space budgets, especially if we intend to increase the number of detectors. Again, we would have a difficult job persuading ESA to accept such connectors. Connectors may dominate the capacitance budgets.

It is advantageous to use connectors wherever cables cross a thermal boundary, for ease of assembly. However, space and mass budgets may preclude this.

Screens: The specification for cross-talk compared to detector impedance will determine how many signal pairs can be bundled within a screen, and we have seen that screens dominate thermal conductance

Alternative technologies such as ribbon cables may be needed to allow adequate screening

- Ribbon Cable technologies
- Kapton encapsulated ribbons: SIRTF will use manganin twisted pairs encapsulated in Kapton. This technology allows twisted pairs and screen wires to be used, and an overall screen of vacuum deposited Titanium. It can therefore be designed for controlled impedance and low thermal conductance, combined with robust NASA-qualified technology.
- Woven ribbons: SCUBA used superconducting woven cables in a Nomex weave, which again is robust and allows controlled impedance and good heatsinking. This technology has not been space qualified, but has been used extensively in ground-based instruments.

Feed-through radiation shields: There are several problems to deal with in taking wire-bundles or ribbon cables through the radiation shields:

Heatsinks: Depending on detailed thermal design, it is likely that heat will need to be intercepted at the 15-K and 4-K structures. This may be done by epoxy encapsulation, or relying on connectors. It is easy to get this wrong, and transmit excessive heat to the 2K stage, so careful thermal design will be needed.

Thermal radiation transmission: Preventing thermal radiation getting through radiation shields where

we have connectors or feed-troughs is not going to be easy. Epoxy connectors are transparent to far-IR & submm, and wire insulation can act as a wave-guide to IR.. Careful design and choice of components will be needed to meet the low-background requirements of the detectors.

Superconducting wires for SQUIDs: The SQUID bias lines will need to conduct quite high currents, and will probably need to be superconducting to avoid dissipation and voltage drops. Again, this will make ESA nervous. We need detailed specs for these bias wires.

Cable lengths: The trade-offs between thermal loads, EMC and space available relative to wire lengths inside the FPU are yet to be made.

Cable cross-section: We need estimates of cross-sectional area and minimum bend radius for the cadidate cable technologies, to see if they will fit in the space available.

Cable mass: We have not included the FPU harnesses in current mass estimates (I think!). For comparison, SCUBA ribbon cables weighed 260 g per metre for 135 detectors, each with a twisted pair and inter-pair screen wire.

Stiffness of wires: We will need to develop a microphonics model to specify cable stiffness and allowable acceleration from our mechanisms.

Mechanical support of harnesses: Support will be needed to survive launch forces. This will probably mean strapping cables to support structures. We decided that there was no point strapping to the thermal straps, as these will be almost isothermal.

14.3 Warm electronics for TES detector readout option (Christophe Cara)

Report to follow.

D

VIEWGRAPHS

1

INTRODUCTION

MATT GRIFFIN

Aim of this meeting

1. Review the whole programme

- The schedule and requirements
- Array technology status and progress since Goddard meeting
- The system designs
- The qualification plans
- The array selection criteria
- The testing and evaluation programme

2. Receive and react to comments from invited experts

Paul Harvey, Ernst Kreysa, Jean-Michel Lamarre

3. Hold splinter meetings on specific topics

Presentations/viewgraph packages to include

- **Overview of the detector concept, principle of operation, advantages for SPIRE, etc.**
- **Summary of development status**
- **System design**
- **Qualification plan**
- **Assessment of technical challenges and risks**
- **Summary of manpower resources available before and after selection**

Status of FIRST and SPIRE

FIRST

- Final mission confirmation and payload approval by the SPC in February (we hope)
- FIRST/Planck funding status was reviewed at a series of meetings in July, October, January
- 3.8-m antenna under study by JPL
- Use of X-band transponders increasingly likely ⇒ available data rate should go up by factor of ~ 4.
- Significant slip in FM delivery date not likely ⇒ PDR before detector selection

SPIRE

- Consortium meeting held in December
- Intensity beam divider FTS option being studied as alternative to classical MP as in proposal
  - Decision in February
- Detailed photometer optical design under review. Division of focal plane between the three FIRST instruments may be changed.
- Second formal meeting with ESTEC project took place on Nov. 17 – several actions on us to be completed by after this meeting
- SPIRE project STILL needs to establish more formal and reliable lines of communication and reporting

Schedule of future detector array meetings

Detector array group meetings:

May 1999	**Caltech. (20/21 May 1999 - TBC)**
September 1999	**Saclay**

Formal selection meeting:

January 2000	**RAL**

Full documentation to be provided by mid-December 1999 (last minute updates in January if necessary).

2

SCHEDULE

KEN KING

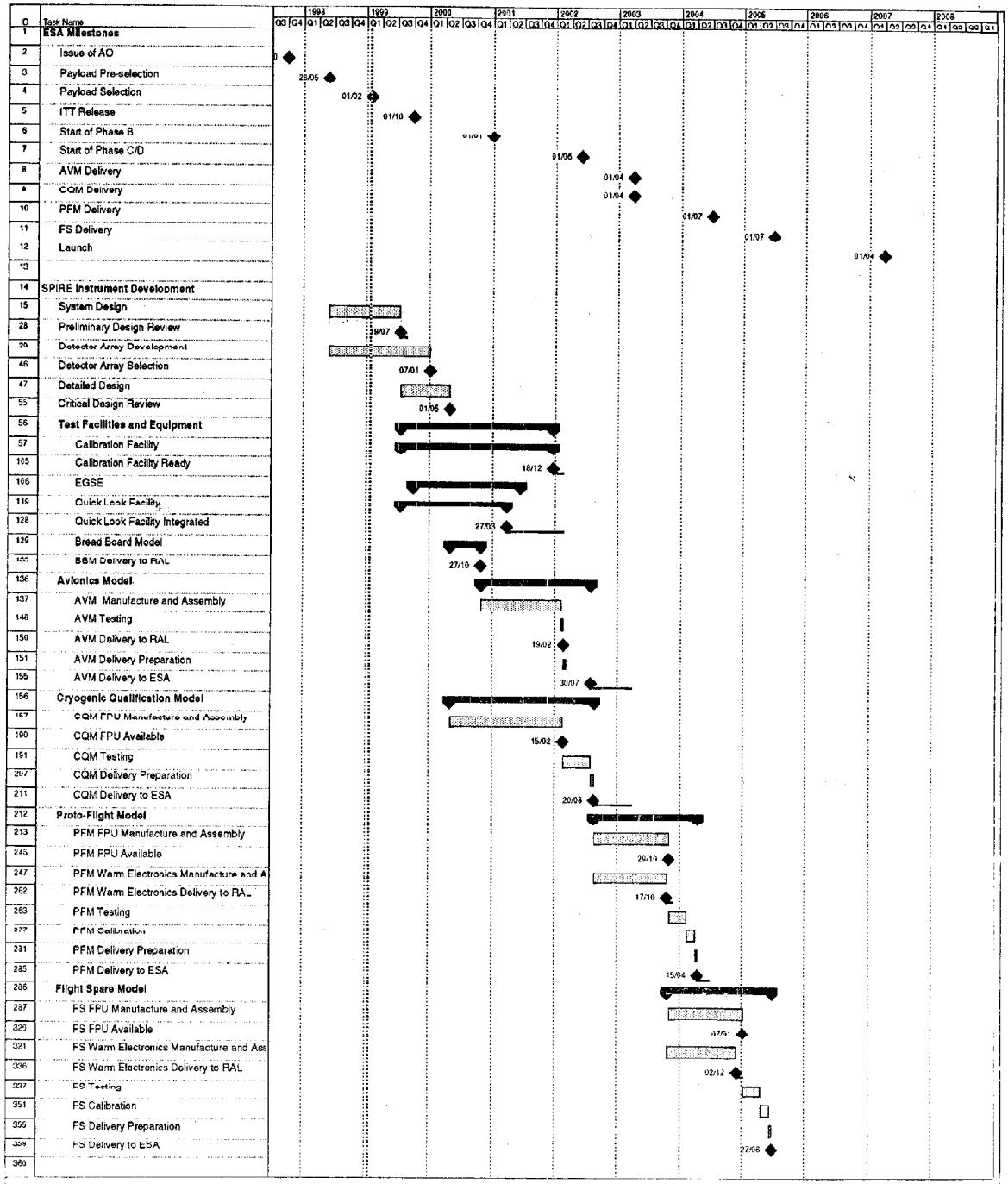
ID
Task Name
1 ESA Milestones
2 Issue of AO
3 Payload Pre-selection
4 Payload Selection
5 ITT Release
6 Start of Phase B
7 Start of Phase C/D
8 AVM Delivery
9 CQM Delivery
10 PFM Delivery
11 FS Delivery
12 Launch
13
14 SPIRE Instrument Development
15 System Design
28 Preliminary Design Review
36 Detector Array Development
46 Detector Array Selection
47 Detailed Design
55 Critical Design Review
56 Test Facilities and Equipment
57 Calibration Facility
105 Calibration Facility Ready
106 EGSE
119 Quick Look Facility
128 Quick Look Facility Integrated
129 Bread Board Model
135 BBM Delivery to RAL
136 Avionics Model
137 AVM Manufacture and Assembly
148 AVM Testing
159 AVM Delivery to RAL
151 AVM Delivery Preparation
155 AVM Delivery to ESA
156 Cryogenic Qualification Model
167 CQM FPU Manufacture and Assembly
190 CQM FPU Available
191 CQM Testing
207 CQM Delivery Preparation
211 CQM Delivery to ESA
212 Proto-Flight Model
213 PFM FPU Manufacture and Assembly
245 PFM FPU Available
247 PFM Warm Electronics Manufacture and A
262 PFM Warm Electronics Delivery to RAL
263 PFM Testing
277 PFM Calibration
281 PFM Delivery Preparation
285 PFM Delivery to ESA
286 Flight Spare Model
287 FS FPU Manufacture and Assembly
320 FS FPU Available
321 FS Warm Electronics Manufacture and Ass
336 FS Warm Electronics Delivery to RAL
337 FS Testing
351 FS Calibration
355 FS Delivery Preparation
359 FS Delivery to ESA
360
1998
1999
2000
2001
2002
2003
2004
2005
2006
2007
2008
28/05
01/02
01/10
01/06
01/04
01/04
01/07
01/07
01/04
19/07
07/01
01/05
18/12
27/03
27/10
19/02
30/07
15/02
20/08
29/10
17/10
15/04
07/01
02/12
27/06

ID	Task Name	Duration	Start	Finish
14	**SPIRE Instrument Development**	**1848 days**	**29/05/1998**	**28/06/2005**
15	System Design	296 days	29/05/1998	16/07/1999
16	Scientific Requirements Definition	26 wks	29/05/1998	26/11/1998
17	System Design	36 wks	29/05/1998	04/02/1999
18	Budgets Specification	8 wks	05/02/1999	01/04/1999
19	Engineering System Reqs. Doc Draft	1 day	02/04/1999	02/04/1999
20	Interface Definition	8 wks	05/02/1999	01/04/1999
21	Interface Control Documents Draft	1 day	02/04/1999	02/04/1999
22	Subsystem Requirements Definition	16 wks	05/02/1999	27/05/1999
23	End User Requirements Definition	20 wks	01/01/1999	20/05/1999
24	End User Reqs. Doc. ssue 1	1 day	21/05/1999	21/05/1999
25	Verfication Requirements Definition	16 wks	01/01/1999	22/04/1999
26	Verfication Reqs. Doc. Issue 1	1 day	23/04/1999	23/04/1999
27	Documentation Update	8 wks	24/05/1999	16/07/1999
28	Preliminary Design Review	2 days	19/07/1999	20/07/1999
29	Detector Array Development	420 days	29/05/1998	06/01/2000
30	PUD Array Development	65 wks	29/05/1998	26/08/1999
31	Delivery of Evaluation PUD Array to QM	0 days	26/08/1999	26/08/1999
32	Feedhorn Array Development	65 wks	29/05/1998	26/08/1999
33	Delivery of Evaluation Feedhorn Array to	0 days	26/08/1999	26/08/1999
34	CEA Evaluation Array Development	325 days	29/05/1998	26/08/1999
35	CEA 1st Evaluation Detector Manufa	40 wks	29/05/1998	04/03/1999
36	CEA 1st Evaluation Detector Deliver	0 days	04/03/1999	04/03/1999
37	CEA 2nd Evaluation Array Manufacti	13 wks	05/03/1999	03/06/1999
38	CEA 2nd Evaluation Array Delivery t	0 days	03/06/1999	03/06/1999
39	CEA 3rd Evaluation Array Manufacti	12 wks	04/06/1999	26/08/1999
40	CEA Evaluation Array Delivery to QMW	0 days	26/08/1999	26/08/1999
41	Evaluation Facility	420 days	29/05/1998	06/01/2000
42	Evaluation Facility Development	35 wks	29/05/1998	28/01/1999
43	Characterise Cryogenics	10 wks	29/01/1999	08/04/1999
44	Integrate and Test BACUS	6 wks	09/04/1999	20/05/1999
45	Array Evaluation	19 wks	27/08/1999	06/01/2000
46	Detector Array Selection	1 day	07/01/2000	07/01/2000
47	Detailed Design	203 days	21/07/1999	28/04/2000
48	Detailed Design	20 wks	21/07/1999	07/12/1999
49	Detailed Design Doc. Issue 1	1 day	08/12/1999	08/12/1999
50	Update Detailed Design	16 wks	10/01/2000	28/04/2000
51	Interface Specification Issue 1	1 day	08/12/1999	08/12/1999
52	AIV Plan	20 wks	21/07/1999	07/12/1999
53	AIV Plan Issue 1	1 day	08/12/1999	08/12/1999
54	Update Documentation	8 wks	10/01/2000	03/03/2000
55	Critical Design Review	2 days	01/05/2000	02/05/2000

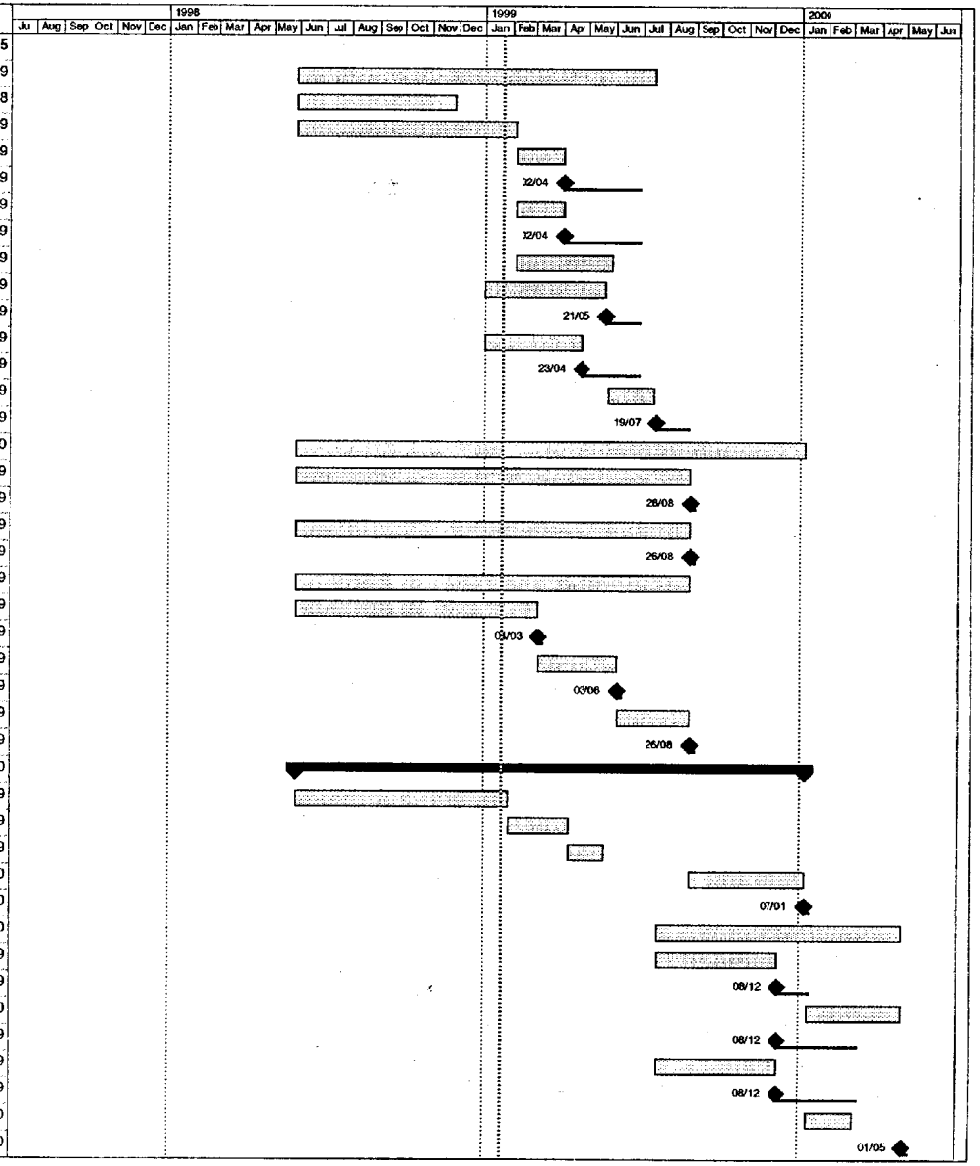

Detector Development Milestones

	Title:	Pop-Up Detector Array
M01	26 Nov 98	He-3 refrigerator from QMW
M02	29 Jan 99	Calibration Module delivery form QMW
M02	3 Feb 99	Mounting hardware design ready
M03	4 May 99	Mounting hardware available
M04	10 May 99	1x 8 PUDs delivered to GSFC
M05	18 May 99	Fanouts delivered to GSFC
M06	31 May 99	Interconnects delivered to GSFC
M07	18 Jun 99	Evaluation array assembled
M08	2 Jun 99	Electrical System ready
M09	6 Jul 99	Cryogenic Dewar System ready
M10	1 Sep 99	Delivery of evaluation array to QMW
M01	18 Jun 99	Delivery of PDR Package

	Title:	Feedhorn Detector Arrays
M01	1 Oct 98	Order JFET ✓
M02	14 Oct 98	Receive JFET dies ✓
M03	16 Oct 98	Order Load Resistor Module ✓
M04	30 Oct 98	Order Feedhorn Array Plates ✓
M05	2 Nov 98	Ship Ti/Nb TES Bolometer #1 to QMW
M06	26 Nov 98	Receive Load Resistor Module
M07	15 Dec 98	Receive Test Dewar and Refridgerator
M08	15 Jan 99	Receive Feed horn Array Plates
M09	15 Jan 99	Receive Calibrator
M10	11 Feb 99	Ship Ti/Nb TES Bolometer #2 to QMW
M11	8 Jun 99	Deliver SPIRE 61-Element Array #1
M12	24 Aug 99	Deliver SPIRE 61-Element Array #2
M01	7 Dec 98	Provide RF Shielding Requirements to QMW
M02	1 Jan 99	Provide preliminary Warm Electronics Requirements to SAp
M03	14 Jan 99	Provide Focal Plane Support Structure Design to QMW
M04	14 Jan 99	Receive revised RF Shielding requirements
M05	18 Jun 99	Delivery of PDR Package

	Title:	CEA Detector Arrays
M01	15 Oct 98	Delivery of prototype detector to QMW ✓
M02	1 Jan 99	1st Receipt of prototype arrays from LETI/SLIR ✓
M03	1 Mar 99	Ship 1st evaluation array to QMW
M04	1 Mar 99	Delivery of Manual Switchbox to QMW
M05	3 May 99	2nd Receipt of prototype arrays from LETI/SLIR
M06	1 Jun 99	Ship 2nd evaluation array to QMW
M07	1 Jun 99	Delivery of Acquisition System to QMW
M08	1 Jul 99	3rd Receipt of prototype arrays from LETI/SLIR
M09	1 Sep 99	Ship 3rd evaluation array to QMW
M01	18 Jun 99	Delivery of PDR Package

	Title:	Array Evaluation Facility
M01	16 Oct 98	Mirrors to QMW ✓
M02	30 Oct 98	Calibration module stray light analysis results from RAL
M03	30 Oct 98	Calibration module electrical interface specifications from QMW (document) ✓
M04	6 Nov 98	Final engineering drawings of calibration module to RAL ✓
M05	18 Nov 98	Connectors delivered ✓
M06	26 Nov 98	He-3 fridge tests complete
M07	26 Nov 98	Delivery of US He-3 fridges & shields to GSFC & JPL
M08	27 Nov 98	Filters complete
M09	18 Dec 98	Cryostat to QMW
M10	24 Dec 98	Illuminator arrays to QMW
M11	31 Dec 98	Construction of calibration modules
M12	29 Jan 99	Calibration module tests completed
M13	29 Jan 99	Delivery of calibrated calibration modules to GSFC & JPL
M14	1 Sep 99	Delivery of Pop-Up Detector Evaluation Array to QMW
M15	1 Sep 99	Delivery of Feedhorn Evaluation Array to QMW
M16	1 Nov 99	Delivery of CEA Evaluation Array to QMW
M17	31 Dec 99	Evaluation of prototype detector arrays completed

3

SPIRE INSTRUMENT DESIGN STATUS

BRUCE SWINYARD

DETECTOR ARRAY MEETING.

QMW 21/22 JAN 1999

INSTRUMENT DESIGN

- "AO" INSTRUMENT DESIGN HAS/IS BEEN REVISTED IN LIGHT OF:
  a) FSEC RECOMMEDATIONS
  b) MORE DETAILED SCIENCE REQUIREMENTS
  c) STARTING TO THINK ABOUT THE DETAILED SYSTEM REQS.
- STILL DUAL CHANNEL WITH 3-BAND PHOTOMETER AND TWO ~~[illegible]~~ BAND FTS.

DETECTOR MEETING

21/22-JAN-1999 QMW

MAJOR CHANGES

- PHOTOMETER OPTICAL DESIGN
  - ⇒ POOR PUPIL IMAGING
  - ⇒ TILTED FIELD ⇒ ABERRATIONS.
  - ⇒ KEETIC'S NEW PHOTOMETER.
    - ⇒ PERFECT PUPIL IMAGING
    - ⇒ STREHL >0.86
    - ⇒ CAPABLE OF TAKING WIDE FOV
    - ⇒ DRAWBACK IS ANAMORPHIC FINAL IMAGE [f/4.2 × f/5]
    - * IS THIS ACCEPTABLE?

DETECTOR MEETING

20-22 JAN '99
OHIO

MAJOR CHANGES.

- FTS DESIGN:

  a) BASELINE – MP POLARISING WITH LINEAR MECHANISM À LA GSFC.

  b) INTENSITY BEAMSPLITTERS

  ⇒ PARA HAS DESIGNED + TESTED BROAD BAND BS WITH 4RT≈1

  ⇒ BREAD BOARD MODEL IS OUTSIDE HIS OFFICE (AND WORKS!)

  ⇒ NEED OPTICAL DESIGN.

⇒ FEEDHORN DESIGN
  * 200 - 300 μm O.K.
  * 2Fλ 350 μm WILL BE USED FOR 300 – 670 μm BAND.

DETECTOR MEETING

20-22 JAN 99
QMW

ADDITIONAL .....

- SHUTTER: THE BACKGROUND INSIDE THE FIRST CRYOSTAT WILL BE V. LARGE. A SHUTTER IS REQUIRED
  - * WHO WILL DO IT ?
  - * WHERE DOES IT GO ?
- STRAY LIGHT CONTROL:

  CRITICAL TO THE INSTRUMENT SENSITIVITY.
  BAFFLE DESIGN - RAL
  BAFFLE PROCUREMENT - ?

⇒ LATEST JPL TELESCOPE DESIGN HAS SECONDARY ϕ 314 mm

DETECTOR MEETING

20-22 JAN '89
QMW

OPTO-MECHANICAL SYSTEM DESIGN.

- NOT MUCH PROGRESS

  ⇒ OLD 'A0' DESIGN HAS LAYOUT PROBLEMS WHICH HAVE BEEN FED BACK TO KJETIL

  ⇒ SOME IDEAS BUT NO SOLUTION TO STRUCTURAL SUPPORT

  ⇒ 2-K MASS MAY BE A "PROBLEM"

  ⇒ SUPPORT AS MUCH AS POS. AT 4-K [COOLER.....

  ✱ ENVELOPE FOR DETECTORS SUGGESTED AS 60×60×400 mm

DETECTOR MEETING 20-22 JAN 1999

WARM ELECTRONICS

BUDGETS:

BAU	2.5 W (80K).	
DRCU	26 W	WHAT IS THE QUALITY.
SPU	15 W	
DPU	10 W	
TOTAL	51 W	

CRYOSTAT WIRING

~ 600 - 800 WIRES.

TELEMETRY BUDGET

BASELINE IS 50 KBITS/S ⇒ ↑ FACTOR OF 4

SYSTEMS: FPU

SPIRE

- Structure

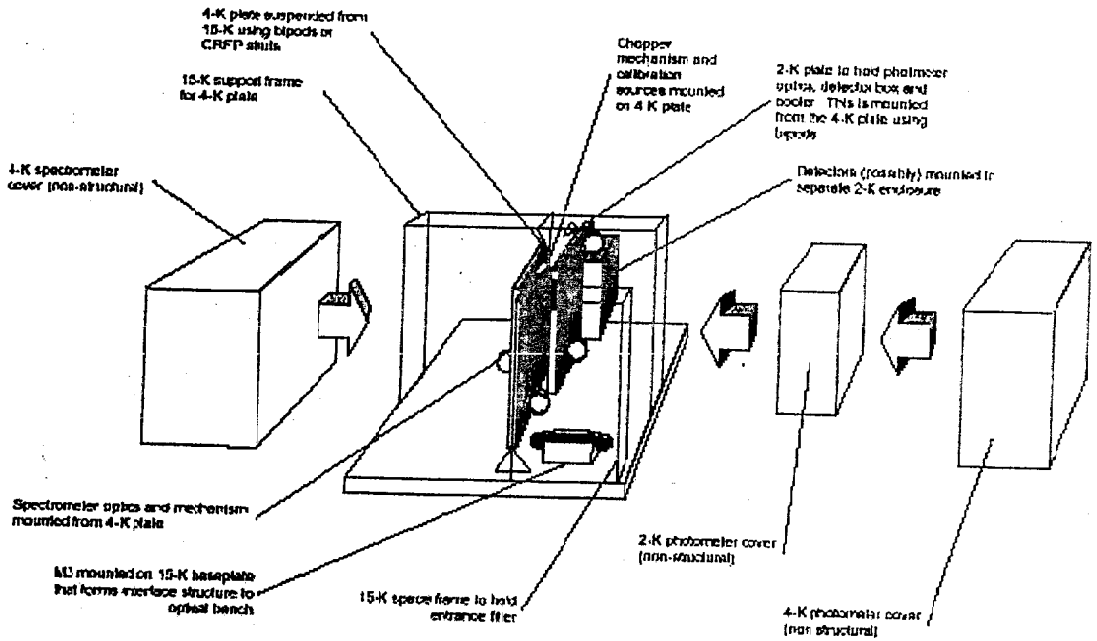

Figure 1: Conceptual layout for the SPIRE structure based on non structural covers (15-K cover not shown)

SYSTEMS: FPU

- Thermal Budgets

Temp. Stage	Item	CEA/TES				Feedhorn (150 dets)			
		ON	OFF	PHOT	SPEC	ON	OFF	PHOT	SPEC
"15-K"		0	0	0	0	15	0	15	15
"4-K"	Wires	1.1	1.1	1.1	1.1	1.1	1.1	1.1	1.1
	Radiation	0.6	0.6	0.6	0.5	0.6	0.6	0.6	0.6
	Mechanisms	0.0	0.0	2.0	7.4	0.0	0.0	2.0	7.4
	Structure	2.0	2.0	2.0	2.0	2.0	2.0	2.0	2.0
	Total	3.7	3.7	5.7	11.1	3.7	3.7	5.7	11.1
"2-K"	Wires	0.1	0.1	0.1	0.1	0.1	0.1	0.1	0.1
	Dissipation	2.0	0.0	2.0	2.0	0.0	0.0	0.0	0.0
	Cooler	1.0	1.0	1.0	1.0	1.0	1.0	1.0	1.0
	Structure	1.0	1.0	1.0	1.0	1.0	1.0	1.0	1.0
	Total	4.1	2.1	4.1	4.1	2.1	2.1	2.1	2.1

4.0 FOR TES OPTIONS.

Notes:
All figures are in mW
Structure: Figures assume temperature of "15-K" shield is 11 K
Cooler: This is the continuous power load of the cooler when at 0.3 K
Feedhorn option: FET box only interfaces to "15-K" stage.

SYSTEMS: FPU

- Mass Budgets

Project code	Instrument unit	# off	Dimensions (mm) *	Mass (kg)
FSFPU	Cold Focal Plane Unit	1	690 x 410 x 410 Irregular shape	31 (TBC) (including JFET box)
FSBAU	Buffer Amplifier Unit	1	200 x 150 x 120 (TBC)	2.5 (TBC)
FSDRC	Detector Read-out and Control Unit	1	285 x 256 x 234	12 (TBC)
FSSPU	Signal Processing Unit	1	240 x 218 x 239	9 (TBC)
FSDPU	Digital Processing Unit	1	200 x 200 x 160	5 (TBC)
FSHAR	Warm interconnect harnesses: FSDRC-FSSPU, FSSPU-FSDPU	3		2 (TBC)
TOTAL				63.5 (TBC)

* Dimensions are given as Length x Width x Height. Length and Width define the fxation baseplate.

Note

1 Dimensions and mass do not include margins

2 Harness FSFPU-FSBAU, FSBAU-FSDRC, FSFPU-FSDRC FSDPU-S/C will be ESA responsibility.

Presented in this note is an outline design fromKjetil Dohlen for a re-optimised photometer channel and a precis of the subsequent exchange of e-mails between us on the 7 and 8 of January 1999.

The design is shown as a sketch in figure 1. In this design M3 is moved to the telescope focal plane to become a Fabry mirror, re-imaging the pupil onto the chopper mirror at M4. Mirror M5 converts the beam from f/8.68 to f/5.0 and re-images the focal plane onto anotherFabry mirror at M6. This mirror also picks off the beam for the spectrometer and sends "over the other side". M6 forms a pupil image at the cold stop, which is now elliptical. Mirrors M7, M8 and M9 form an off axis Offner relay to take the image formed at M6 onto the detectors with a sufficiently long back focal length to allow the dichroics and folding mirrors to be incorporated with plenty of room for the detectors and fridge.

The pupil image quality is now very good as well as the final image quality with Strehl>0.86 across the 4x4 arcmin FOV. Kjetil reckons this same design is capable of taking up to 4x8 arcmin still with reasonable imaging. The image distortion is less than 5% across the FOV.

The final focal ratio is optimised in the XZ plane, so here it is 5.00 and doesn't vary across the FOV. In the XY plane it has the following values:

Image coord	Fy
(0,2')	4.24
(0,0)	4.35
(0,-2)	4.42

So this design has a smallanamorphism in the final image plane and a rectangular field on the sky, but the focal ratio does not vary as a very much function of the FOV. Kjetil reckons it will be difficult to get equal focal ratio in the two directions. A question for the array groups is – does this matter?

There are some minor adjustments to be made to the design some we have already discussed are as follows – comments on these from the appropriate people would be appreciated:

i) The chopper mirror is placed in the centre of the chopper structure in the sketches I have seen. This means that as presently designed the chopper structure would penetrate into the input beam. Kjetil says it is not a problem to open the angle on M4 but doesnt know how far he can go. Is it possible to move the chopper mirror with respect to the chopper structure (GFM)

ii) There isn't a lot of room around the beams for filters and apertures (except at the cold stop). Careful thought will have to be given to where the 2-K structure went. One would like to wrap it around M7,M8, M9 etc to make sure that no higher temperature radiation had a path through the cold stop. Also one would have to think about what temperature M3 was now placed at.

Kjetil is sanguine about the possibility of opening up the angles on the mirrors slightly to allow structure and filtering much the same as in the present deign.

All in all this design looks to be robust and solves the pupil imaging and image quality problems of the original. There are some slightly tricky aspects – the chopper is placed high in the instrument

for instance - but once these have been addressed I recommend we adopt it as our new baseline for the photometer and look at its accommodation.

Figure 1: Fax from Kjetil 7/1/99

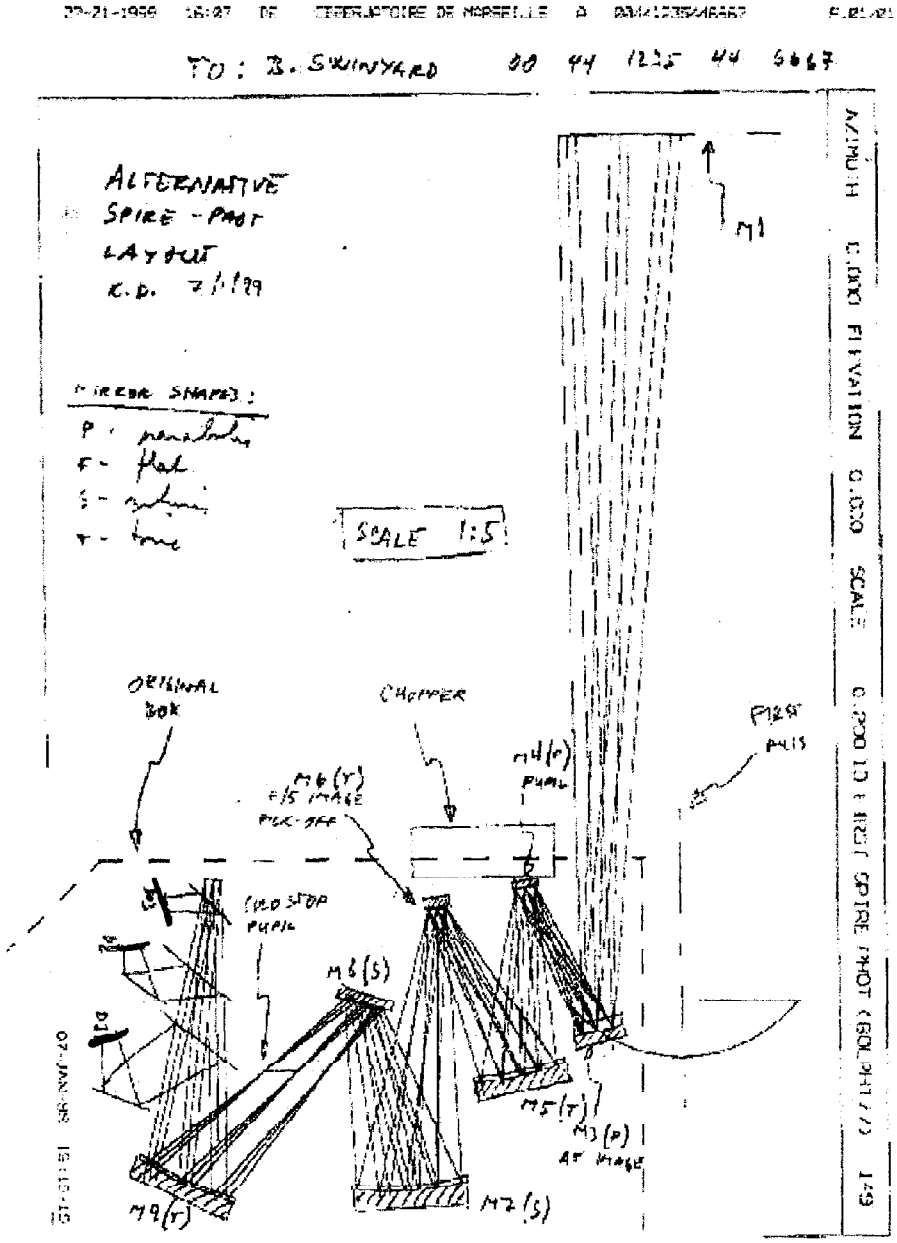

Open actions from Goddard meeting, Sept. 17, 18 1998 (As updated at the meeting)				
No.	**Action**	**Responsible**	**Deadline**	**Status**
		Closed		
13	Provide monthly reports on progress on the development programme to Matt Griffin, copied to Ken King	Rodriguez, Moseley, Bock, Hargrave	End of each month	Closed – superseded by need for all groups to provide monthly reports from now on
15	Produce draft array selection plan	King	Oct. 10	Closed
16	Define 3He fridge stability requirements for BACUS	Hargrave?		Closed (subsumed under 8)
18	Provide summary of FET box options to Thomas Passvogel based on input from Jamie Bock	Cunningham	Oct. 9	Closed
23	Provide written comments on existing draft of array selection criteria document to Matt Griffin	All	Oct. 30	Closed
28	Investigate creation of new SPIRE workpackage for a cold shutter	Griffin	Oct. 9	Closed - discussions with Canadians underway
29	Array splinter meeting actions	QMW, CEA, GSFC, Caltech/JPL	Various	Closed – to be updated in the minutes of this meeting
		Open		
20	Provide first-draft of Systems Design Document	Bock, Moseley, Rodriguez	Feb 28	CEA: Closed GSFC: Open JPL: Open
8	Specify 3He cold stage temperature requirements for SPIRE and BACUS.	Rodriguez, Moseley, Bock	21 Jan. 99	Open
24	Revise array selection criteria document	Griffin	Nov. 13	Open
25	Ask Lionel Duband to provide cooling power vs. temperature curve for baseline He-3 fridge	Swinyard	Feb. 18	Open
27	Define limiting resource dictating maximum permitted number of detectors in the focal plane for feedhorn option	Cunningham	March 20	Open

5

CEA ARRAYS

LAURENT VIGROUX
LOUIS RODRIGUEZ

See also Annex 1

Goals of the CEA developments

1) design of bolometer arrays optimised for FIRST
   - Large format
   - image quality by sampling of PSF
   - immune to cosmic ray
   - $T_{op} = 0.3\ K$

2) Design compatible with ESA space mission constraints
   - based on existing technology
   - production line compatible with ESA planning

CEA organization

- DSM / DAPNIA / Service d'Astrophysique
  - Overall scientific and technical responsibility
  - specification
  - electrical and Optical characterization (with QMW)
  - Space qualification
- DTA / DOPT / Laboratoire d'Infrarouge
  - design of the bolometer arrays
  - process of the different subsystem and integration
    - grids
    - ~~—~~ MUX
    - Read Out
    - connecting support

MONOLITHIC FILLED BOLOMETER DETECTOR ARRAYS & READOUT DEVELOPMENT FOR THE FIRST / SPIRE PROJECT AT CEA

P. AGNESE, C. BUZZI
CEA/LETI/LIR

J.L. AUGUERES, C. CARA, Y. LEPENNEC, L. RODRIGUEZ, L. VIGROUX
CEA/DAPNIA/SAp

BOLOMETER ELEMENTARY PIXEL

THERMOMETER

IMPLANTED SILICON THERMISTOR COMPATIBLE WITH INTEGRATED CIRCUIT COLLECTIVE MANUFACTURE .

PHOSPHRUS IMPLANTATION COMPENSATED BY 50 % BORON NEAR METAL/INSULATOR TRANSITION
α SLOPE ~ 40.

Noise~ 1 $\mu K/\sqrt{Hz}$

BOLOMETER STRUCTURE

A STANDING CRYSTALLINE SILICON MESH TO REDUCE HEAT CAPACITY AND IONIZING PARTICLES SUSCEPTIBILITY.

THERMAL CONDUCTANCE TAILORED TO WANTED VALUES BY GEOMETRIC CONTROL OF THE SILICON SUSPENSION BEAMS

SILICON SENSORS MICROMACHINING TECHNIQUES AT LETI

SUBMM EM WAVES ABSORPTION

VERTICAL RESONANT ABSORPTION :
METAL ABSORBER MATCHED TO VACUUM IMPEDANCE ON $A\lambda/4$ REFLECTIVE CAVITY

HORIZONTAL RESONANT ABSORPTION:
METALLIC PERIODIC PATTERN
(inductive mesh, capacitive loops or crosses)
ADJUSTED TO 377W/□
DEPOSITED ON THE SILICON GRID

FIRST/SPIRE

THE DETECTOR PRINCIPLE

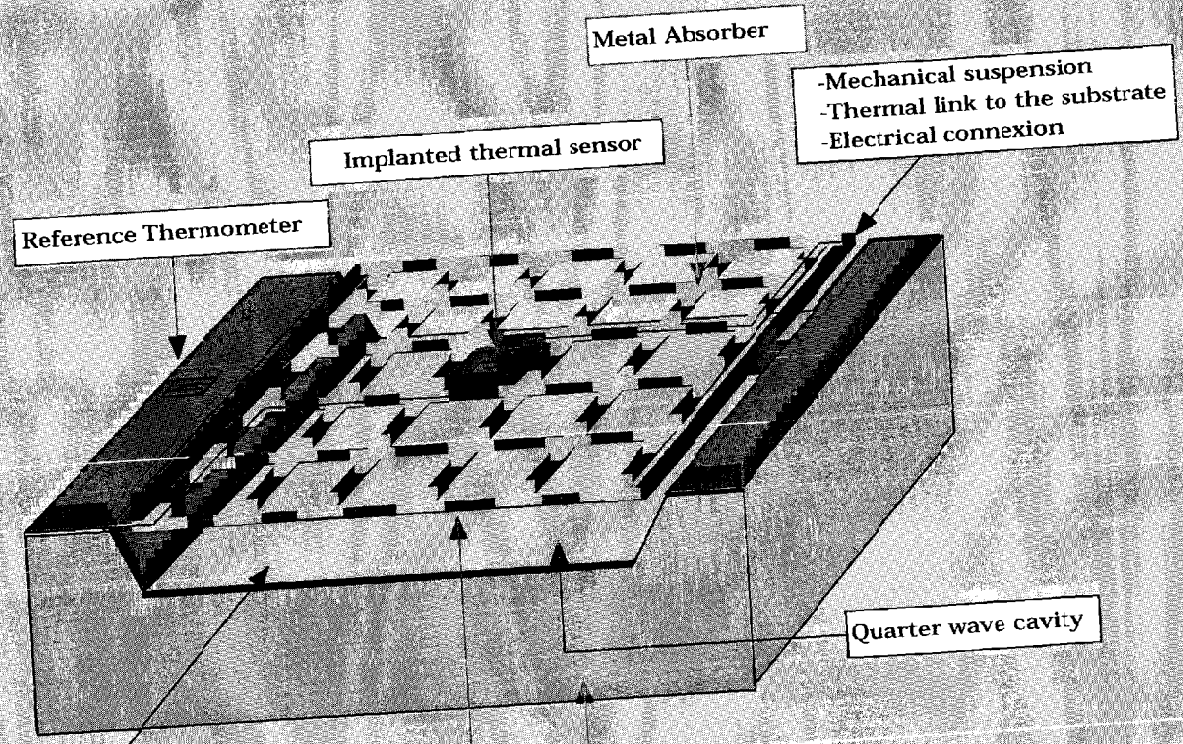

FIRST/SPIRE

THE ARRAY CONCEPT

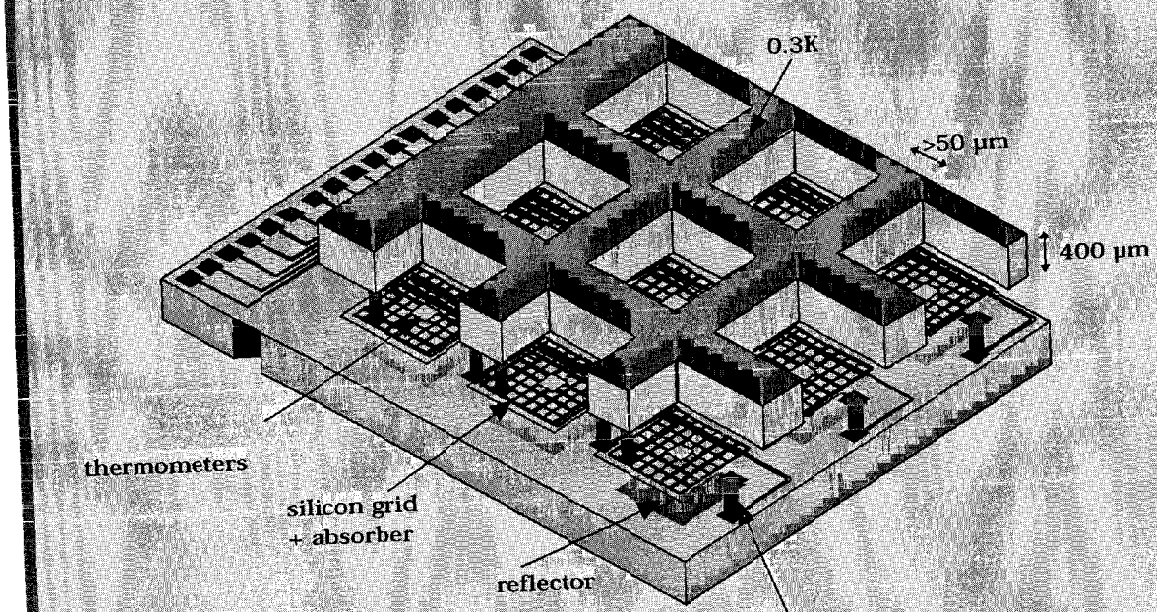

TO BUILD BOLOMETER ARRAYS

TO HAVE ACCESS TO A TECHNOLOGY :
HERE AT CEA/LETI
Manufacture of integrated electronic circuits,
and microsensors for industry.
TO HAVE KNOWLEDGE OF CRYOGENIC DETECTORS
FOR SCIENTIFIC SPACE PLATFORMS: ISO and CASSINI.

TO HAVE ACCESS TO PHYSICAL PROPERTIES:

OPTICAL ABSORPTION DATA.

THERMAL CONDUCTANCES OF MATERIALS:
Si, metal wires, others.

SPECIFIC HEAT DATA to compute heat capacity of the bolometer.

A THERMOMETER with known response ard noise density
to compute SENSITIVITY.

TO DEVELOP MODELS :

For observations

For optical absorption.
For thermal behaviour of the bolometers: bandpass and expected sensitivity
For electrical read out and signal processing.
For thermal requirements of the focal planes.

TO ENSURE THAT SOLUTIONS ARE CONSISTANT WITH AVIABLE THECHNOLOGIES FOR SCIENTIFIC SPACE BASED INSTRUMENTS.

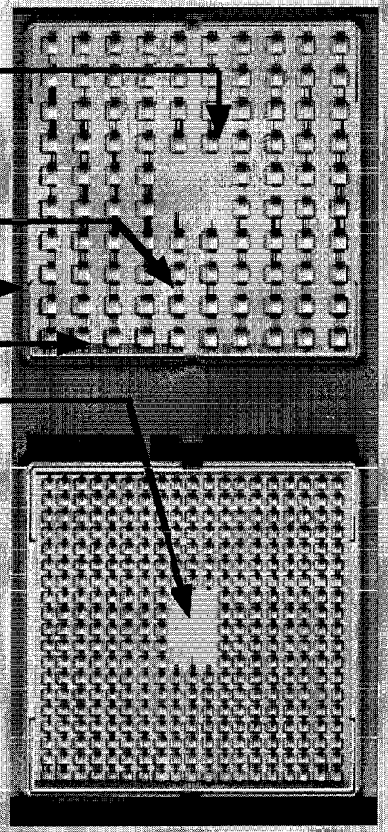

Description de la zône motifs thermiques(D)

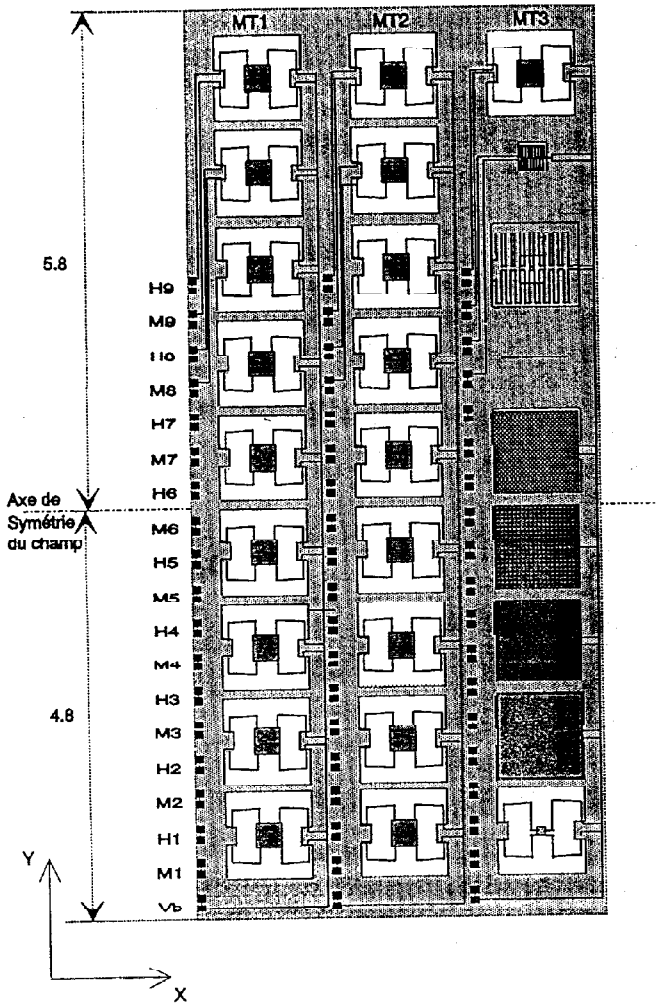

Détail d'une structure type MT1 & MT2

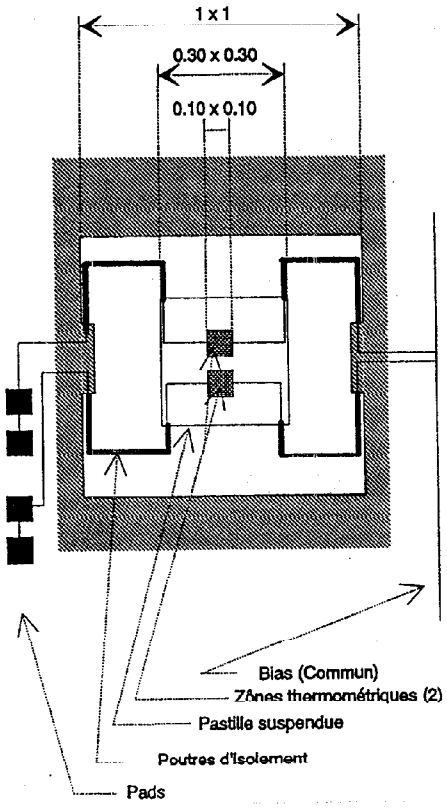

- PAS en X: 1.3
- PAS en Y: 1.1
- Mur d'isolement en X: 0.3
- Mur d'isolement en Y: 0.1
- Pas des pads en Y: 400 µm. Nombre: 19 (1 bias + 18 ponts bolos) dont 12 au dessous de l'axe de symétrie du champ, 7 en dessus.
- Cf. document pour définition des géométries des poutres et des membranes suspendues

Définition du Pad élémentaire (dédoublé)
Côtes en µm

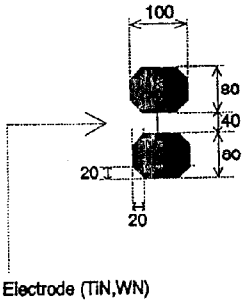

97 PROTOTYPE ARRAY

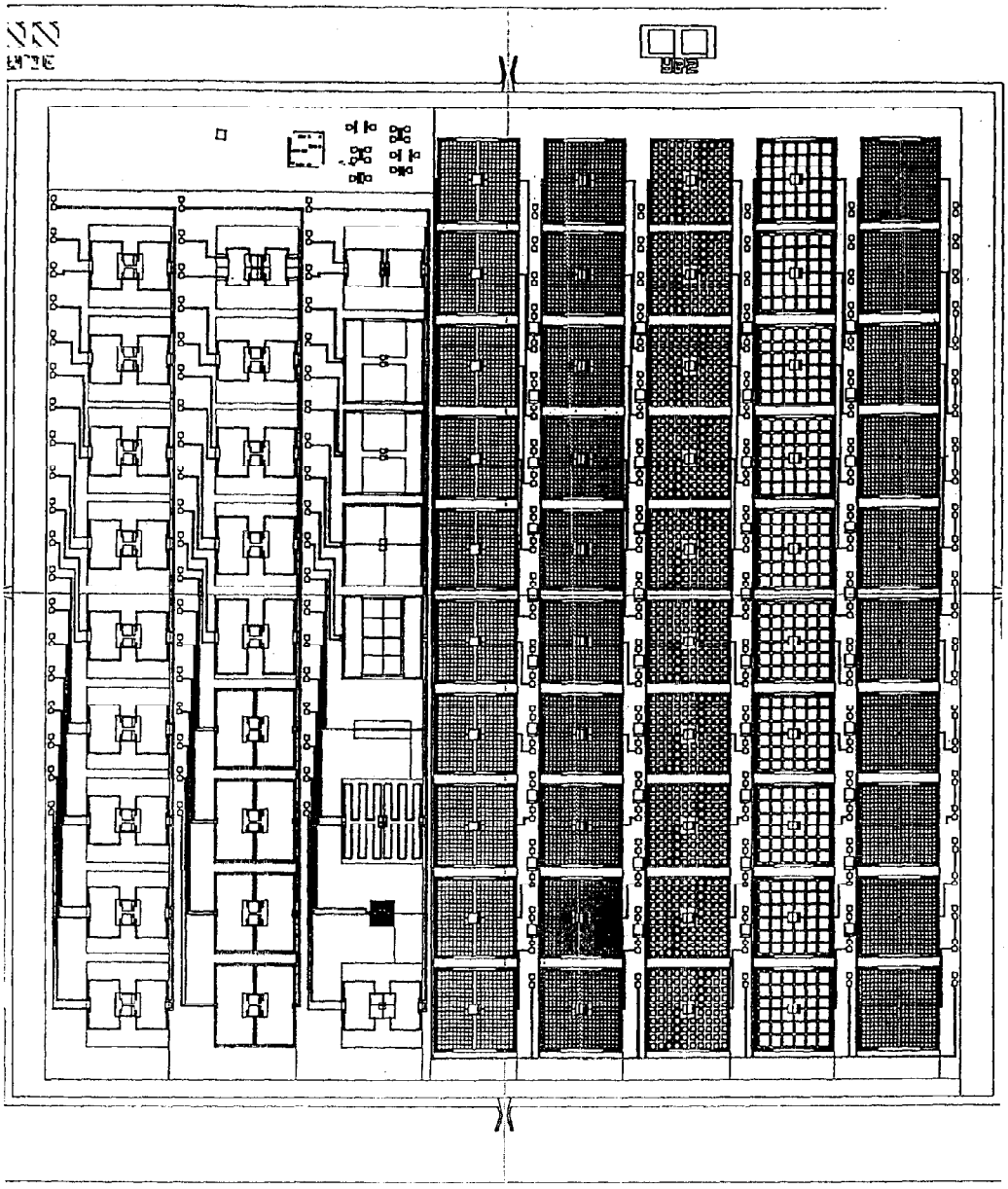

THERMOMETER PERFORMANCES

THERMAL RESPONSE

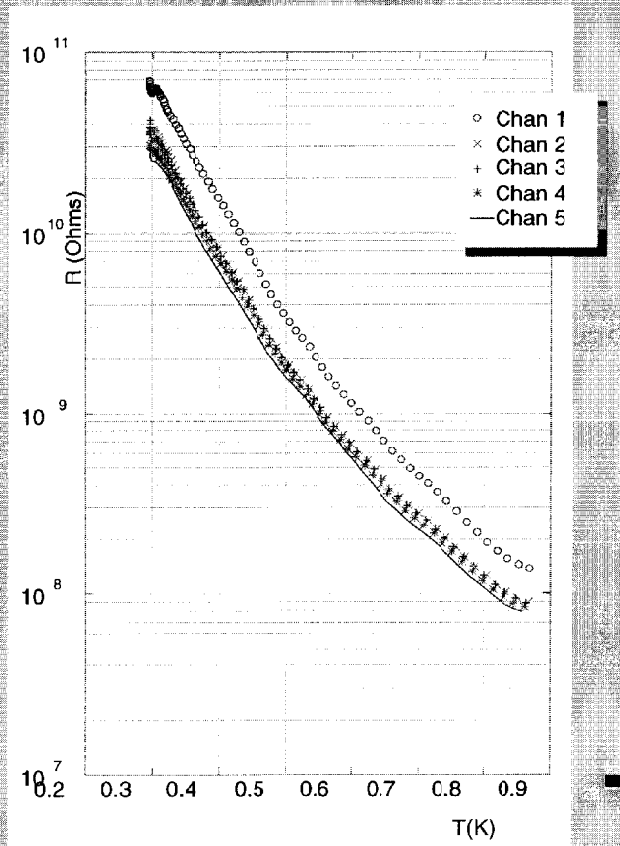

NOISE MEASUREMENTS

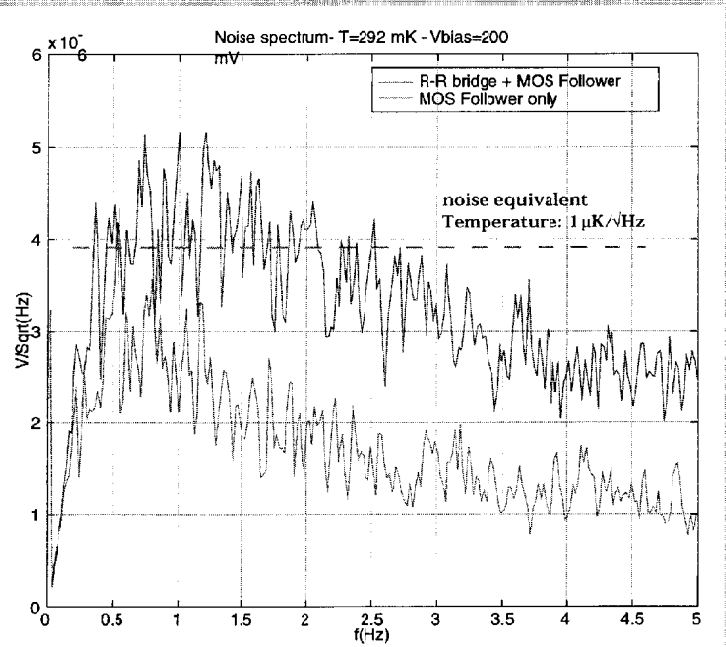

$\alpha \sim 40$

FIRST/SPIRE

VERTICAL RESONANCE

HORIZONTAL PATTERN RESONANCE

ABSORPTION SIMULATIONS

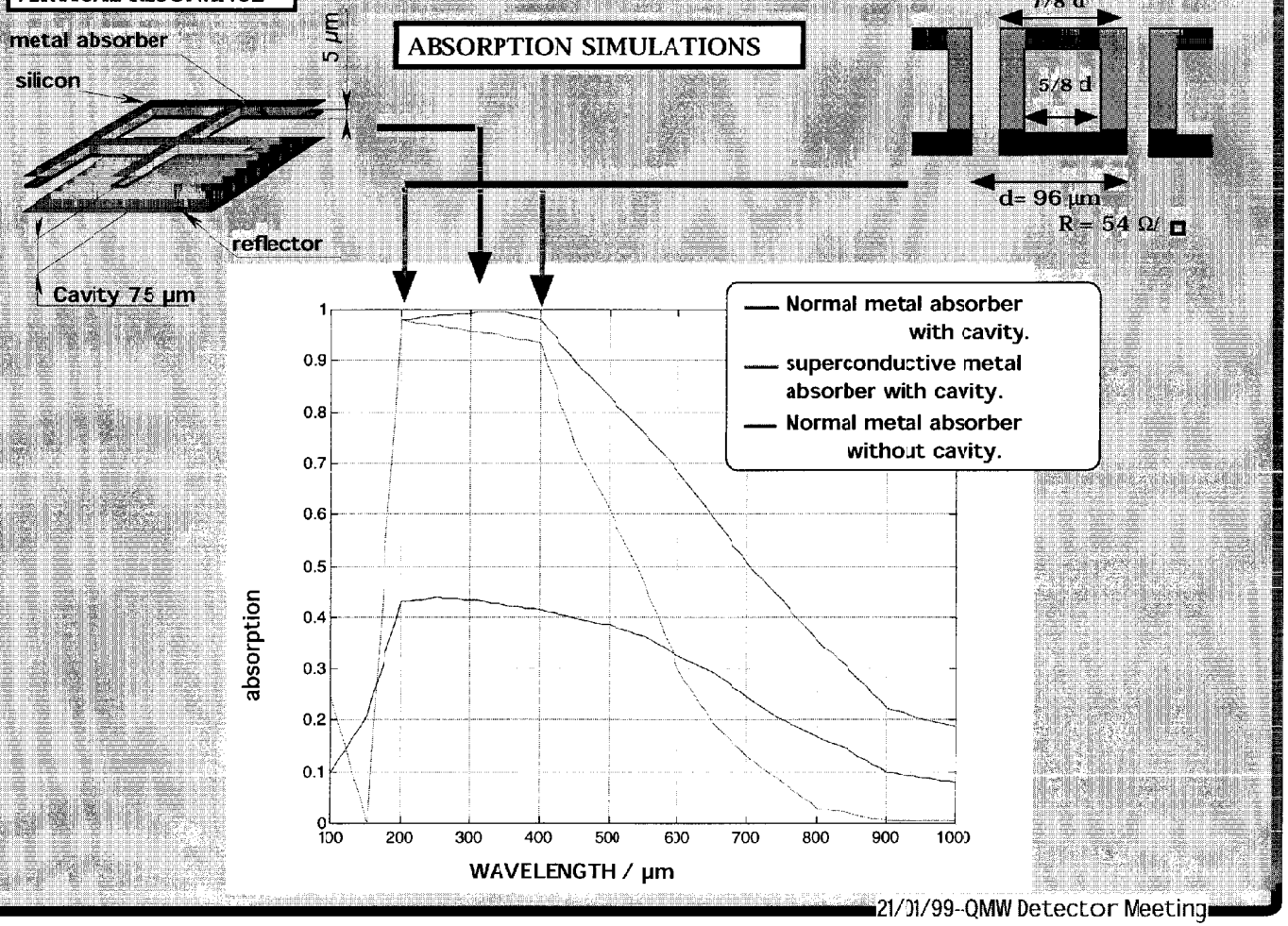

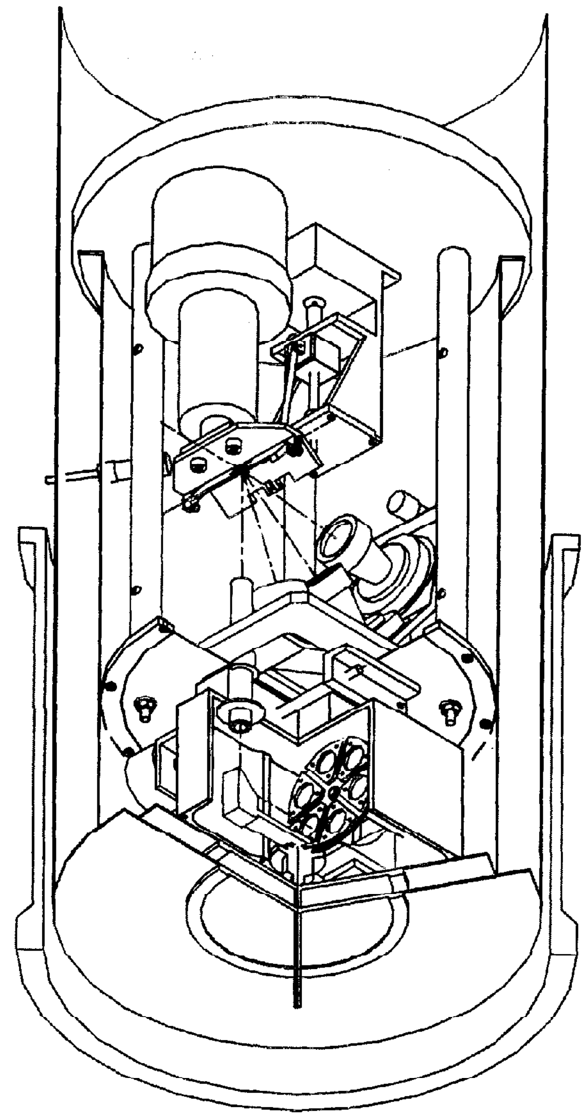

FIRST/SPIRE

300 mK BOLOMETER THERMODYNAMIC PROPERTIES

HEAT CAPACITY
J/K/mm²

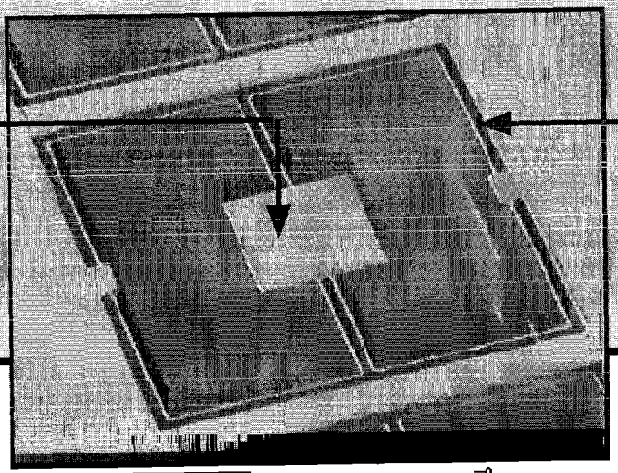

THERMAL
CONDUCTANCE
W/K
700µmx5µmx4µm

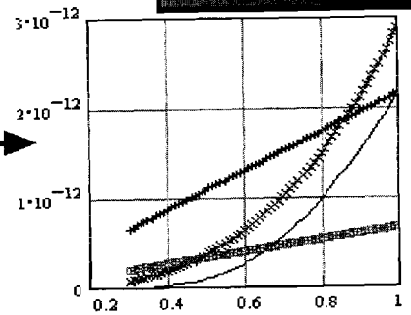

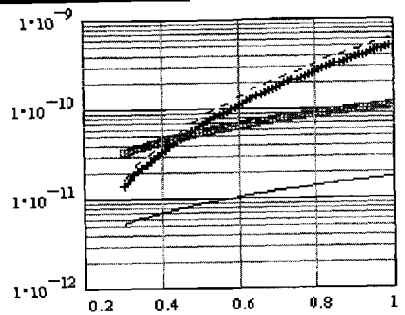

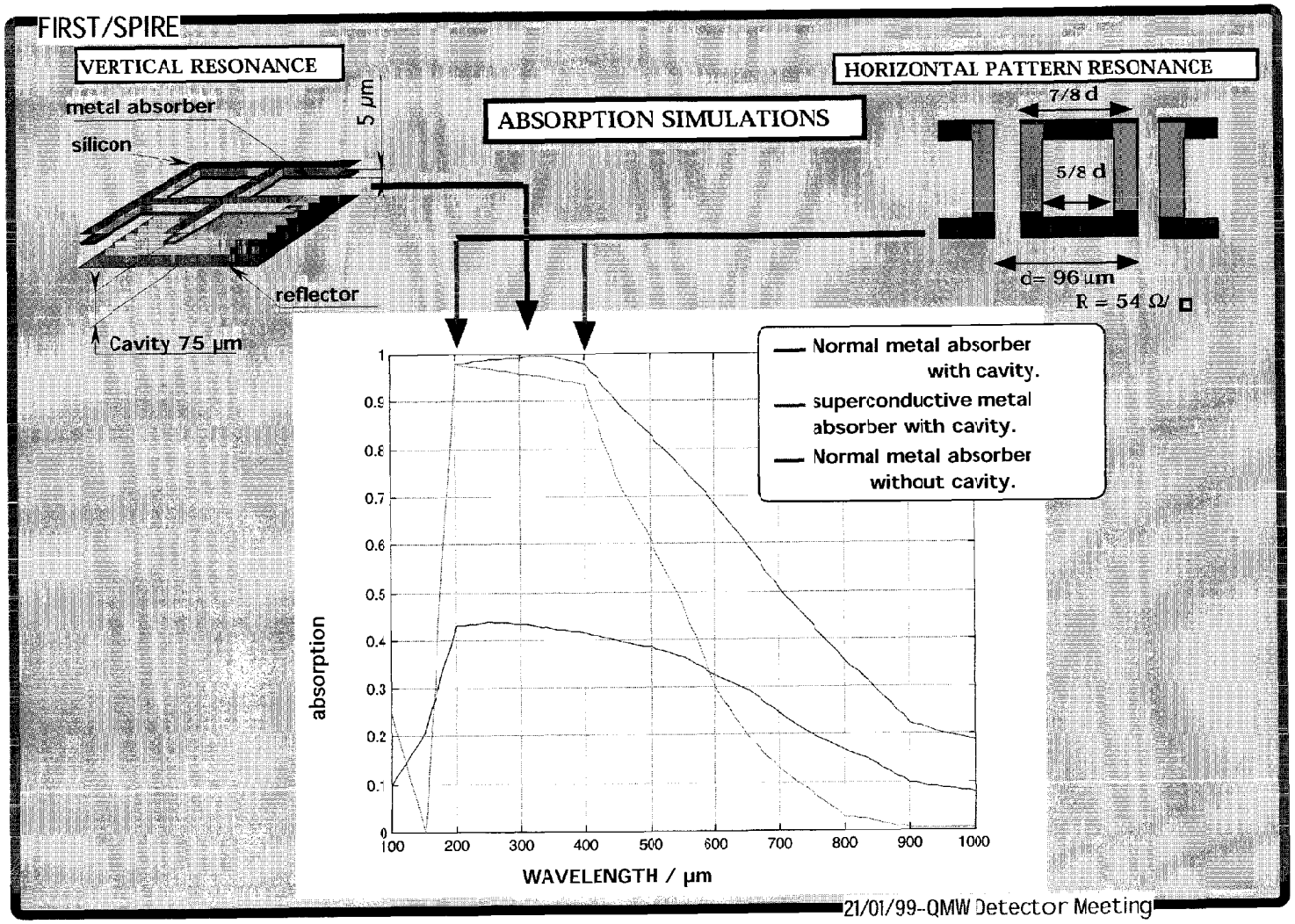
FIRST/SPIRE
VERTICAL RESONANCE
metal absorber
silicon
5 μm
reflector
Cavity 75 μm
ABSORPTION SIMULATIONS
HORIZONTAL PATTERN RESONANCE
7/8 d
5/8 d
d= 96 μm
R = 54 Ω/□
Normal metal absorber with cavity.
superconductive metal absorber with cavity.
Normal metal absorber without cavity.
absorption
WAVELENGTH / μm
21/01/99-QMW Detector Meeting

OPTICAL ABSORPTION MODEL (I)

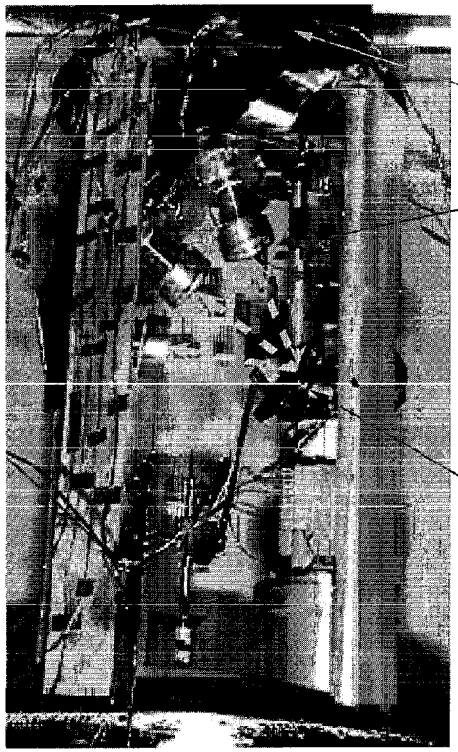

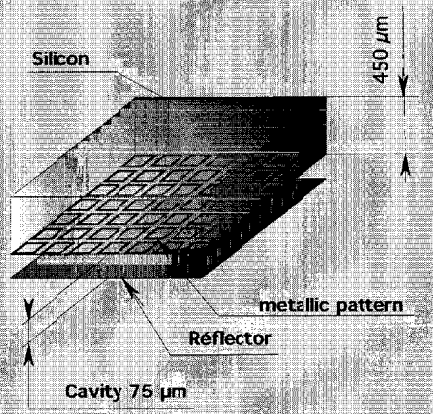

SIMULATION

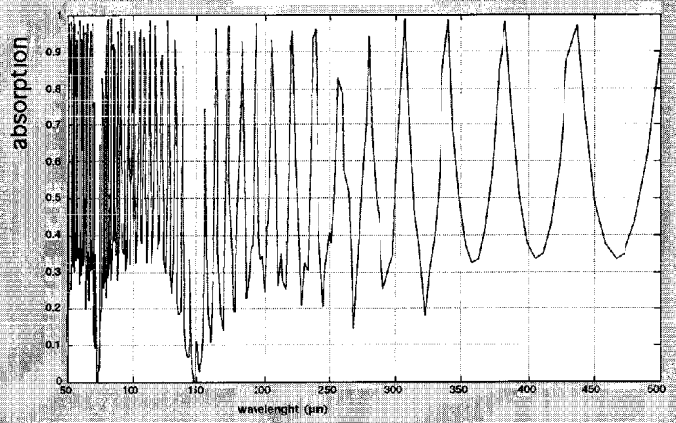

OPTICAL ABSORPTION MODEL (II)

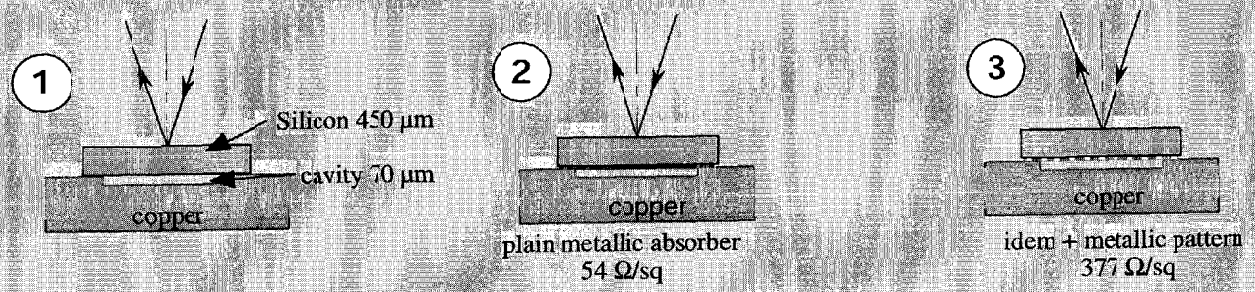

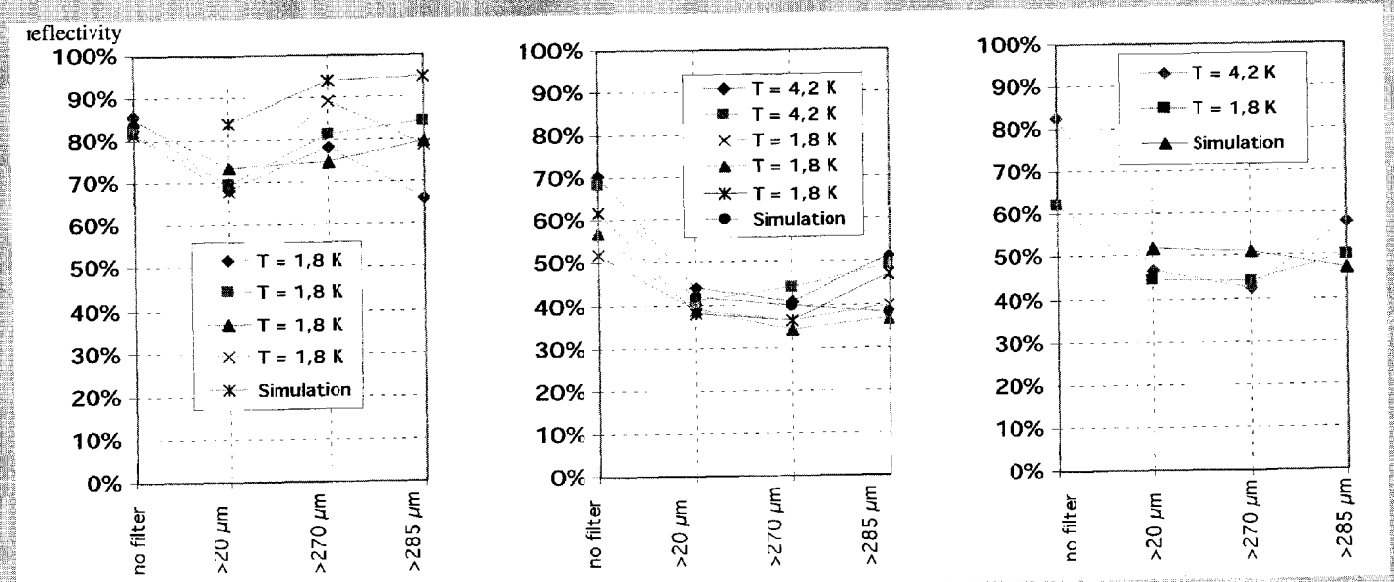

LONG LEGGED THERMOMETER

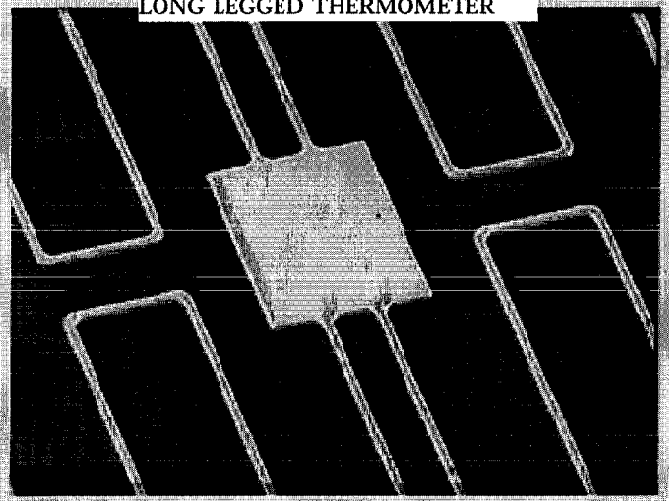

NORMAL DESIGN

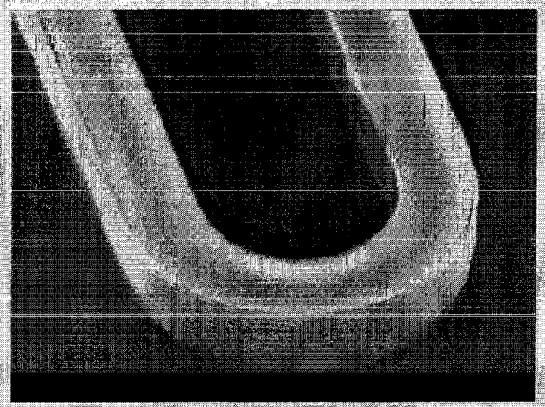

SUSPENSION LEGS DETAILS

WIGGLED DESIGN

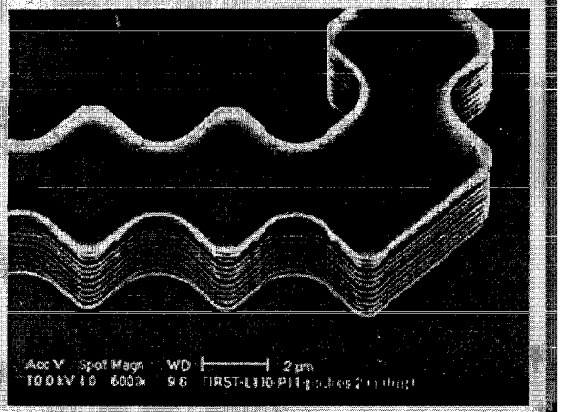

INDIUM BUMPS THERMAL CONDUCTIVITY

Using high power dissipation on bolometers and measuring substrate (reference) temperature, we deduced the thermal conductivity of the indium bumps. They were supposed to isolate the cold read out circuit at 1,8 K from the 300 mK stage .

We measured a conductivity variation with T^3 in place of T, incompatible with admitted thermal load on the ^{3}He fridge.

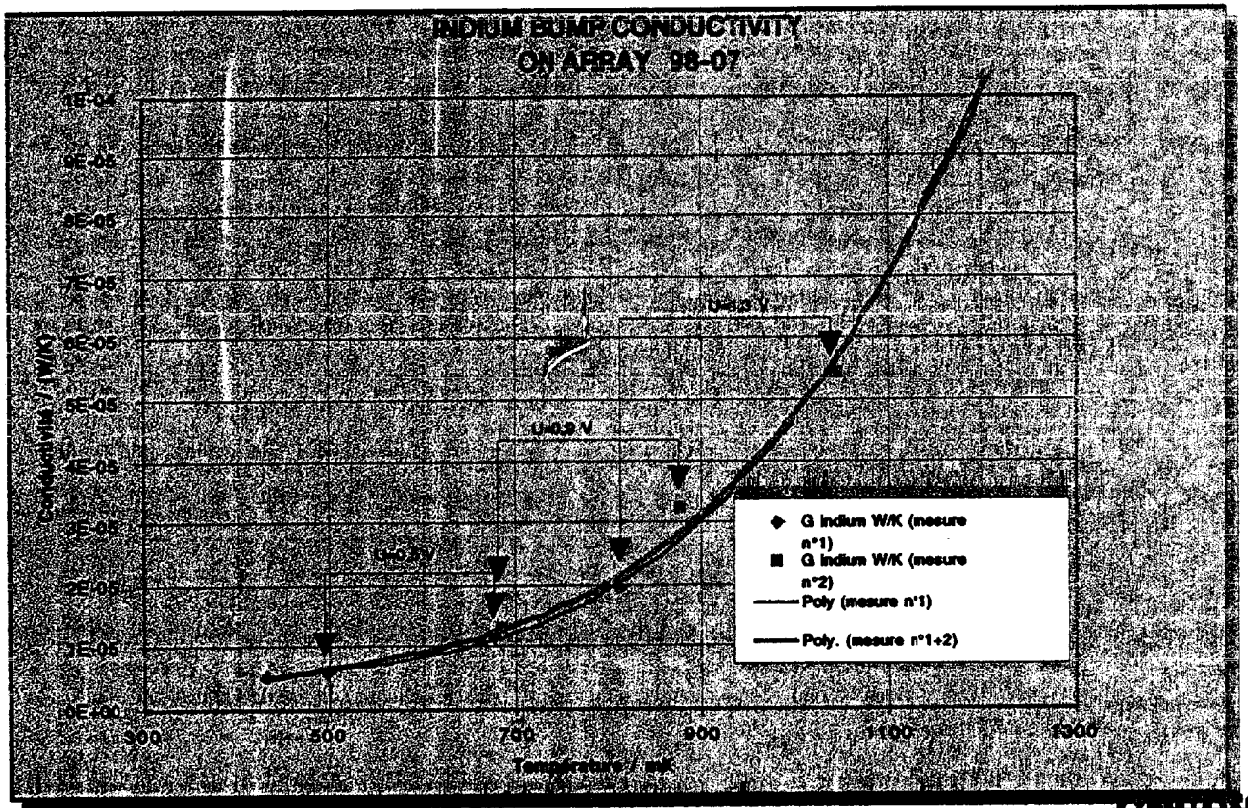

THE COLD READOUT ELECTRONICS

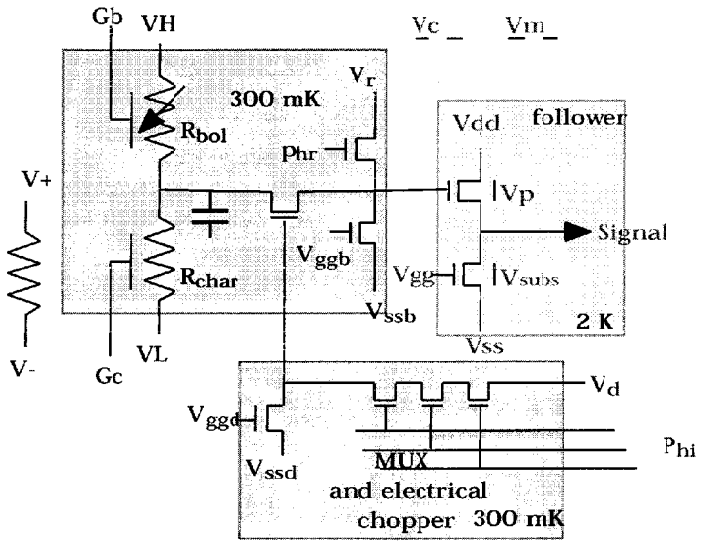

SPIRE ANALOG CHAIN BLOCK DIAGRAM (LETI/LIR BOLOMETER)

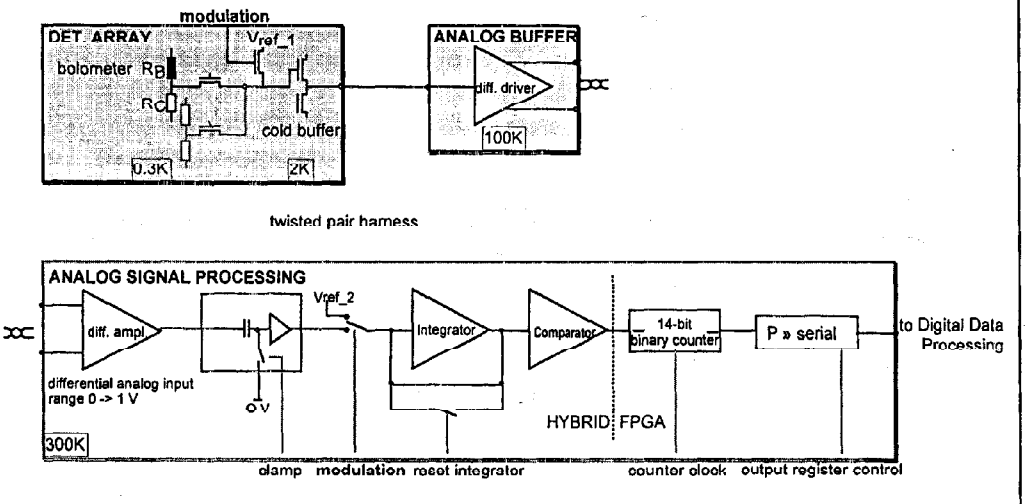

Note : all signals are generated by the Detector Array Sequencer

ANALOGUE CHAIN TIMING

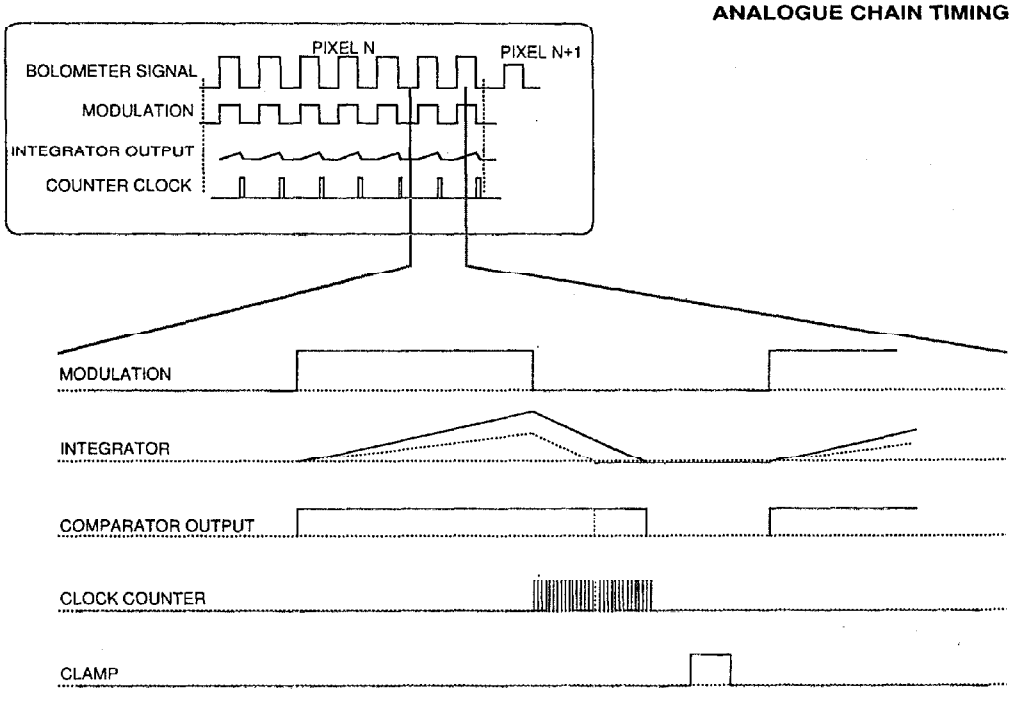

COLD BUFFER 1/f NOISE
(2 µV/√Hz - 2 Hz)

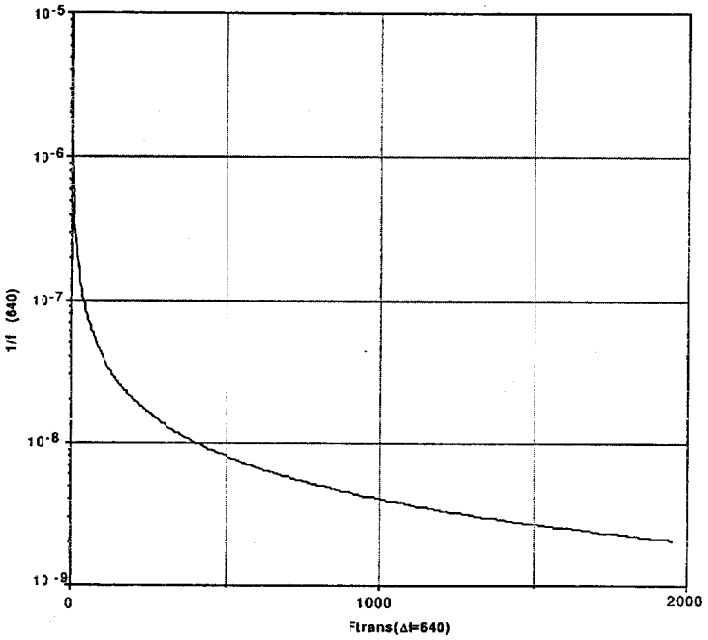

ANALOGUE CHAIN RESPONSE vs FREQUENCY
(Fmod = 1 kHz - Fpix = 320 Hz)

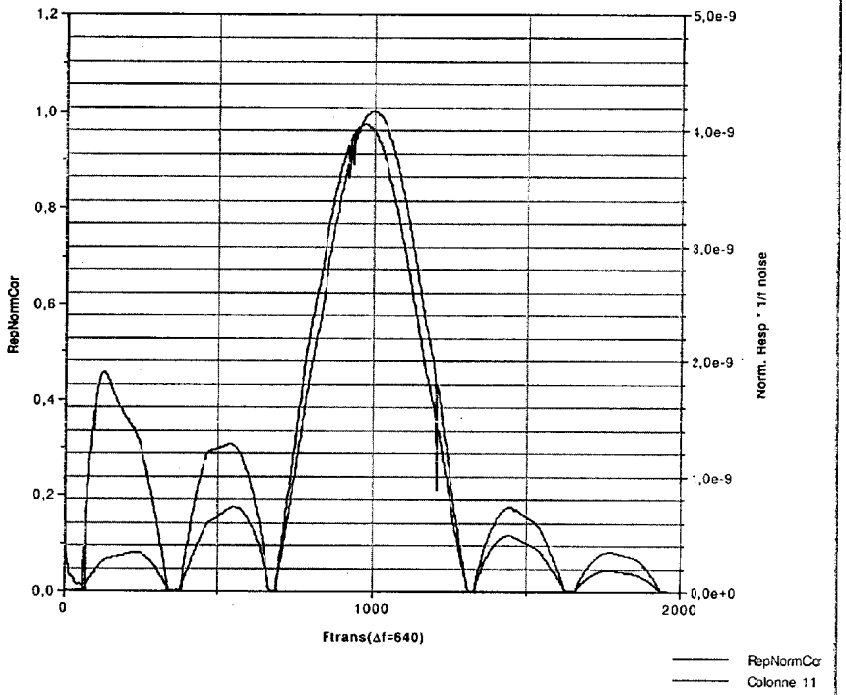

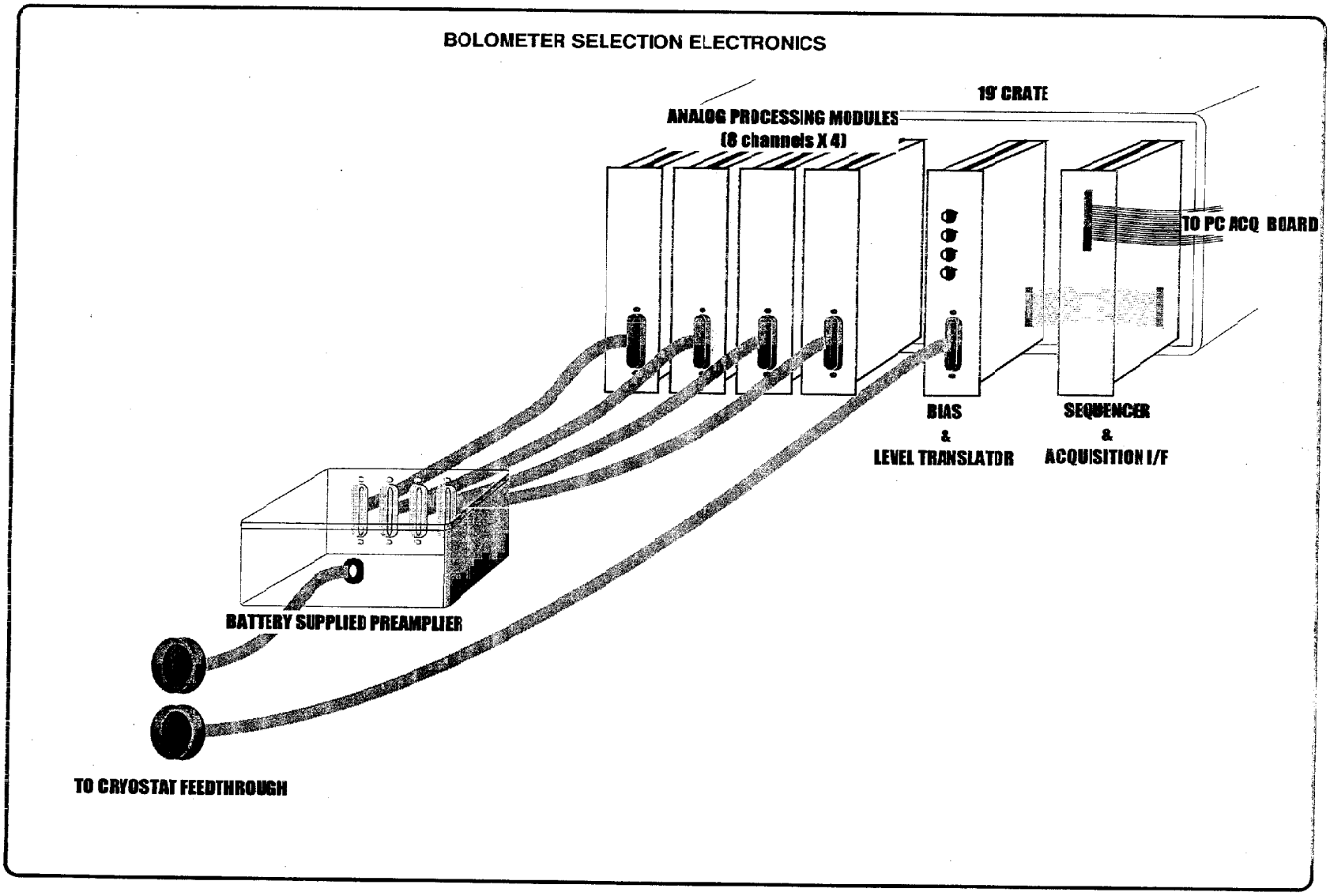
BOLOMETER SELECTION ELECTRONICS
19' CRATE
ANALOG PROCESSING MODULES
(8 channels X 4)
TO PC ACQ BOARD
BIAS
&
LEVEL TRANSLATOR
SEQUENCER
&
ACQUISITION I/F
BATTERY SUPPLIED PREAMPLIER
TO CRYOSTAT FEEDTHROUGH

NEW DETECTORS ELEMENTARY PIXEL

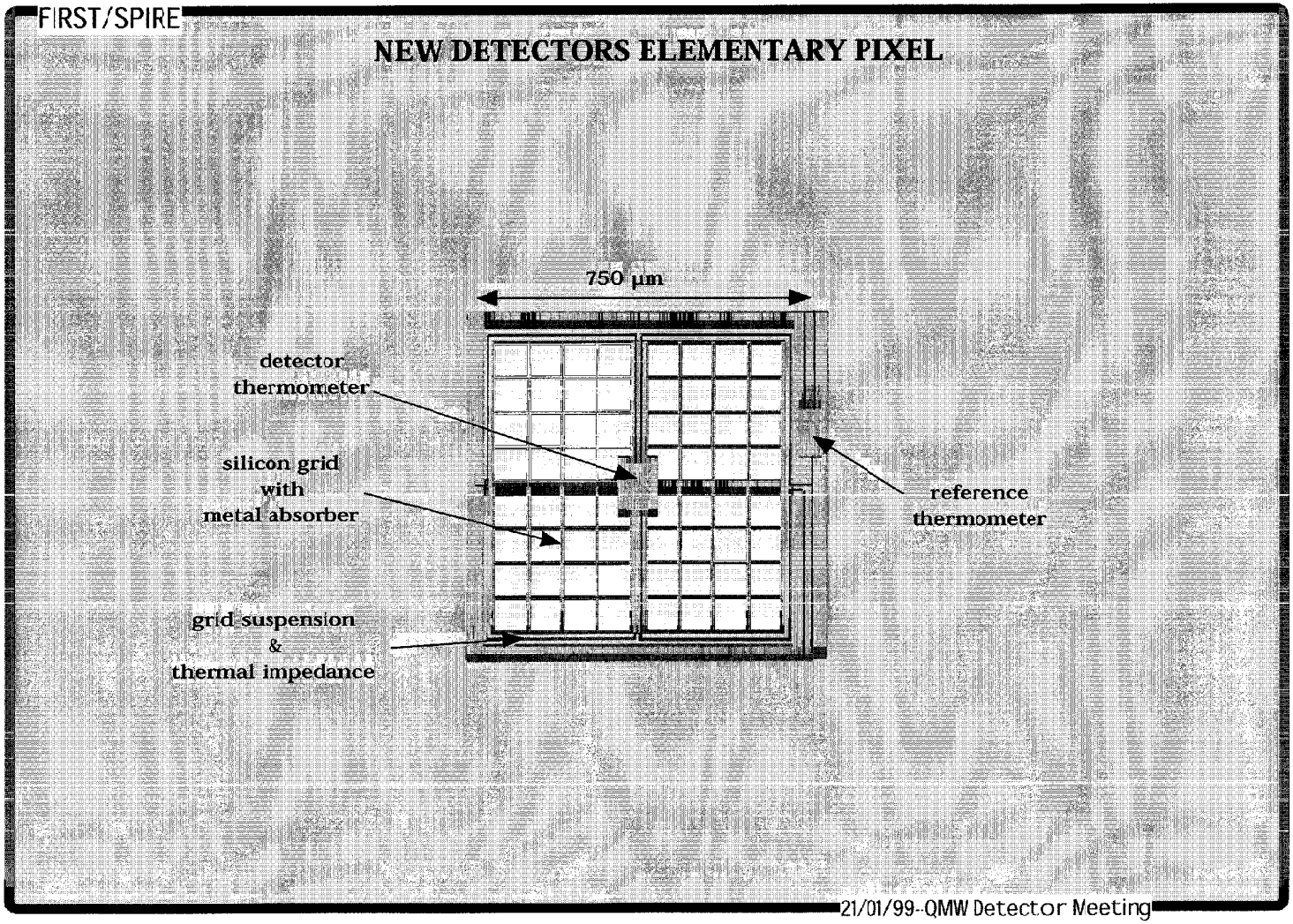

NEW DETECTORS PIXEL BOLOMETERS

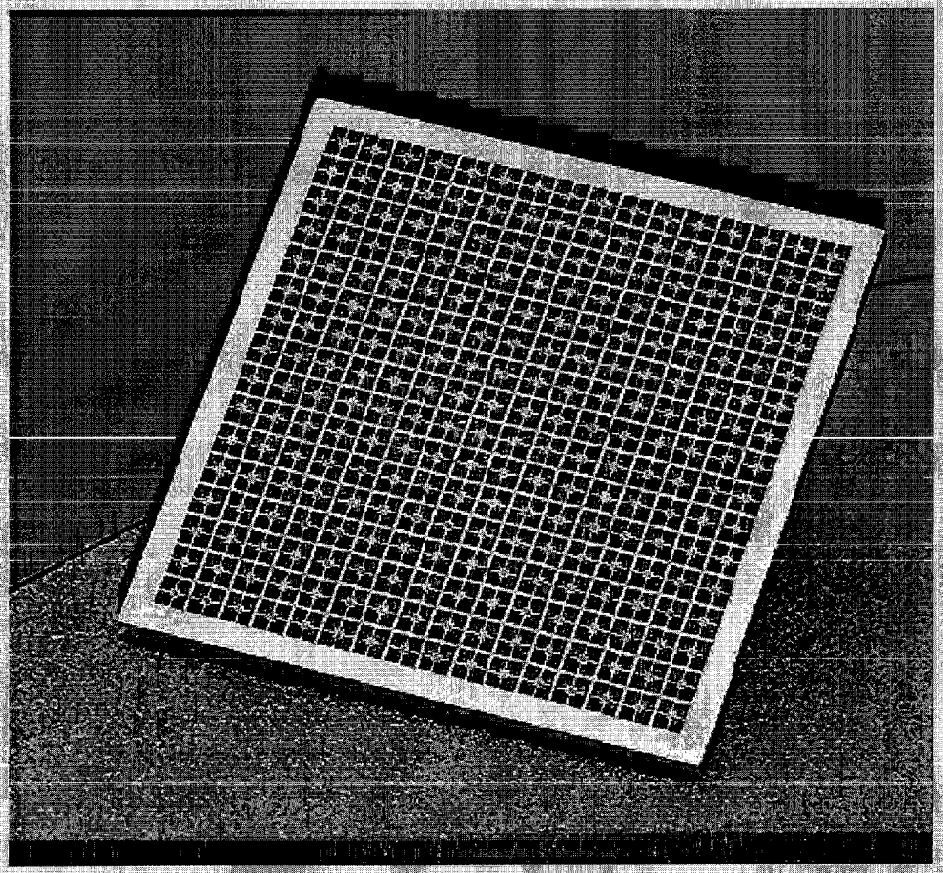

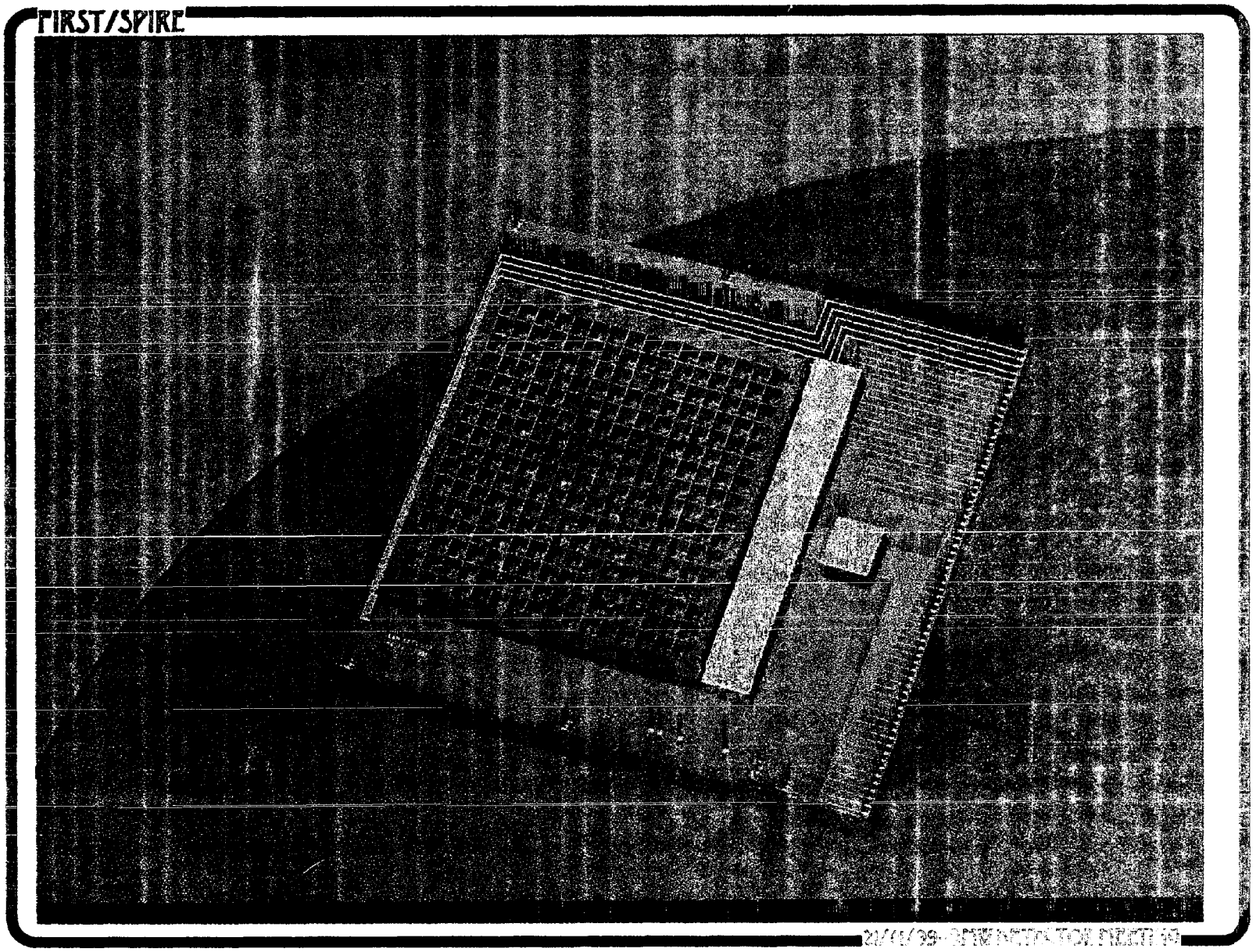
FIRST/SPIRE

FIRST/SPIRE

CEA BOLOMETER ARRAYS : SYSTEMS DESIGN IMPACTS

ADVANTAGES

LIGHT COLLECTION
- Airy disc sampling

BOLOMETER STRUCTURE
- Low heat capacity
- controled thermal conductance
- Good immunity to ionizing particles
- high mechanical resonances=
- low microphonic susceptibility

LIGHT->HEAT CONVERSION
- close to 100% efficiency.
- Absorption profile tailored by
- horizontal pattern

THERMOMETRIC PERFORMANCES
- High T dependence a~40.
- can be adjusted in flight (TBC)
- Noise level OK->goal NEP $_{opt}$~10^{-17}W/√Hz

GENERAL
- Complete focal plane sampling
- Easy baffling
- small devices (8 x 5 x 2 cm ^{3})
- High elect. Integration MUX 8->1

DRAWBACKS

LIGHT COLLECTION
- Low directivity-need baffling

BOLOMETER STRUCTURE

LIGHT->HEAT CONVERSION
- TBC

THERMOMETRIC PERFORMANCES
- High impedance thermometer
- Need 2K close readout.
- Complex lock-in amplifier
- Noise performances< NTD Ge

GENERAL
- COST
- Success oriented development
- Few physic properties still to evaluate

FIRST/SPIRE

CEA Detector Development Schedule

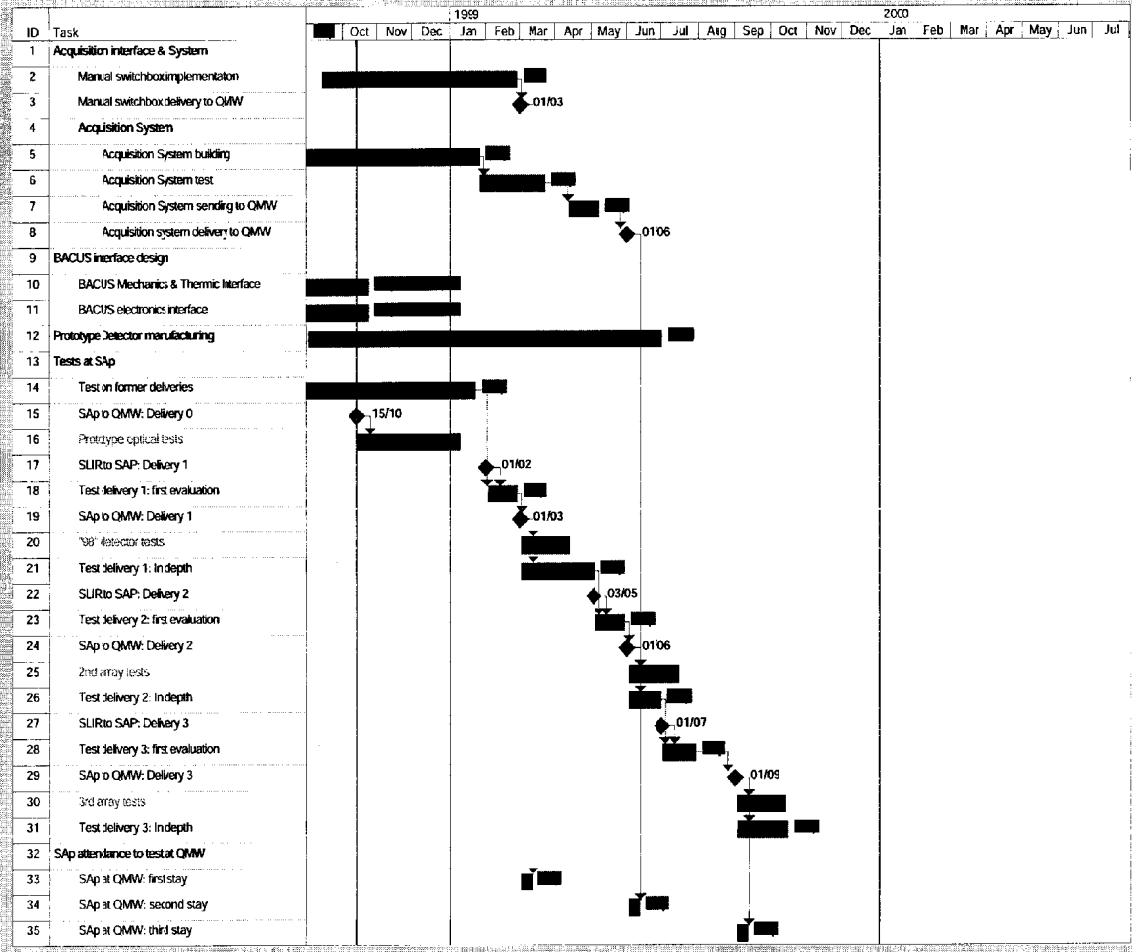

CONCLUSIONS AND PROSPECT

- These last years have been a very exciting period. We started, two years ago, from a single concept, to end up with a new detector in hands.

- Although, all the physical principles at work in these arrays are (well?) known, this realisation is an original combinaison of sophisticated techniques (not alwaws under control!).

- For this reason, most of the final (before evaluation) design is frozen.

- A few aspects have yet to be explored (mesa detectors, gate effect on the thermistors etc.)

- A large amount of work is still necessary to sort out a satisfactory array.

- In parallel to the detector caracterisations, an important effort will be done to manufacture the warm signal processing electronics.

- A pre-qualification process will be done internally at Grenoble (vibration tests).

- Susceptibility to ionising particles will be soon tested also. The simulation program has already started. The bonus is, maybe, to be able to measure easily the individual electro- thermal bolometer characteristics without a calibrated sub millimeter source.

6

GSFC/NIST ARRAYS

HARVEY MOSELEY
JIM CALDWELL
JUAN ROMAN
KENT IRWIN

THE NIST TEAM

KENT IRWIN

JAY CHERVENAK

ERICH GROSSMAN

TODD HARVEY

JOHN MARTINIS

CARL REINTSEMA

DAVE RUDMAN

OUTLINE

- SINGLE PIXEL PERFORMANCE
  - SCALING TO SMALL TES
  - EXCESS HIGH FREQ. NOISE ELIMINATED
  - TES FABRICATION
    Al/Ag + Mo/Au + Mo/Cu
- 4×8 FABRICATION STATUS
  - CONTACT PADS, GRANULAR Al LEADS, Pd Au ABSORBER, BACKSIDE KOH ETCH, FRONTSIDE PUNCH-THRU MASK — DONE
  - SOME MICROMACHINING, TES DEPOSITION — REMAINING
  - RISK REDUCTION THROUGH REDUNDANT FABRICATION @ GSFC + NIST
- SQUID MUX CHIPS (1×8)
  - SUFFICIENT INVENTORY FOR DOWNSELECT OF BOTH SQUID MUX AND NYQUIST FILTER CHIPS.

Thermal Circuit Model

Fit to two free parameters:

$G^* = 300\ G_{pud}$ Thermal conductance within pud

$C^* = C_{TES}$ Extra heat capacity (from granular Al)

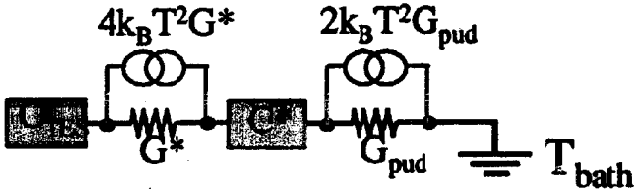

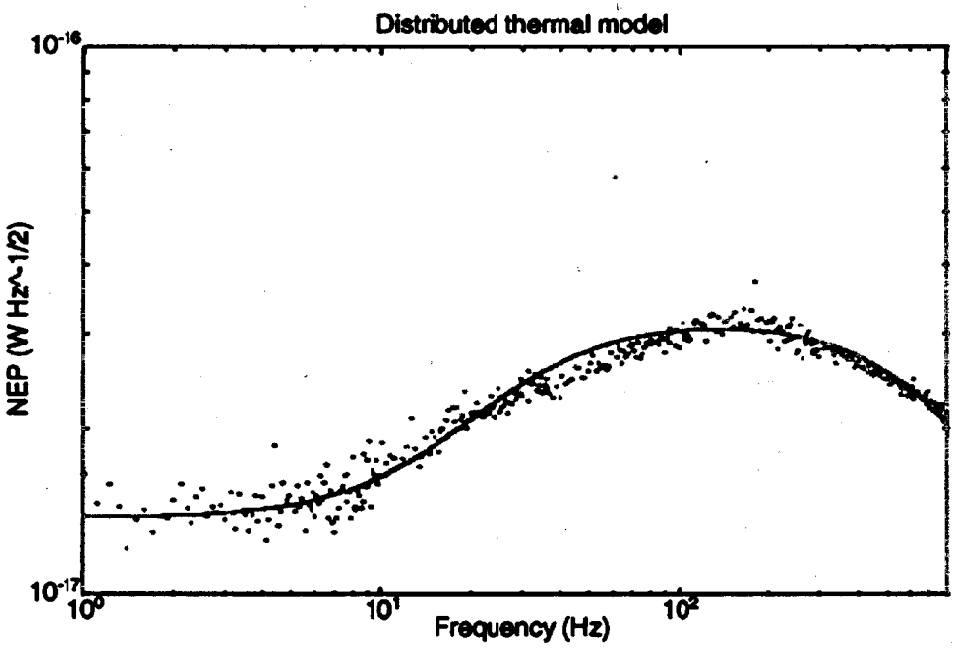

NIST Boulder

RECENT, PRELIMINARY RESULT:
NOISE BUMP ELIMINATED

Mo/Au Superconducting Transition

Thermal anneal tests (400 C) very promising

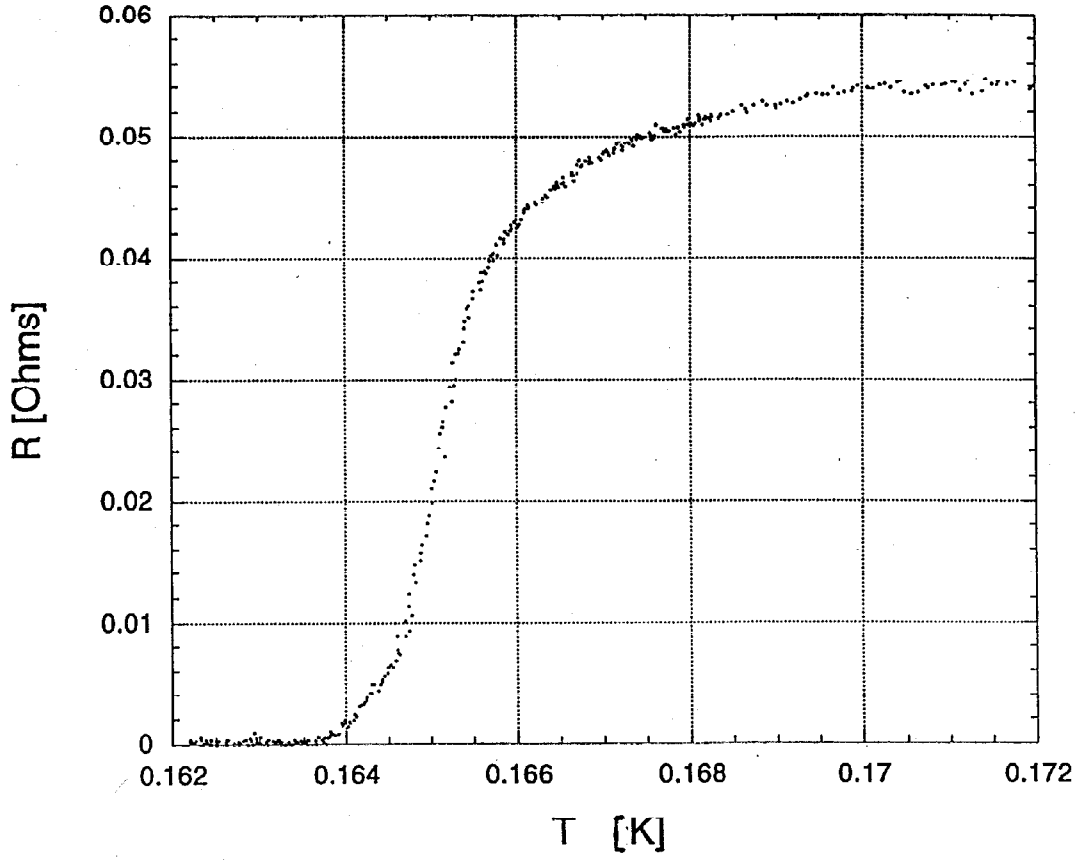

TES/PUD FAB PROCESS

① FRONTSIDE METALLIZATION
(CONTACTS, LEADS, ABSORBER)

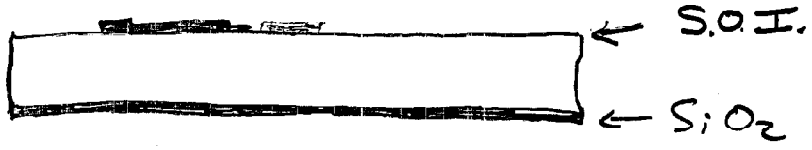

② BACKSIDE ETCH MASK

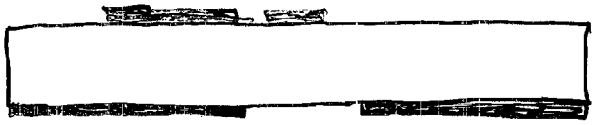

③ KOH ETCH OF Si

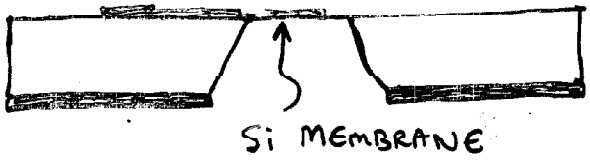

④ FRONTSIDE Si PUNCH-THROUGH ETCH

⑤ SHADOWMASK DEPOSITION OF TES

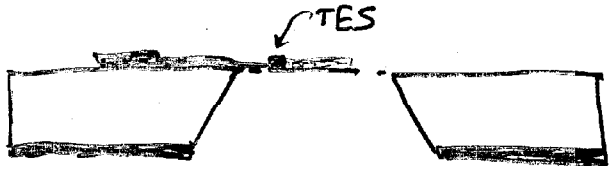

One Pixel of a Partially Fabricated 1 x 8 TES Bolometer Array

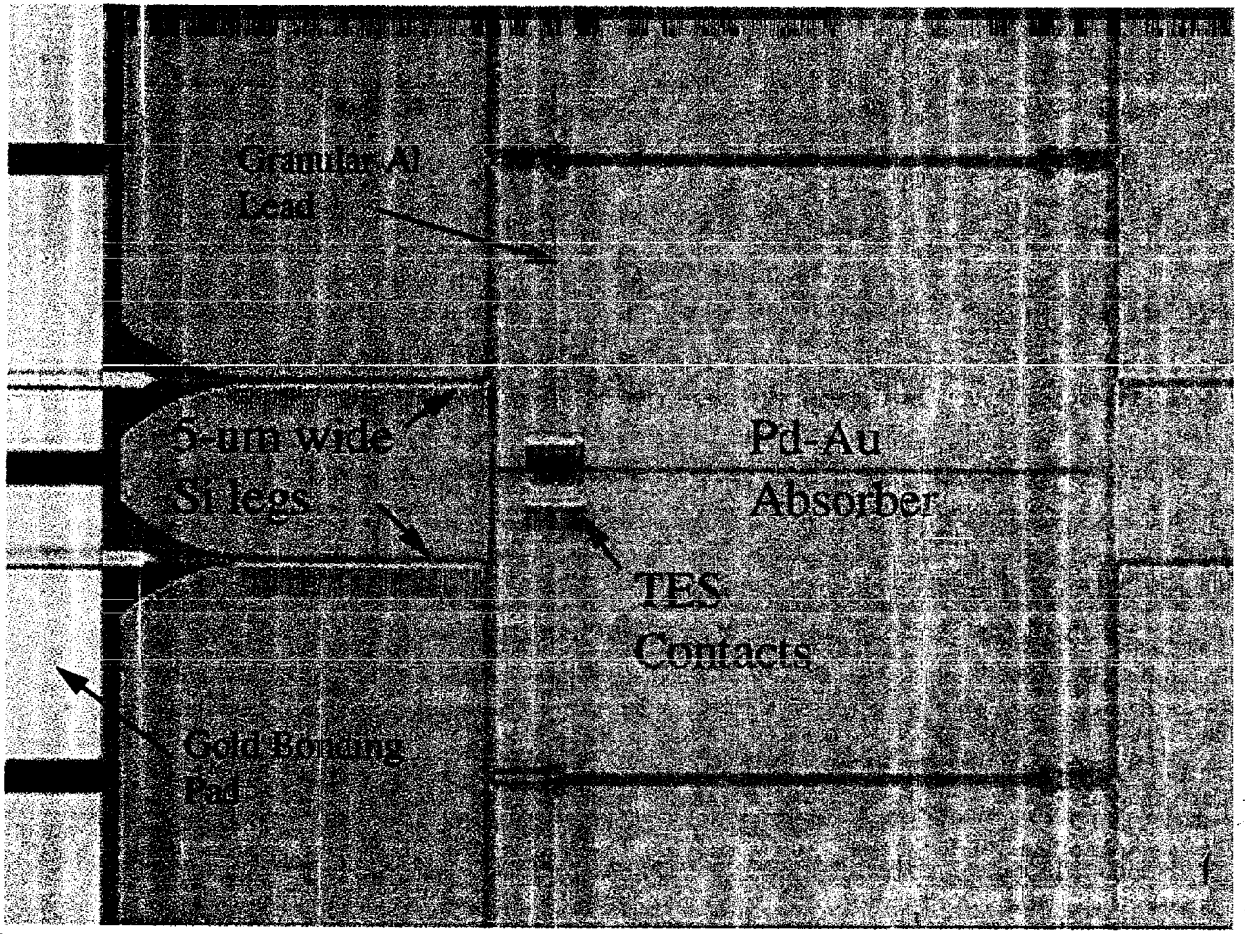

TWO-TES DEVICE

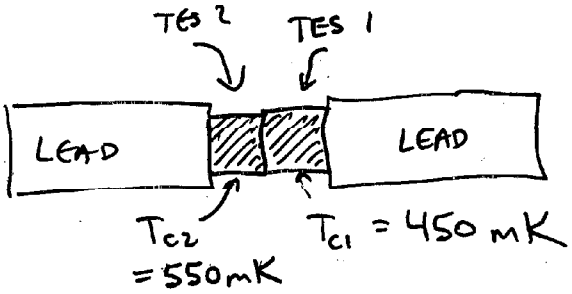

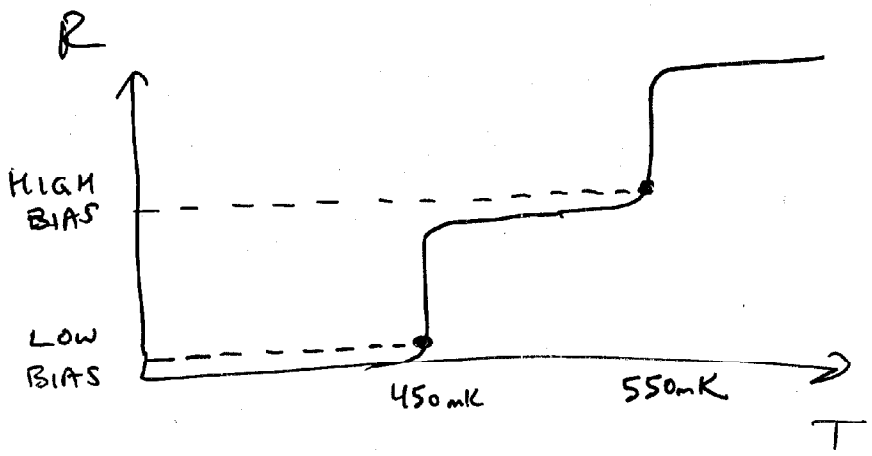

BY CHOOSING EITHER THE LOW OR HIGH BIAS POINT, THE ARRAY CAN BE OPERATED AT TWO POWER LOAD/NEP TRADEOFF POINTS.

A RISK REDUCTION MEASURE

James N. Caldwell

NASA/GSFC

Detector Development Meeting

Jan 21, 1999

- Assumptions:
  - Each Detector Array has its own Front end Electronics
  - Instrument configurable to Photometer OR Spectrometer
  - Electronics design is same for FTS or Photometer arrays
  - Simultaneous sampling of Photometer arrays
  - Buffer Amplifier in the TES system is located in the Warm Electronics box.
  - Chopper Motion and FTS Scan Mechanism synchronized with DRCU/SPU

- Physical properties are being determined
  - Warm Electronics Box
    - Footprint; Height . . . . . TBD
    - Mass . . . . . TBD
    - Power . . . . . TBD
      - Input . . . . . TBD
      - Dissipation . . . . . TBD
  - Detectors and Cold Electronics
    - Preliminary Wire Count 1010
    - Power Dissipation at 4K, 1.8K and 0.3K are in agreement with the specification

ID	Description	No. of Cond	No. of Shields	R (ohm)	C (F)	L (H)	I (A)	Duty Cycle	Voltage	End Temp
	32 x 32 Photometric Array Signals entering from warm (300K) electronics									
1	Detector Signal	64	32							0.3 K
2	Row Bias	33	1							2K
3	Column FB	64	32							2K
4	Detector Bias	64	32							0.3K
	Subtotal	225	97							
	24 x 24 Photometric Array Signals entering from warm (300K) electronics									
5	Detector Signal	48	24							0.3 K
6	Row Bias	25	1							2K
7	Column FB	48	24							2K
8	Detector Bias	48	24							0.3K
	Subtotal	169	73							
	16 x16 Photometric Array Signals entering from warm (300K) electronics									
9	Detector Signal	32	16							0.3 K
10	Row Bias	17	1							2K
11	Column FB	32	16							2K
12	Detector Bias	32	16							0.3K
	Subtotal	113	49							
	Total	507	219							

TBD's

TBD's

TBD's

ID	Description	No. of Cond	No. of Shields	R (ohm)	C (F)	L (H)	I (A)	Duty Cycle	Voltage	End Temp
1	Detector Signal	32	16							0.3K
2	Row Bias	17	1							2K
3	Column FB	32	16							2K
4	Detector Bias	32	16	← TBD's →						0.3K
	Subtotal	113	49							
	12 x 12 FTS Array Signals entering from warm (300K) electronics									
5	Detector Signal	24	12							0.3 K
6	Row Bias	13	1							2K
7	Column FB	24	12							2K
8	Detector Bias	24	12	← TBD's →						0.3K
	Subtotal	85	37							
	Total	198	86							
	Grand Total	705	305							
	Total Wires & Shield	1010								

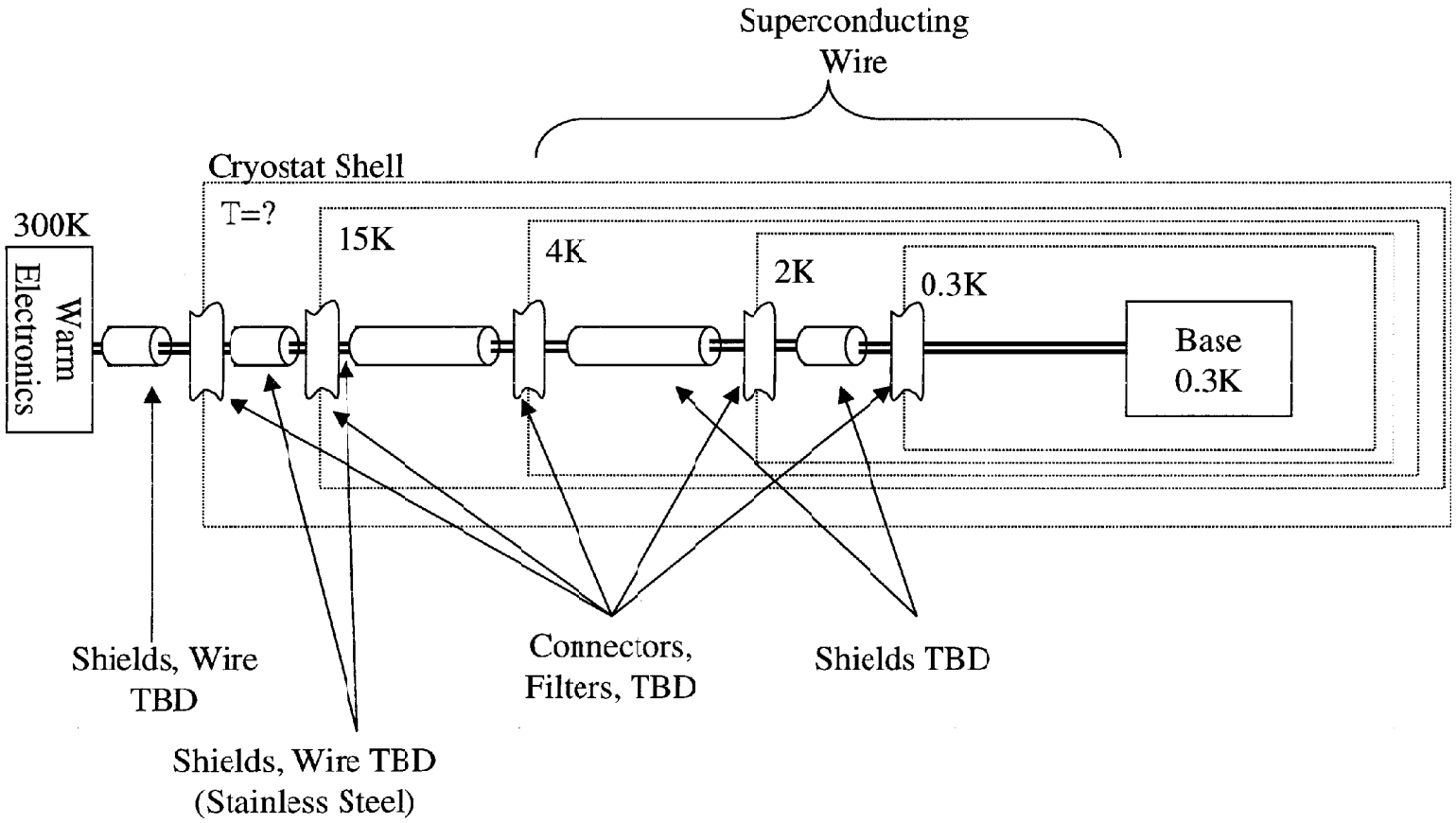
Superconducting
Wire
Cryostat Shell
T=?
300K
Warm
Electronics
15K
4K
2K
0.3K
Base
0.3K
Shields, Wire
TBD
Shields, Wire TBD
(Stainless Steel)
Connectors,
Filters, TBD
Shields TBD

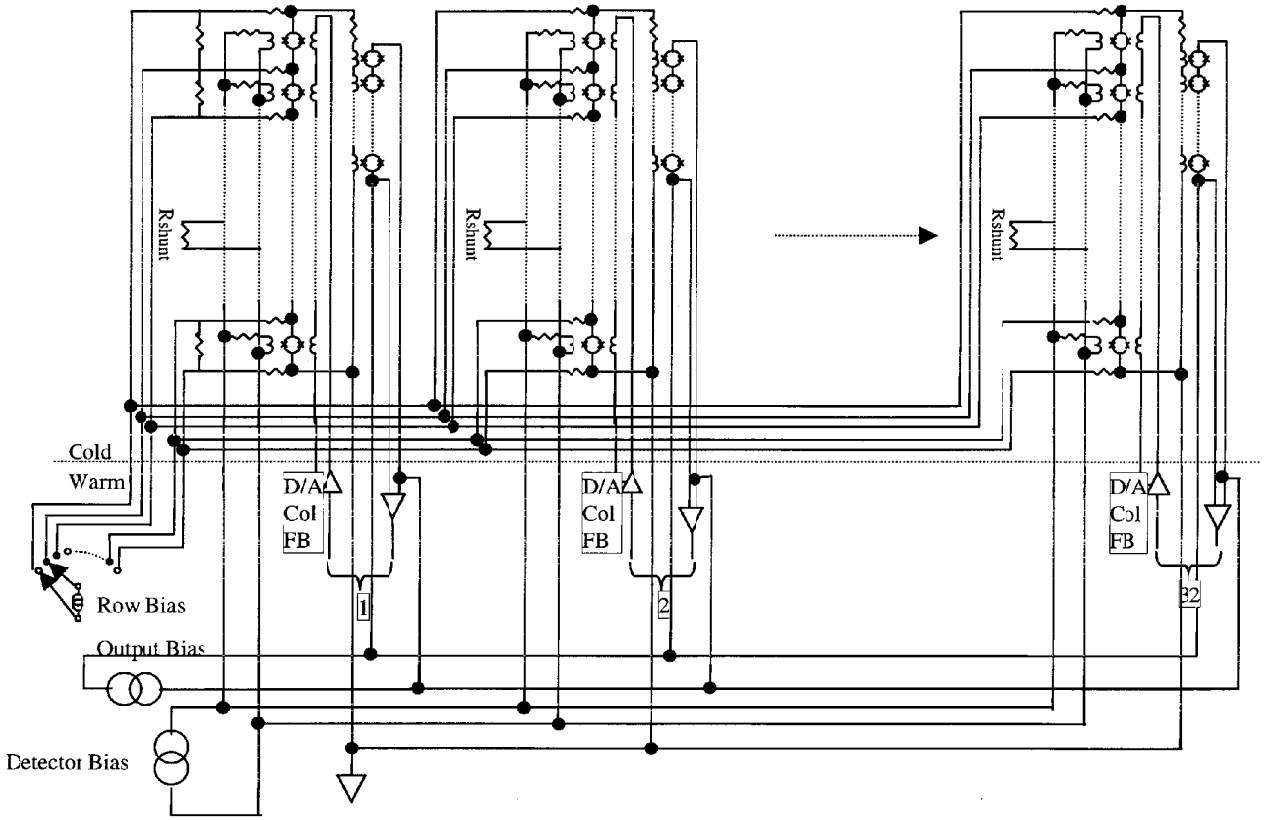
Rshunt
Rshunt
Rshunt
Cold
Warm
D/A
Col
FB
D/A
Col
FB
D/A
Col
FB
1
2
32
Row Bias
Output Bias
Detector Bias

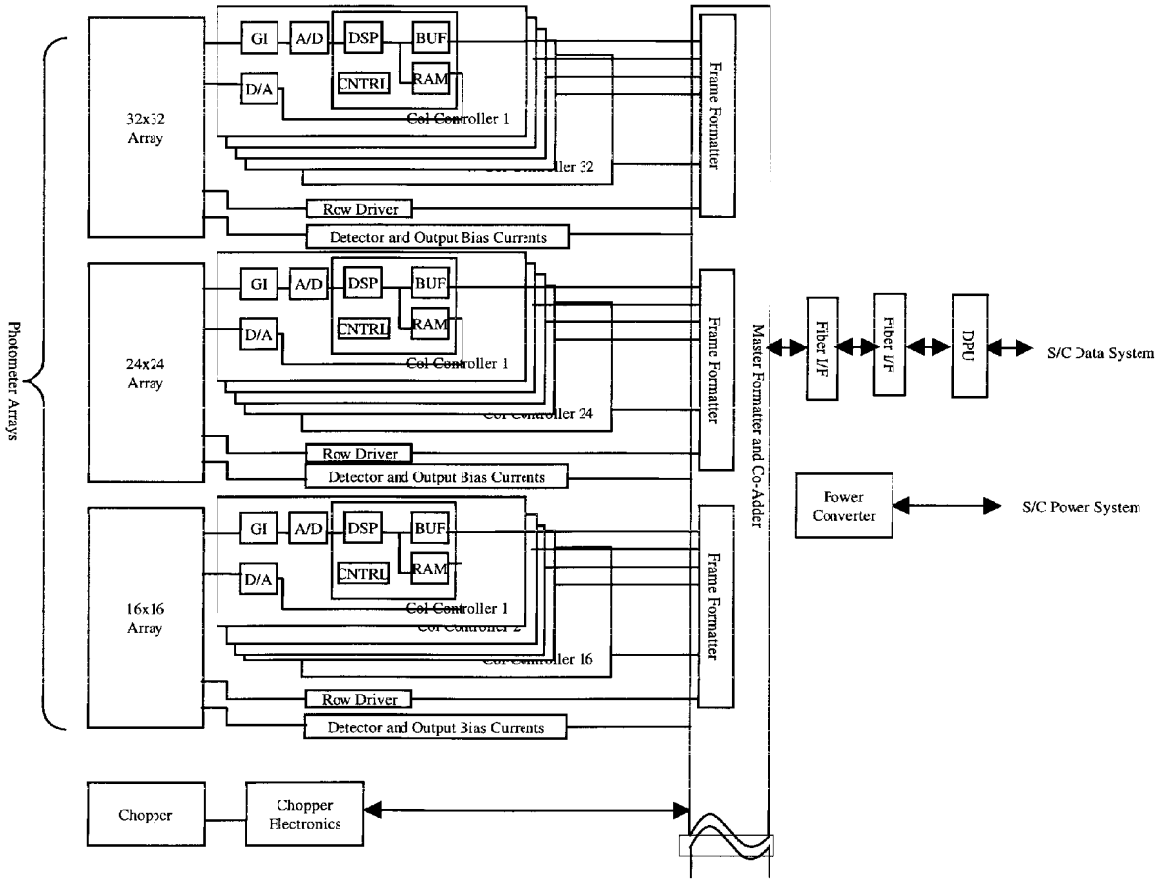
Photometer Arrays
32x32 Array
24x24 Array
16x16 Array
GI
A/D
DSP
BUF
D/A
CNTRL
RAM
Col Controller 1
Col Controller 32
Col Controller 24
Col Controller 16
Row Driver
Detector and Output Bias Currents
Frame Formatter
Master Formatter and Co-Adder
Fiber I/F
Fiber I/F
DPU
S/C Data System
Fower Converter
S/C Power System
Chopper
Chopper Hectronics

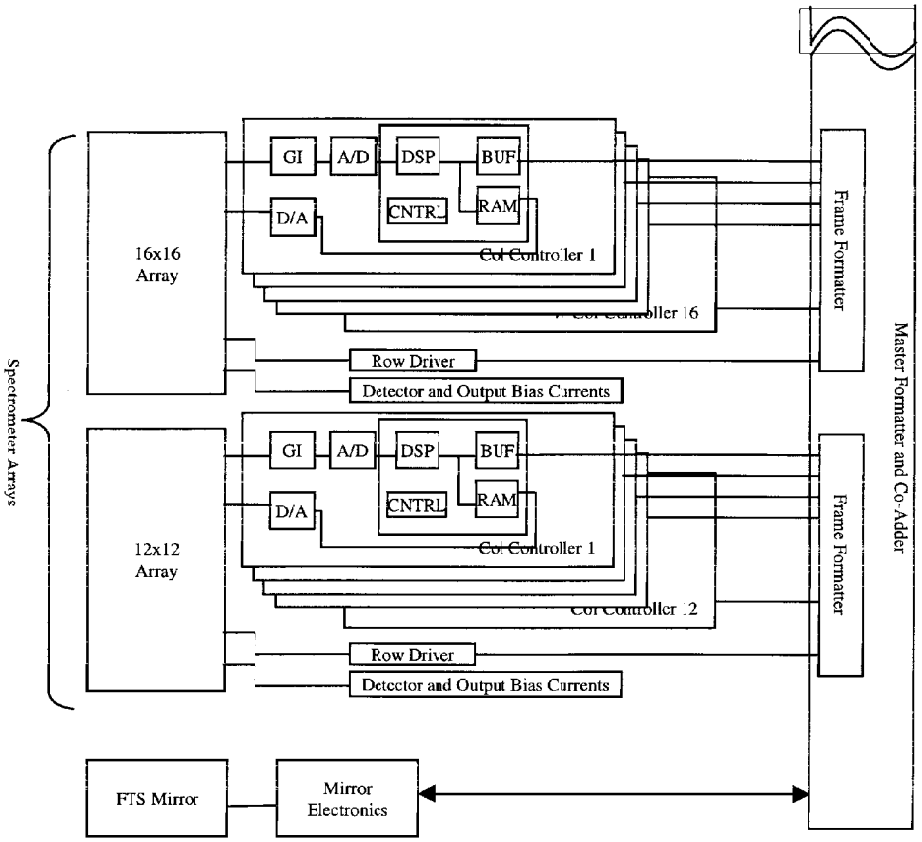
Spectrometer Arrays
16x16
Array
GI
A/D
DSP
BUF
D/A
CNTR
RAM
Col Controller 1
Col Controller 16
Row Driver
Detector and Output Bias Currents
12x12
Array
GI
A/D
DSP
BUF
D/A
CNTRL
RAM
Col Controller 1
Col Controller 12
Row Driver
Detector and Output Bias Currents
Frame Formatter
Frame Formatter
Master Formatter and Co-Adder
FTS Mirror
Mirror
Electronics

Sample Rate 5 - 50 Hz

Memory data size DPU

With Co-adding in DPU

< 3 Mbytes in DPU and < 20 Kbytes in Master Formatter

With Co-adding in Master Formatter

< 20 Kbytes in DPU and < 3 Mbytes in Master Formatter

Data Throughput < 40 Kbps and Mode dependant

ID	Task Name	Start	Finish
1	**Design & Fab of SPIRE Prototype H/W**	**Thu 10/12/98**	**Wed 10/03/99**
2	Fab Dummy Bus Bars	Thu 10/12/98	Thu 10/12/98
3	Fab Ceramic Mount Parts	Thu 10/12/98	Thu 04/02/99
4	PITA Jig Design	Thu 10/12/98	Thu 10/12/98
5	Folding Jig Match Drilling	Thu 10/12/98	Mon 18/01/99
6	Design Kevlar Glue Jig	Fri 11/12/98	Thu 24/12/98
7	DWGS Kevlar Glue Jig	Mon 04/01/99	Wed 06/01/99
8	"C" Jig Design	Thu 07/01/99	Wed 13/01/99
9	Fab Kevlar Glue Jig	Thu 07/01/99	Wed 03/02/99
10	"C" Jig Dwgs	Thu 14/01/99	Tue 19/01/99
11	Fab "C" Jig	Wed 20/01/99	Tue 16/02/99
12	PITA Jig Dwgs	Wed 20/01/99	Fri 22/01/99
13	Design Bridge Chip Glue Jig	Mon 25/01/99	Tue 02/02/99
14	Bridge Chip Glue Jig Dwgs	Wed 03/02/99	Wed 10/02/99
15	Fab Bridge Chip & PITA Jigs	Thu 11/02/99	Wed 10/03/99
16			
17	**Mechanical Prototype Testing**	**Thu 10/12/98**	**Tue 16/03/99**
18	Select Suspension Motion Sensor	Thu 10/12/98	Wed 16/12/98
19	Purchase / Fab Sensor	Thu 17/12/98	Thu 07/01/99
20	Tryout sensor	Fri 08/01/99	Thu 21/01/99
21	Assemble Mount & Sensor	Fri 05/02/99	Thu 18/02/99
22	Mount Mechanical / Cold Testing	Fri 19/02/99	Thu 11/03/99
23	Stiffness test	Fri 12/03/99	Tue 16/03/99
24			
25			

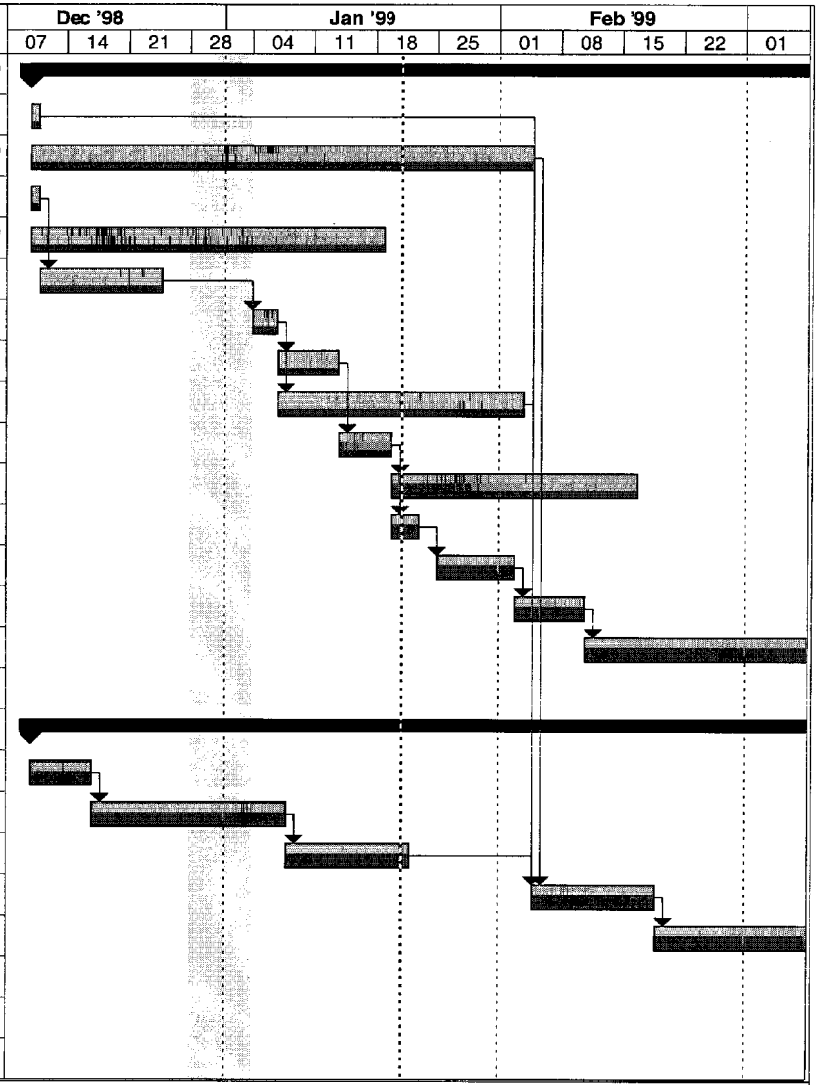

ID	Task Name	Start	Finish
26	**NIST PUD Processing**	**Mon 11/01/99**	**Fri 30/07/99**
27	**Planar PUD Fab**	**Mon 11/01/99**	**Mon 08/02/99**
28	Contact/Absorber/Lead/SiO2 Mask/Metali	Mon 11/01/99	Mon 18/01/99
29	Micromachining	Tue 19/01/99	Fri 29/01/99
30	TES/Thermal Mass Deposition	Mon 01/02/99	Mon 08/02/99
31	Develop Wafer Thining Step	Wed 27/01/99	Fri 05/02/99
32	Test Planar PUD's	Mon 08/02/99	Thu 11/03/99
33	**Foldable PUD Fab**	**Mon 08/02/99**	**Thu 11/03/99**
34	Contact/Absorber/Lead/SiO2 Mask/Metali	Mon 08/02/99	Mon 15/02/99
35	Micromachining	Tue 16/02/99	Tue 23/02/99
36	First Laser Dice	Wed 24/02/99	Wed 03/03/99
37	TES/Thermal Mass Deposition	Thu 04/03/99	Thu 11/03/99
38	Test Foldable PUD's	Fri 12/03/99	Fri 19/03/99
39	Ship PUD's to GSFC	Mon 22/03/99	Fri 30/04/99
40	Laser Trim and Fold	Mon 22/03/99	Wed 05/05/99
41	Fab Backup 1x8 PUD'd	Thu 06/05/99	Fri 30/07/99
42			
43	**GSFC PUD Processing**	**Mon 04/01/99**	**Fri 07/05/99**
44	Mask Fabrication: 2 layers	Wed 06/01/99	Fri 15/01/99
45	Mask Fabrication: Remaining layers	Mon 18/01/99	Wed 27/01/99
46	TES Deposit on wafer 1 (Iteration 1)	Mon 01/02/99	Wed 10/02/99
47	Test Wafer 1 (He3, Tc, Jc)	Mon 15/02/99	Fri 19/02/99
48	TES Deposit on wafer 2 (Iteration 2)	Mon 22/02/99	Mon 08/03/99
49	Test Wafer 2 (He3, Tc, Jc)	Tue 09/03/99	Mon 15/03/99
50	TES Deposit on wafer 3 (Iteration 3)	Tue 16/03/99	Tue 30/03/99

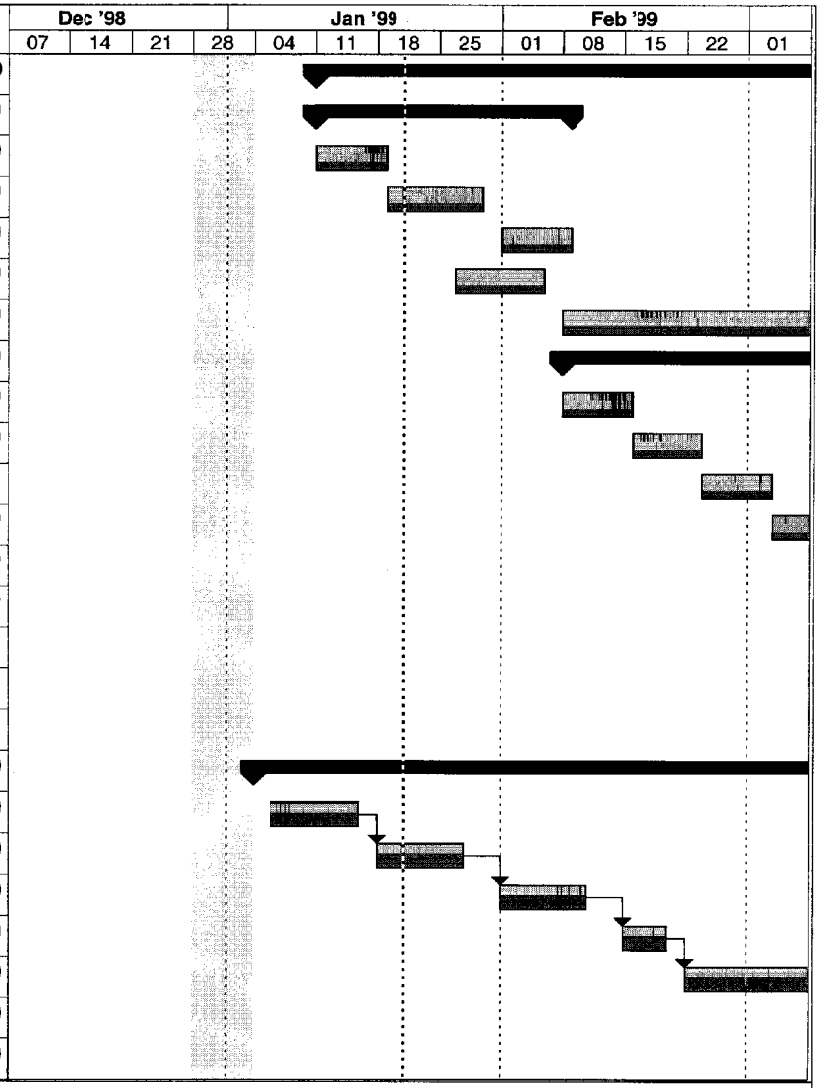

ID	Task Name	Start	Finish
51	Test Wafer 3 (He3, Tc, Jc)	Wed 31/03/99	Tue 06/04/99
52	TES Deposit on wafer 4	Wed 07/04/99	Mon 19/04/99
53	Test Wafer 4 (He3, Tc, Jc)	Tue 20/04/99	Mon 26/04/99
54	TES Deposit on wafer 5 to ?	Tue 27/04/99	Fri 07/05/99
55	Silicon Bridge Design, Mask Fabrication	Mon 04/01/99	Mon 01/02/99
56	Silicon Bridge Fabrication (IRAC reject wafers to start)	Tue 02/02/99	Wed 10/03/99
57	Silicon Bridge Testing (Tc & Critical Curent)	Thu 11/03/99	Wed 17/03/99
58	Silicon Bridge Fabrication (IRAC reject wafers to start)	Thu 18/03/99	Wed 21/04/99
59	Silicon Bridge Continuity Test	Thu 22/04/99	Wed 28/04/99
60	Grainy Aluminum Development	Mon 11/01/99	Mon 08/02/99
61	Grainy Aluminum Testing	Mon 18/01/99	Mon 15/02/99
62			
63	**Electrical and S/W Testing**	**Thu 10/12/98**	**Thu 15/07/99**
64	Mk 1.8 I & T w. SQUID simulator	Tue 05/01/99	Wed 13/01/99
65	Mk 1.8 Delivery to NIST	Wed 13/01/99	Wed 13/01/99
66	Run 1.8 with SQUIDS	Thu 14/01/99	Wed 20/01/99
67	Fab Single Pixel TES	Mon 04/01/99	Fri 08/01/99
68	Single Pixel Testing	Mon 11/01/99	Fri 15/01/99
69	Run 1.8 w single pixel TES's	Thu 21/01/99	Wed 27/01/99
70	Run 1.8 w. planer 1x8's	Thu 18/02/99	Tue 09/03/99
71	Mk 1.8 to GSFC	Wed 10/03/99	Tue 16/03/99
72	Mk 2 delivery @ GSFC, 2 units	Thu 14/01/99	Thu 04/03/99
73	NELL S/W to drive Mk 1.8	Thu 10/12/98	Mon 04/01/99
74	NEMO S/W to drive Mk 2 (functional)	Tue 05/01/99	Mon 01/03/99
75	NEMO S/W to drive Mk 2 (upgrade 1)	Tue 02/03/99	Tue 01/06/99

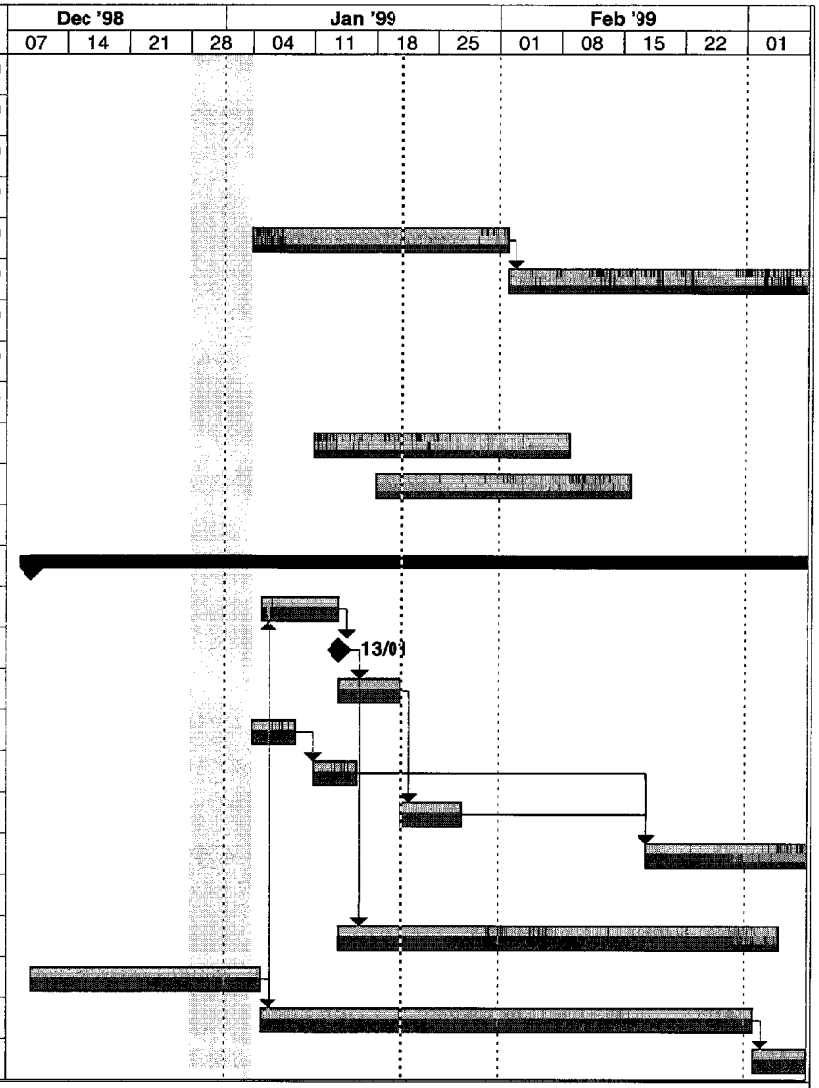

SPIRE Detectors
TES/Popup Option

- Mechanical and Electronics — Harvey Moseley
- Bolometer Fabrication — Kent Irwin
- Electronics System Design — Jim Caldwell
- Plans and Schedule — Juan Roman

SILICON "POPUP" BOLOMETER

0.5 fλ OPTION

- 3-DIMENSIONAL MICROMACHINED SILICON STRUCTURES

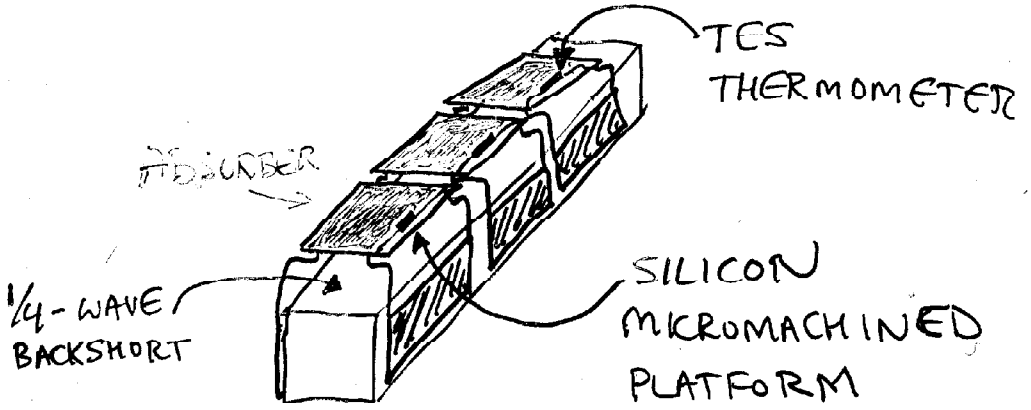

Silicon Popup Detectors

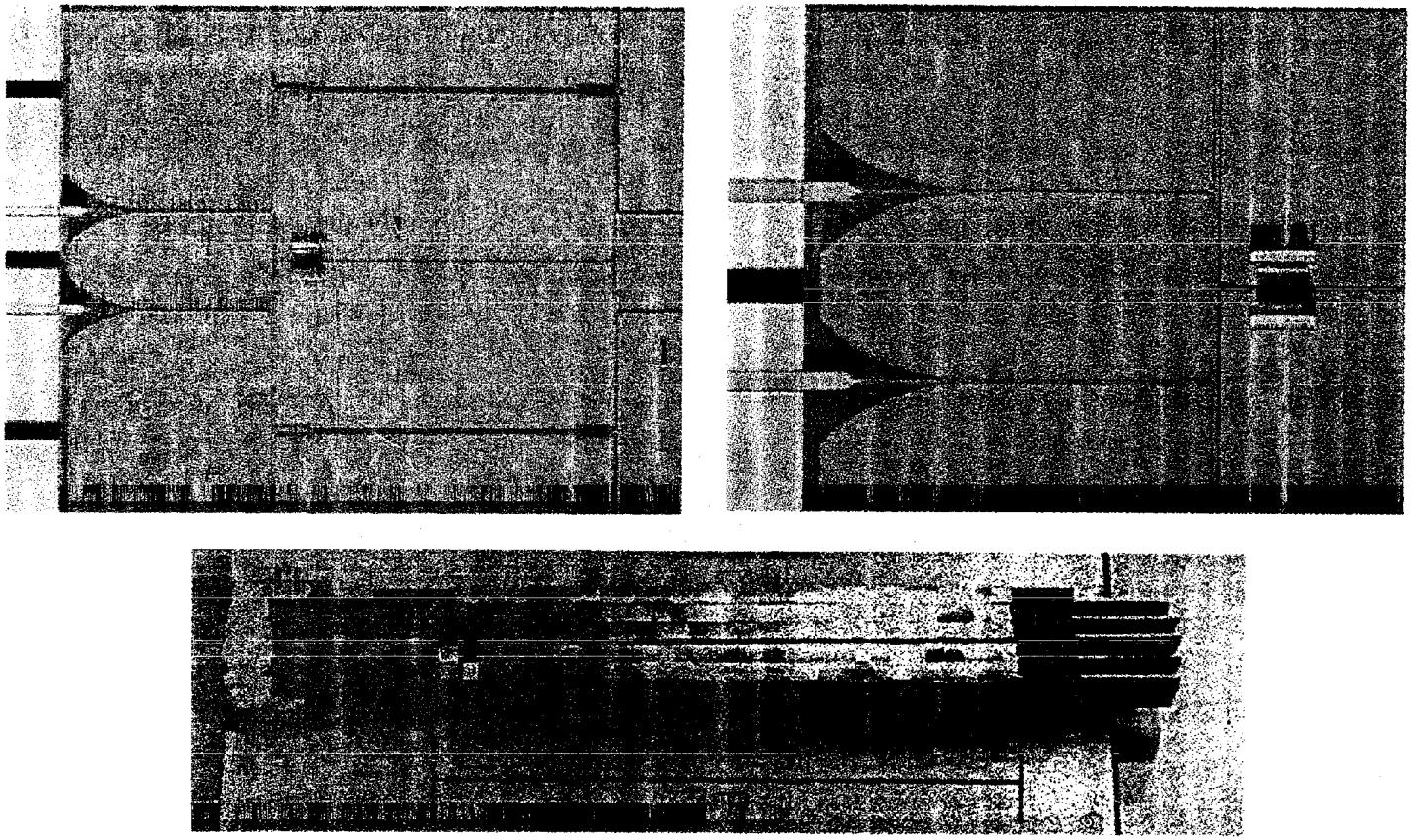

A 5 x 32 array of 1 mm x 1 mm popup structure

NIST Boulder

Superconducting Transition-Edge Sensor (TES) Thermometer

Advantages of TES Thermometer

- High Sensitivity (α is 10-100 x higher than thermistors. Allows absorber heat capacity 10-100 x bigger)
- Uses low power SQUID amplifiers instead of FETs
- Low Impedance (less microphonics)

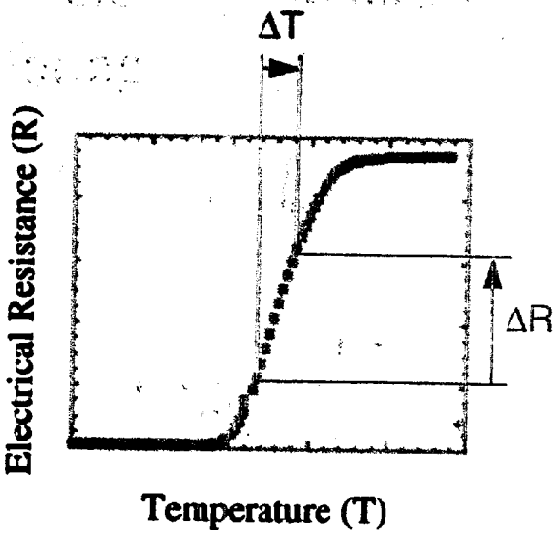

Superconducting Quantum Interference Device (SQUID) Current Amplifier

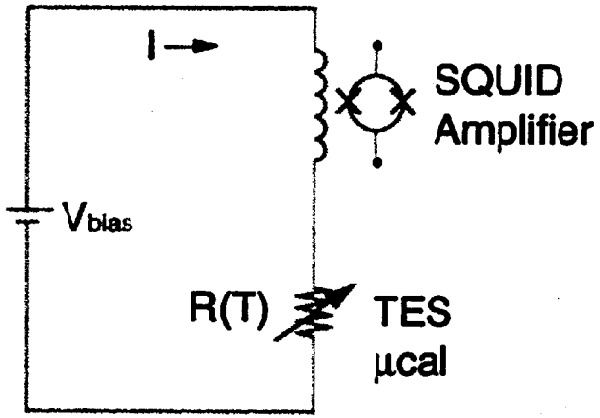

Advantages of SQUID readout

- Low Power (SQUID ~ 1 nW, FET~ 1 mW)
- Low Temperature (SQUID < 100 mK, JFET ~ 77K)
- Low Noise (Noise T: SQUID << 100 mK, FET ~ 1 K)
- Low Impedance (better microphonics)

NIST Microcalorimeter EDS system

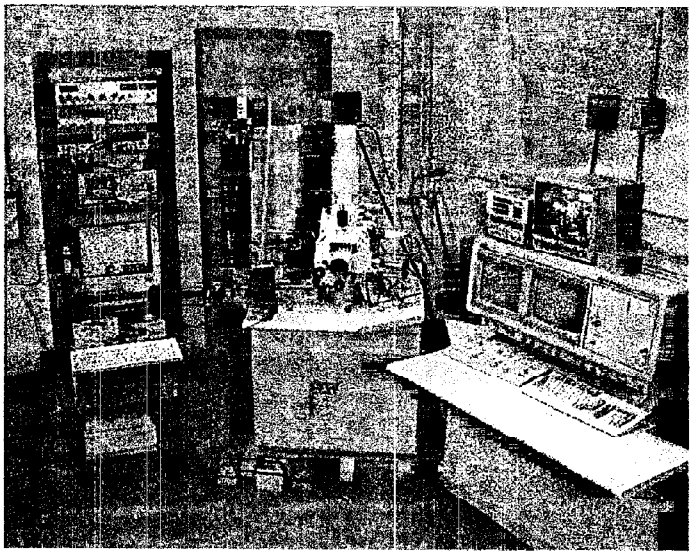

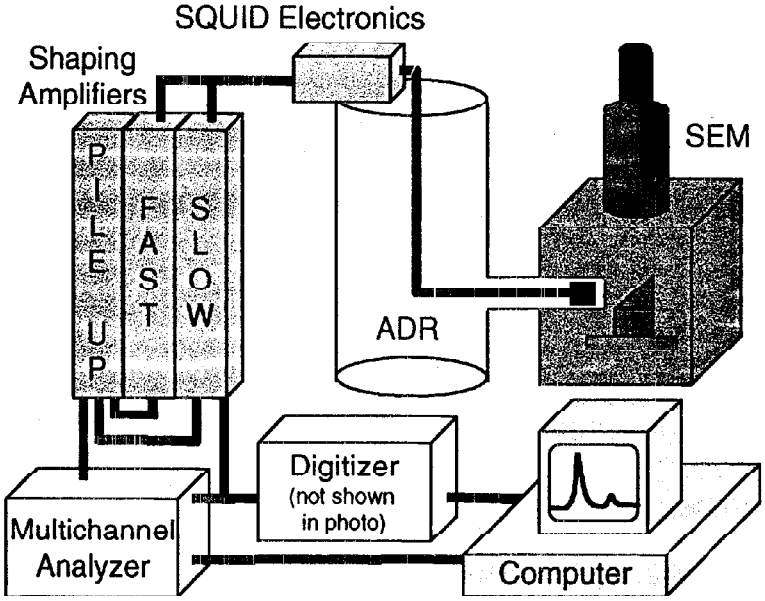

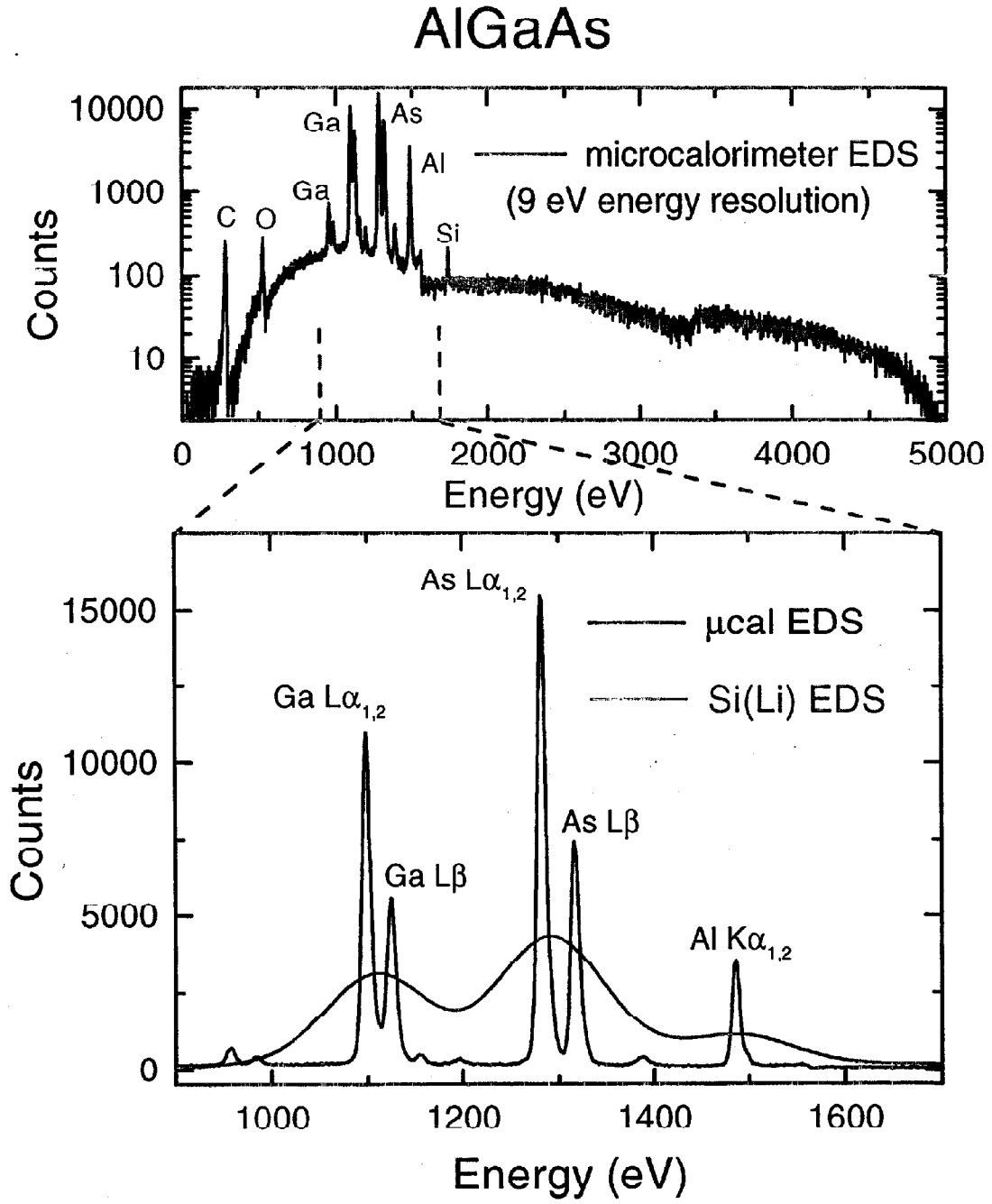
AlGaAs
10000
1000
100
10
Counts
C
O
Ga
Ga
As
Al
Si
microcalorimeter EDS
(9 eV energy resolution)
0
1000
2000
3000
4000
5000
Energy (eV)
15000
10000
5000
0
Counts
As Lα1,2
Ga Lα1,2
Ga Lβ
As Lβ
Al Kα1,2
μcal EDS
Si(Li) EDS
1000
1200
1400
1600
Energy (eV)

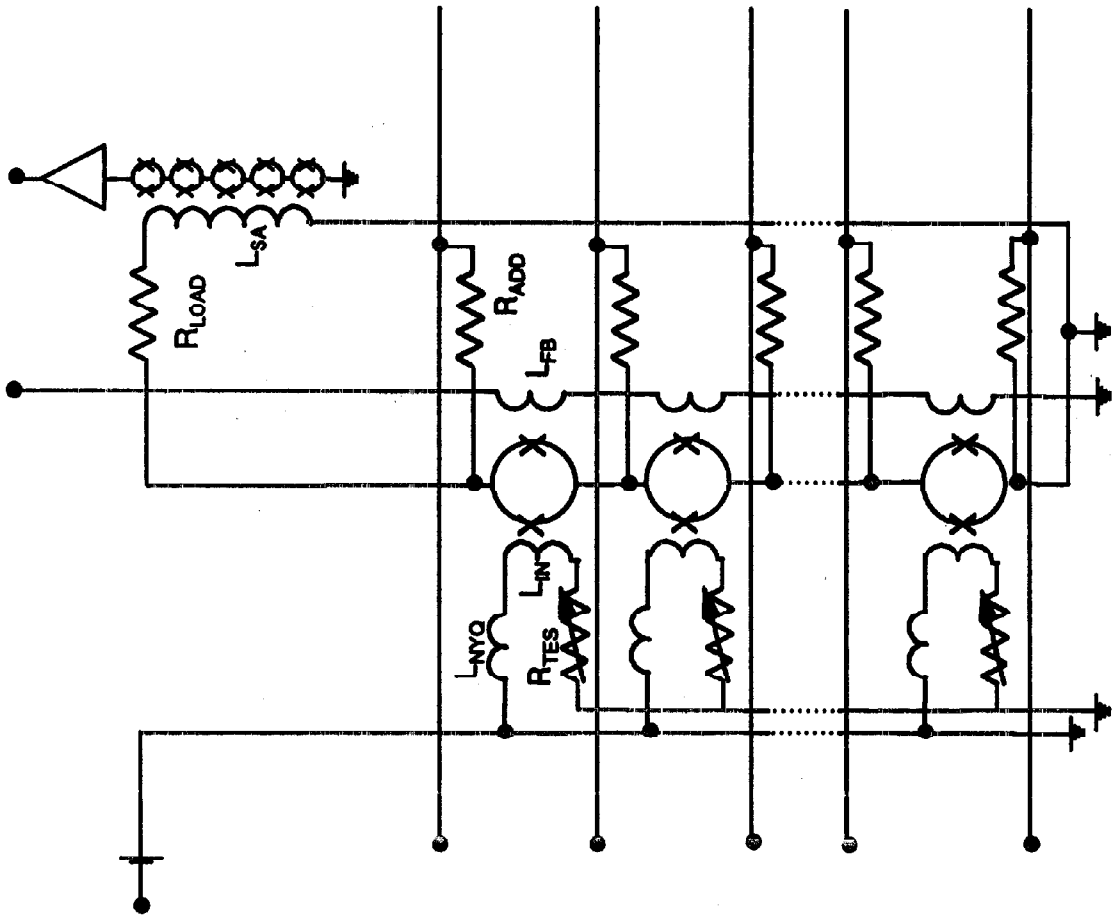
R_{LOAD}
L_{SA}
R_{ADD}
L_{FB}
L_{IN}
L_{NYQ}
R_{TES}

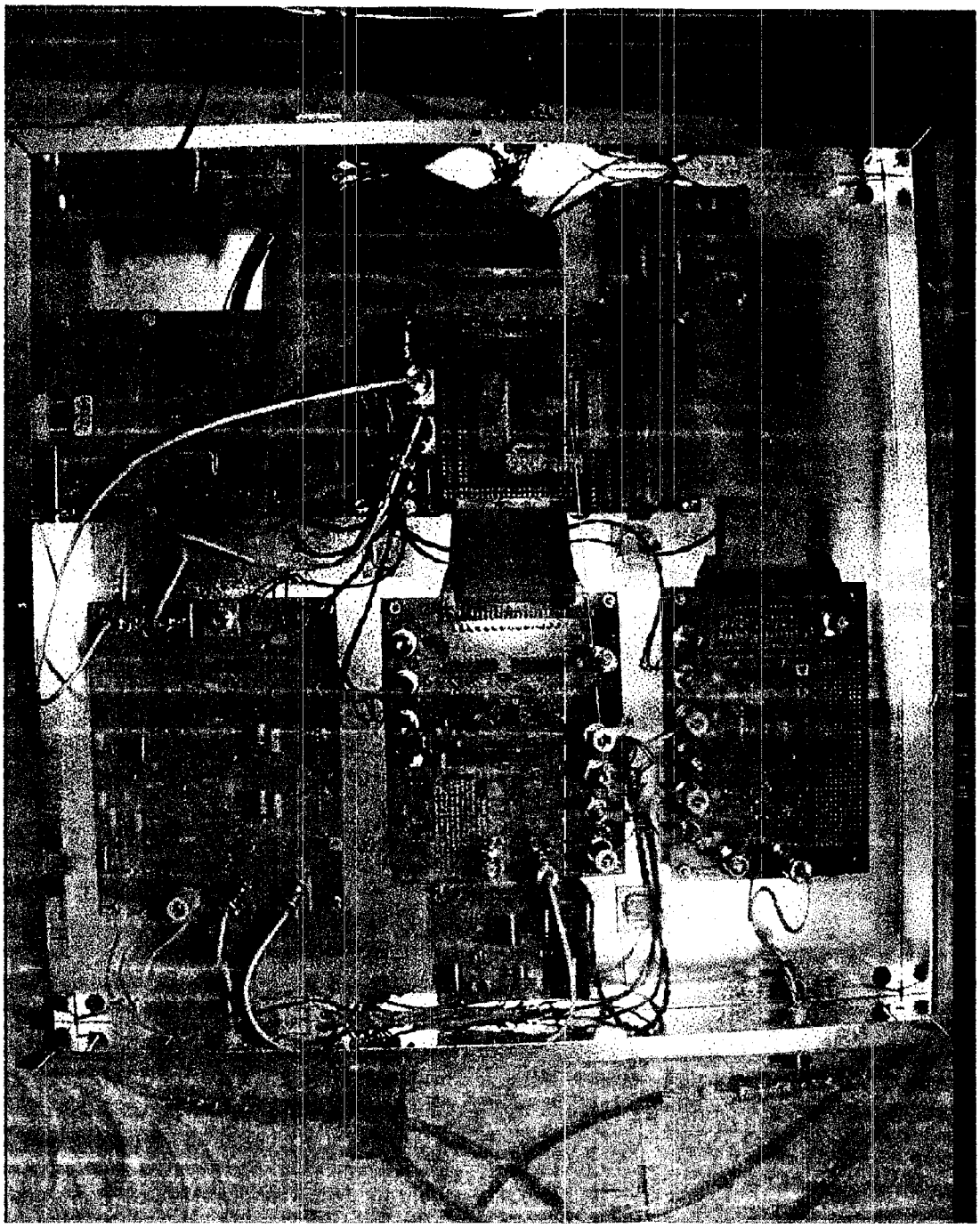

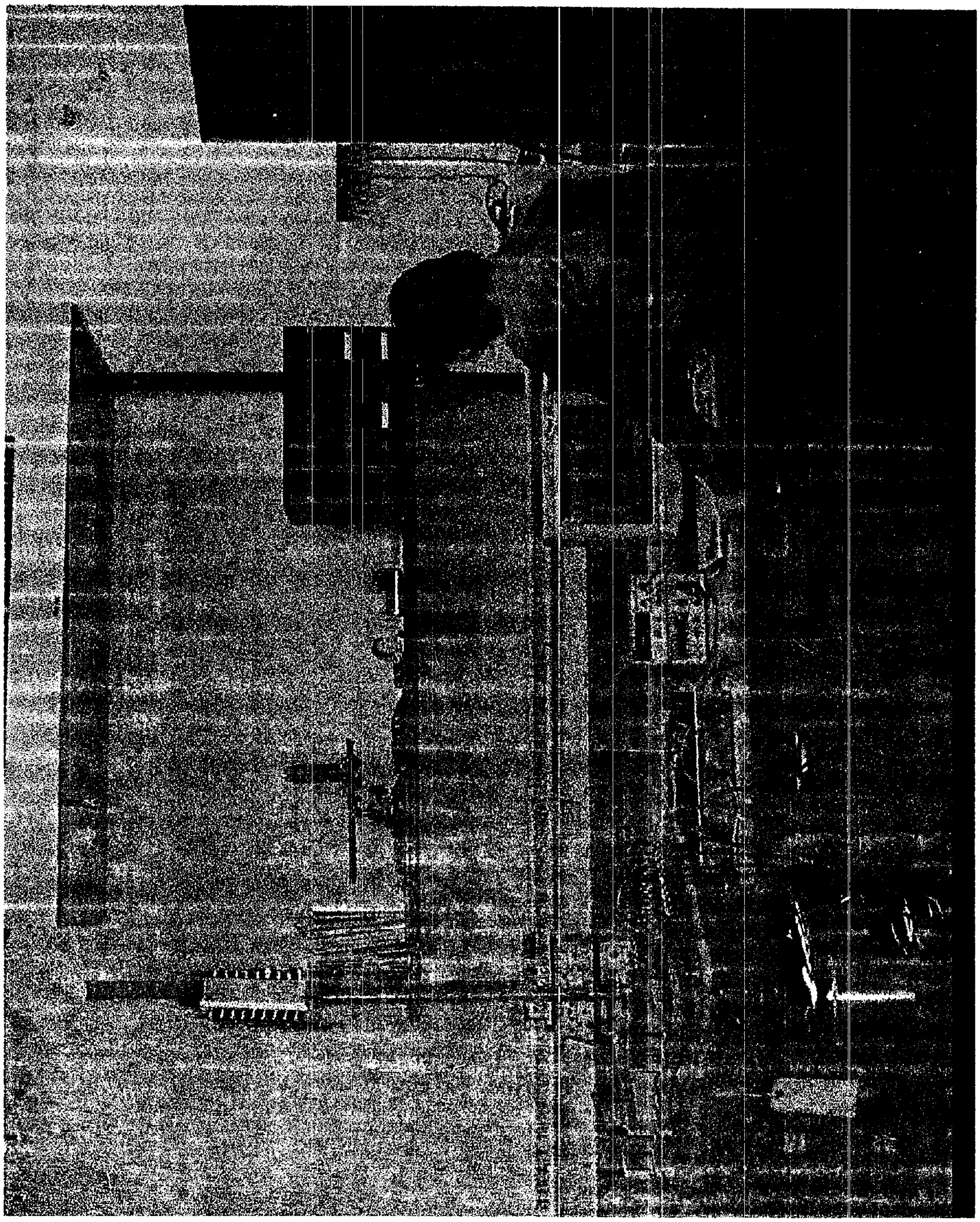

SQUID multiplexer design & layout

1 x 8 SQUID multiplexer (one column)

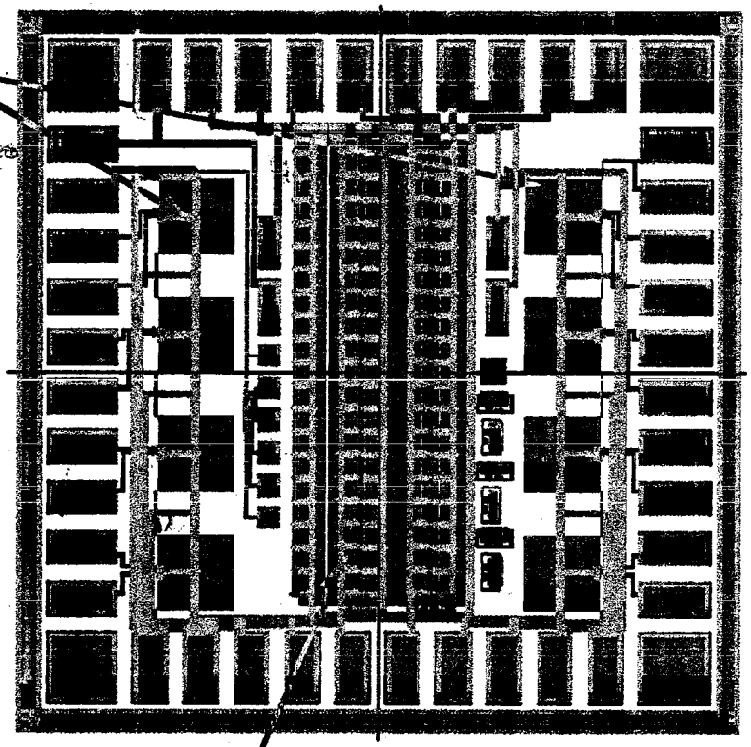

100 SQUID series array

NIST Boulder

1 x 8 Multiplexed SQUID Channels

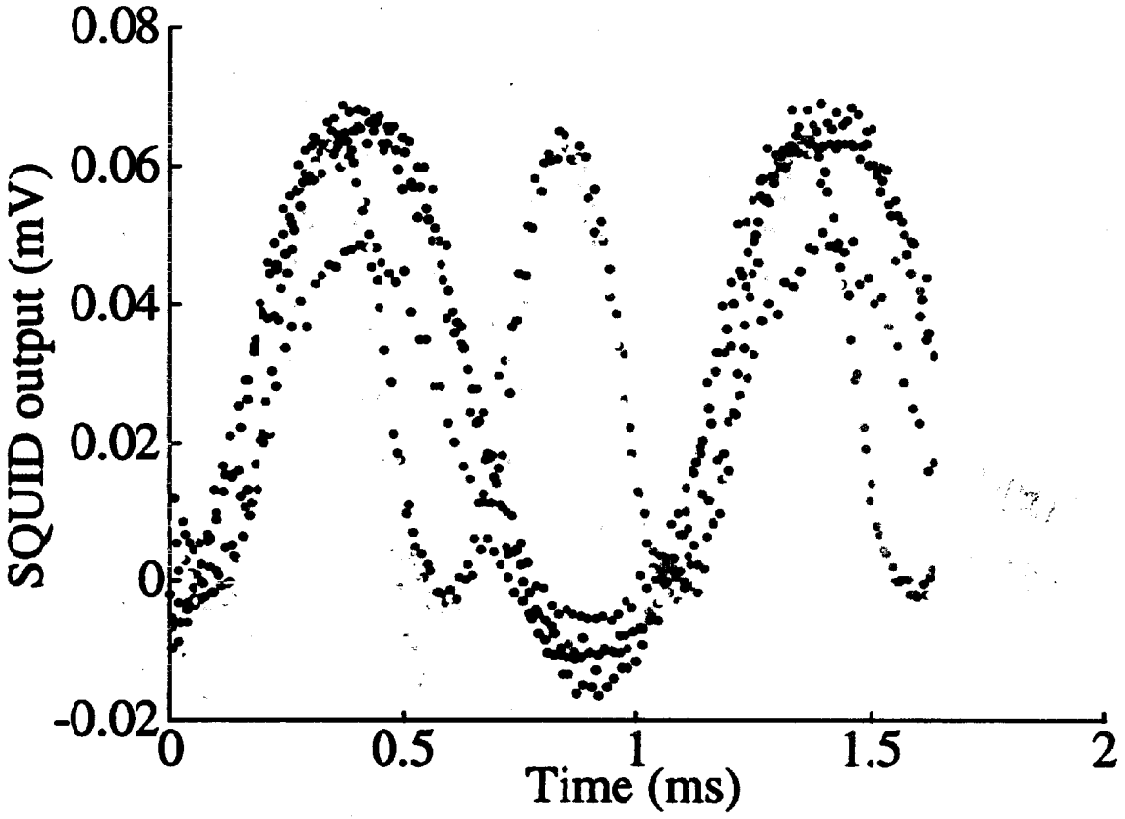

NIST Boulder

1 x 8 De-Multiplexed SQUID Channels

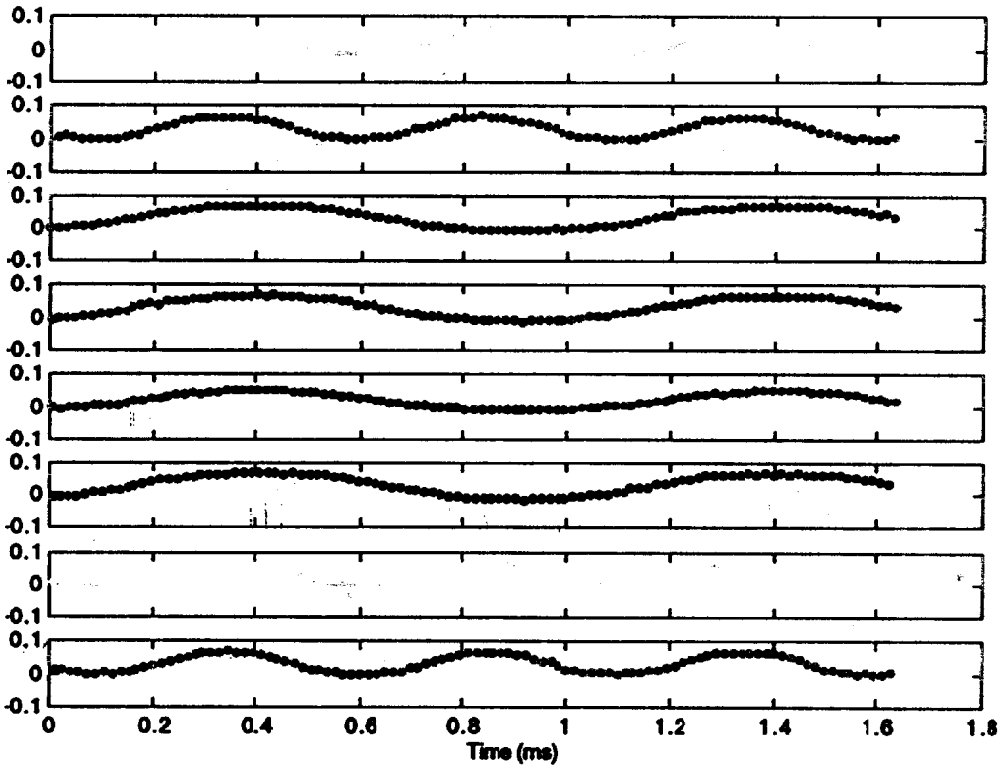

NIST Boulder

SPIRE Personnel

GSFC

- Project Manager — Juan Roman.
- Detector Fab Lead — Christine Allen
- Mechanical Lead — Mike Amato
- Electronics Lead — Dave Bergman
- Electrical Systems Lead — Jim Caldwell
- Systems Engineer Lead — George Voellmer.

Detector mechanical design

- Current design can accommodate various array sizes (25x32, 1mm pitch for example) with minor changes.
- Planning static load and cryo tests of prototype to confirm design stability.
- Design conduction thermal losses between coldest stage and slightly warmer stage of detector assembly should be less than ~10 microwatts for 12x32 array.

Detector mechanical design

- The diameter of the assembly is under 10.2 cm (4 in)
- Prototype design has detector pixel row spacing of 1 mm (currently working with +/- ~ .025 mm (.001 in) mechanical tolerance goal).
- Prototype designed to handle 50G static equivalent loads in any direction (can accommodate higher)

PUD Detectors

- **Detector mechanical design** - A good way to describe the detector subassembly is to work from the inside out which is also how the system is, in a simplified sense, assembled.

PUD Detectors

- The PUD chips are folded and epoxied to the buss bars.

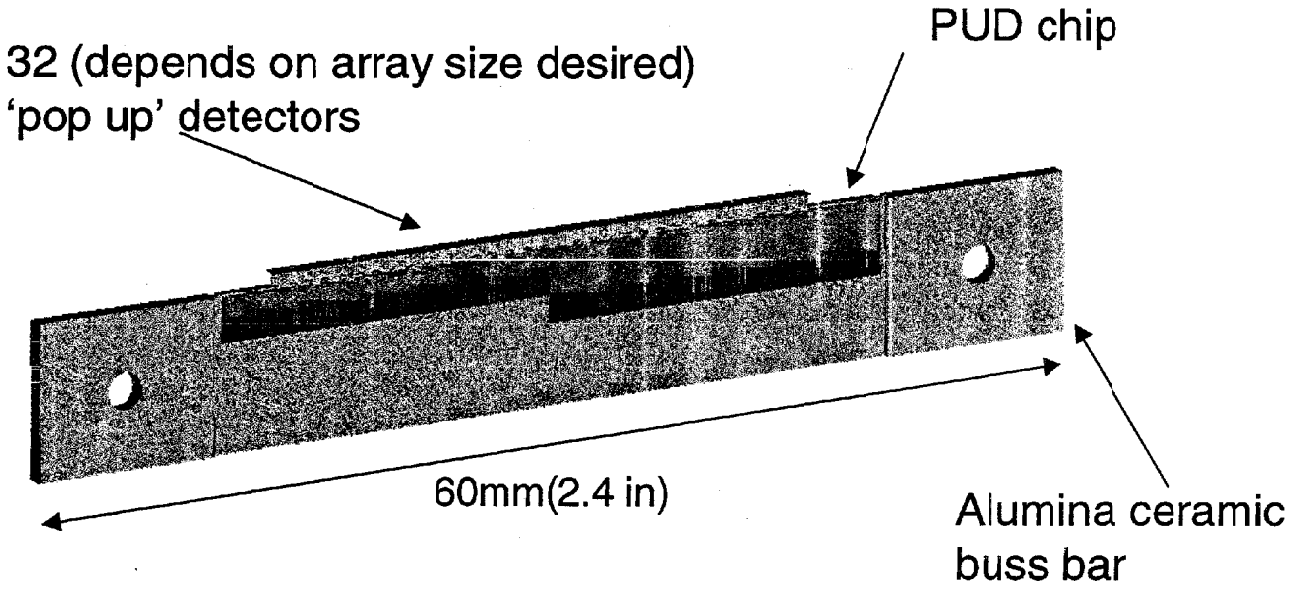

PUD Detectors

- The bridge chips are epoxied to a buss bar and a squid-mux boa

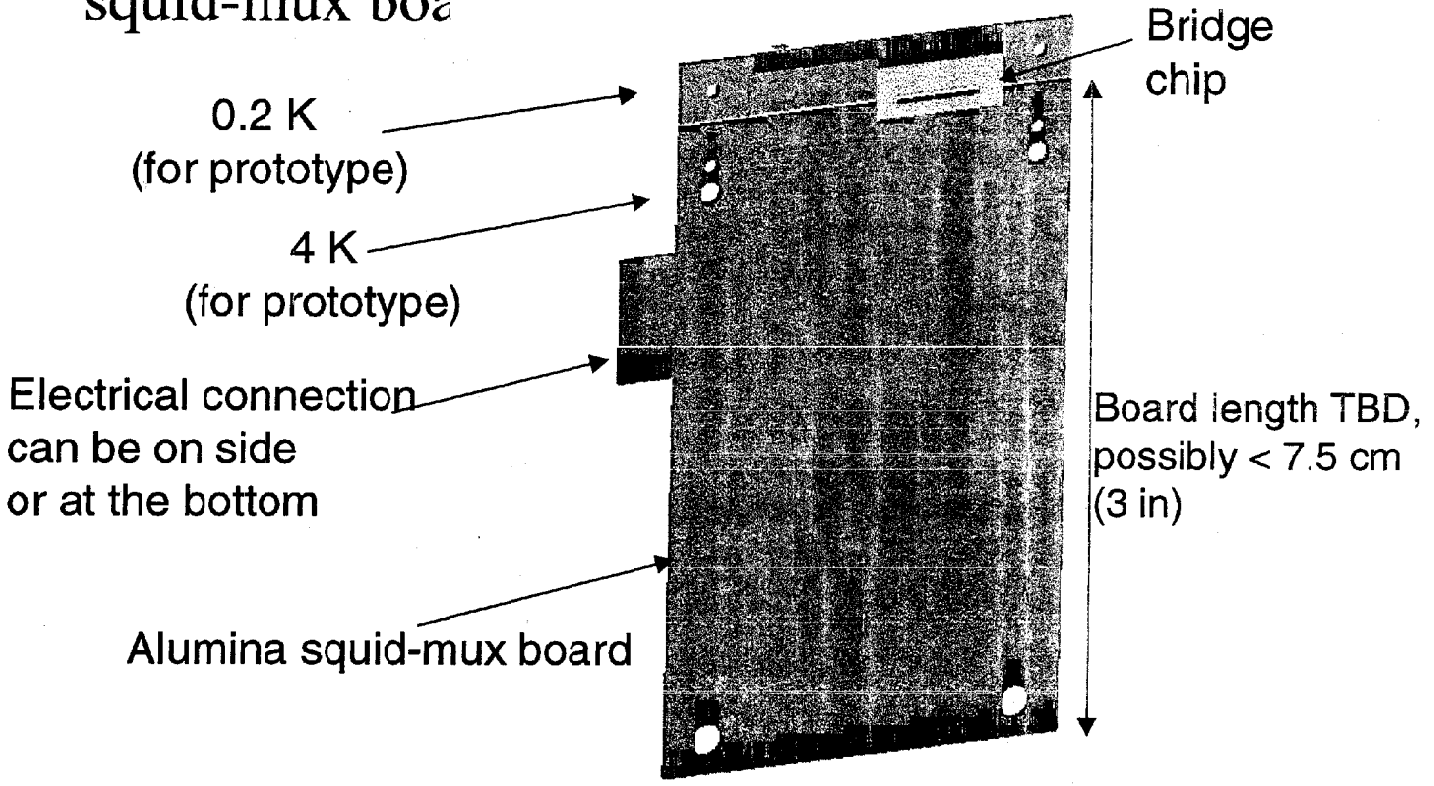

PUD Detectors

- Six buss bar/bridge chip/squid-mux board subassemblies are aligned and epoxied to each ceramic 'C' subassembly.

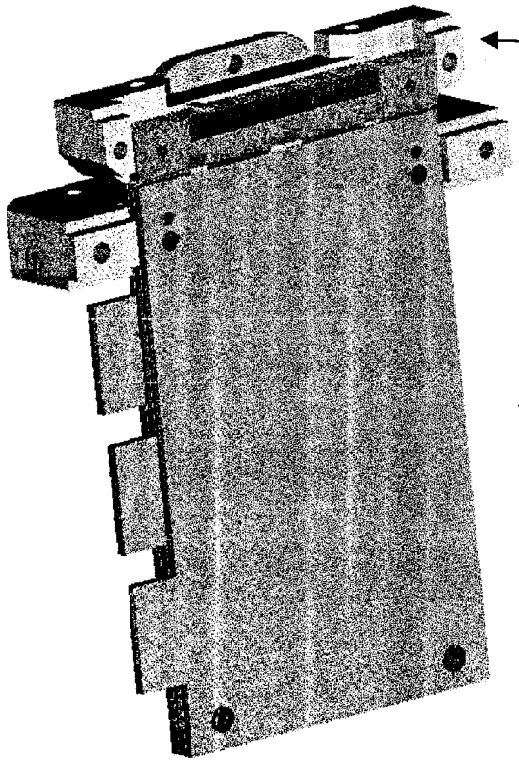

PUD Detectors

- Two of the resulting subassemblies are aligned and bolted together to form an array (12X32 shown here).

Two half detector subassemblies joined into one full detector array subassembly

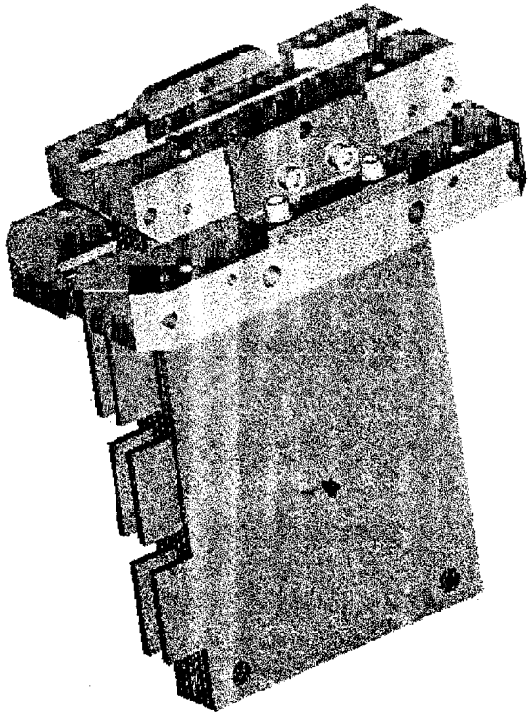

PUD Detectors

- The resulting detector assembly is lowered into and bolted to the card-cage interface structure.

Full detector array subassembly from previous picture

Card cage interface structure (ceramic, or titanium)

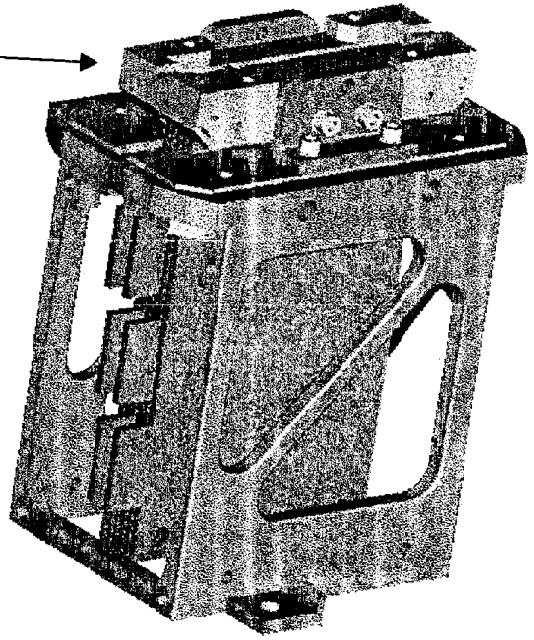

PUD Detectors

- The six kevlar straps are epoxied to end hardware and tensioned into the claw with a Belleville spring stacks on the top ends.

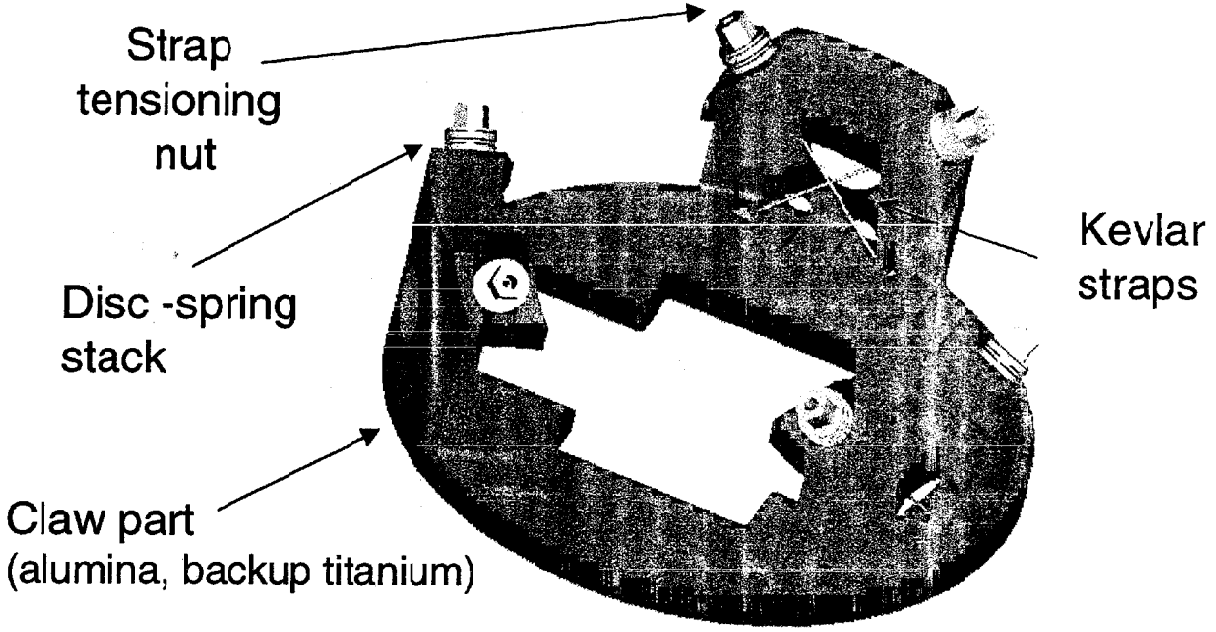

PUD Detectors

- The claw is lowered over the detector array and bolted to the lower 'C's

Suspension claw with tensioned kevlar straps

Full detector array in card cage structure

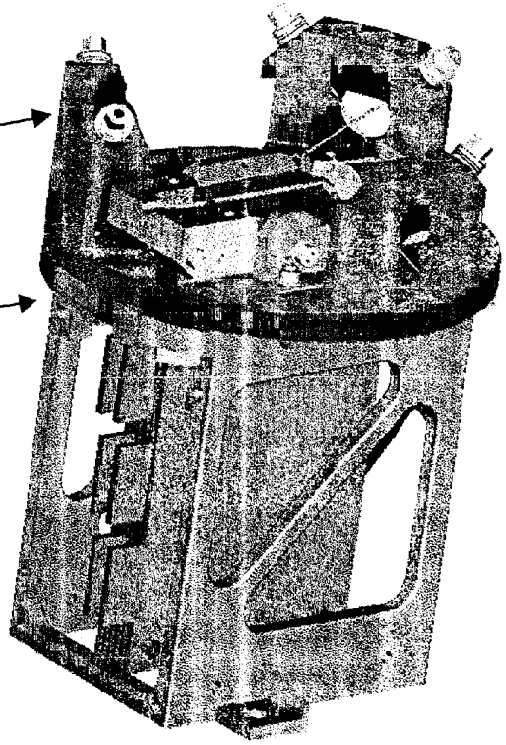

PUD Detectors

- The cold plate is lowered, twisted into position with its 'hooks' or 'grooves' at the kevlar straps, and bolted or epoxied to the upper 'C's.

Cold plate epoxied to kevlar straps at each strap set crossing point

Cold plate (alumina)

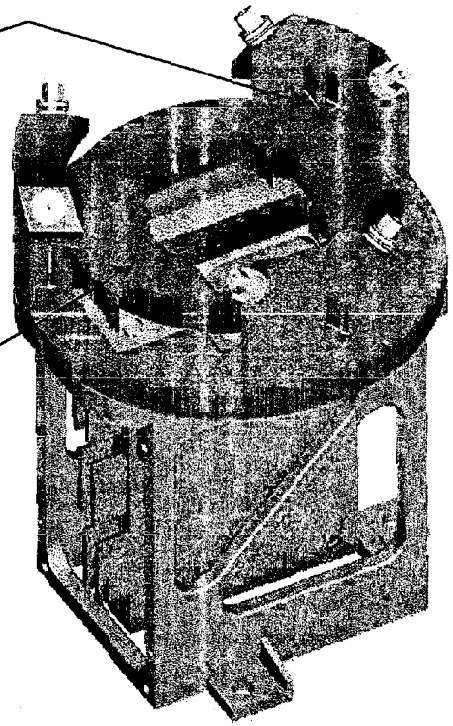

PUD Detectors

- The ADR heat strap is attached to the cold plate, electrical connections made and the suspension brackets which suspended the detectors during the assembly are removed.

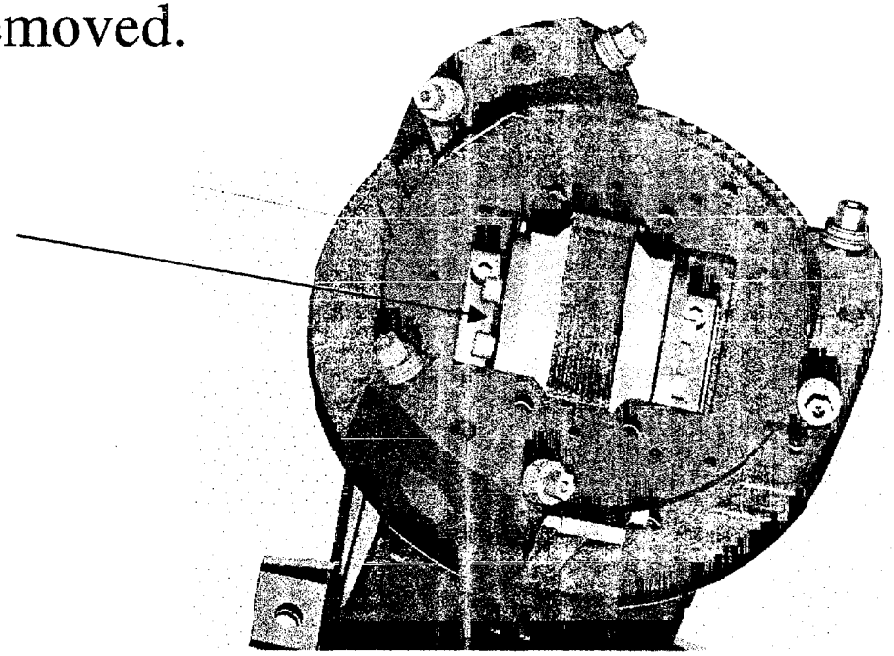

PUD Detectors

- Filter baffle

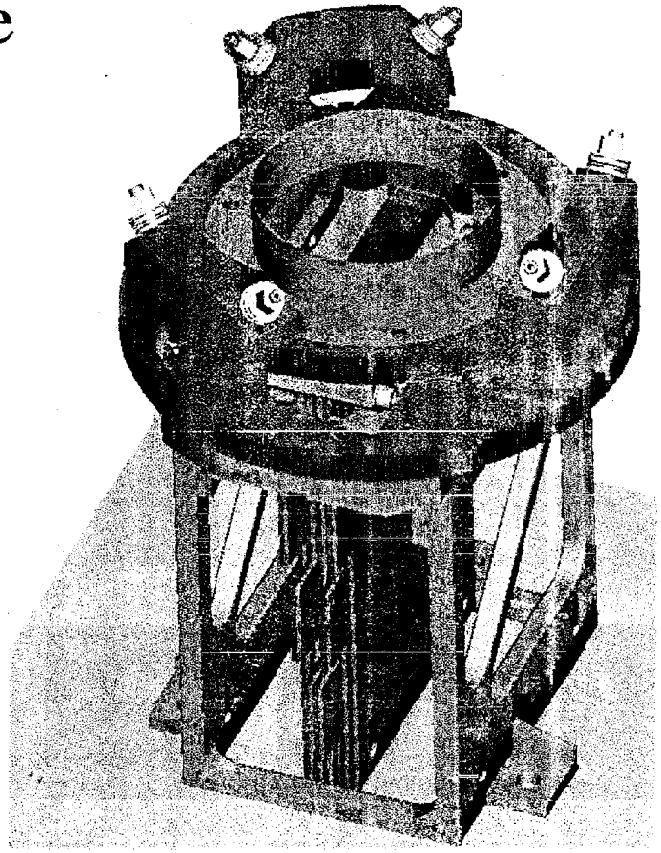

7

JPL/CALTECH ARRAYS

JAMIE BOCK

[TO FOLLOW]

8

BACUS AND THE ARRAY TEST PLAN

PETER HARGRAVE

See also Annex 2

BACUS Status & Array Test Plan

P.Hargrave, B.Maffei, F.Gannaway,
G.Gannaway, M.Griffin, P.Ade &
R.Hermoso

Design of BACUS Module

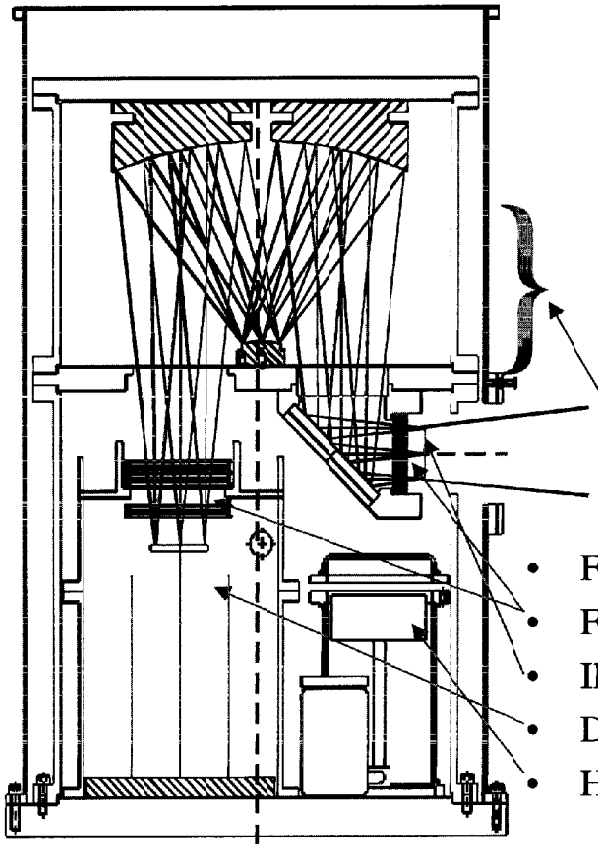

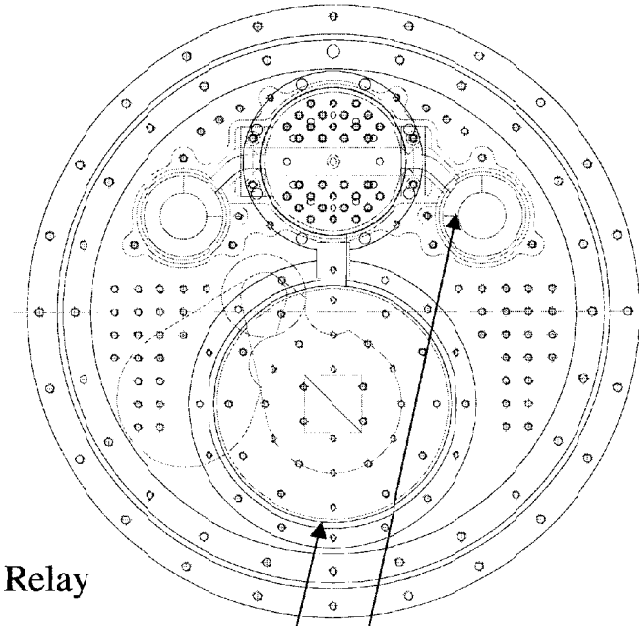

- F5 Offner Relay
- Filters
- Illuminators
- Detector Module & Shields
- He-3 Fridge & Shields

Cryogenics

- Cryostat from Precision Cryogenics (Indiana)
- Optics at 1.5K (Pumped L^{4}He Bath)
- Detector stage at 300mK - Kevlar isolated stage linked to ^{3}He fridge (Chase Research)
- Array providers will supply 300mK detector shields

Optics

- F5 Offner Relay
- Mirrors from Symons Mirror Technology (diamond turned Al-6061)
- All optics at 1.5K
- Baffling scheme will be finalised once stray light analysis is completed (RAL)

Optics

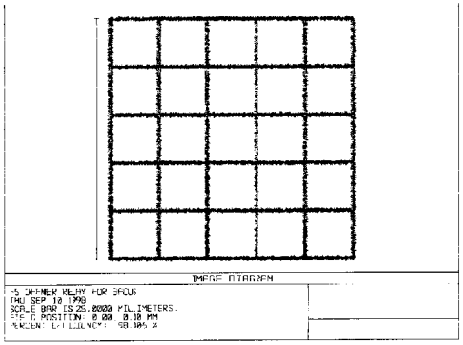
IMAGE DIAGRAM
FS OFFNER RELAY FOR BACUS
THU SEP 10 1998
SCALE BAR IS 25.0000 MILLIMETERS.

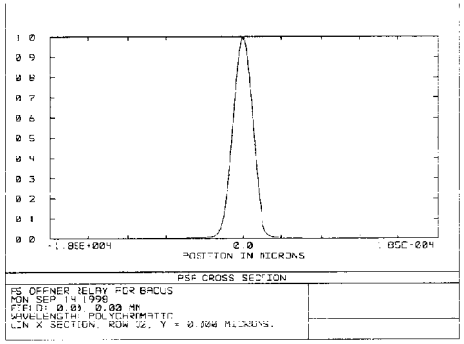
1.0
0.9
0.8
0.7
0.6
0.5
0.4
0.3
0.2
0.1
0.0
-1.8E+004
0.0
1.8E-004
POSITION IN MICRONS
PSF CROSS SECTION
FS OFFNER RELAY FOR BACUS
MON SEP 14 1998
FIELD: 0.00, 0.00 MM
WAVELENGTH: POLYCHROMATIC
LIN X SECTION, ROW 32, Y = 0.3048 MICRONS.

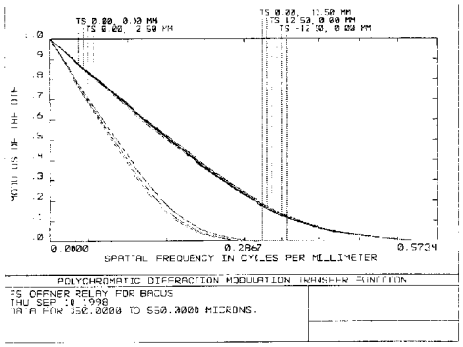
TS 0.00, 0.10 MM
TS 0.00, 2.50 MM
TS 0.00, 12.50 MM
TS 12.50, 0.00 MM
TS -12.50, 0.00 MM
1.0
0.9
0.8
0.7
0.6
0.5
0.4
0.3
0.2
0.1
0.0
0.0000
0.2867
0.5734
SPATIAL FREQUENCY IN CYCLES PER MILLIMETER
POLYCHROMATIC DIFFRACTION MODULATION TRANSFER FUNCTION
FS OFFNER RELAY FOR BACUS
THU SEP 10 1998
DATA FOR 350.0000 TO 550.0000 MICRONS.

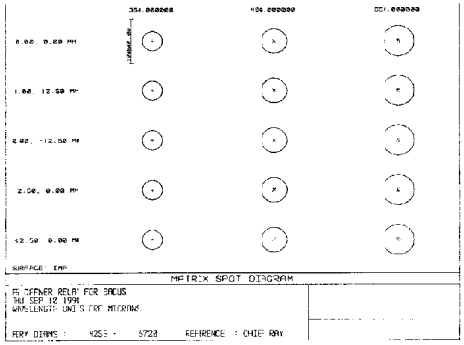
SURFACE: IMA
MATRIX SPOT DIAGRAM
FS OFFNER RELAY FOR BACUS
THU SEP 10 1998
WAVELENGTH UNITS ARE MICRONS.
REFERENCE : CHIEF RAY

Illuminators

- ND + Edge filters for work in R-J region
- GSFC illuminator evaluated - new design being built for optimisation at 350 μm
- Need to be modulated ~10Hz or more
- Uniform source plate - variable temp.
- QMW dewar will have window to outside

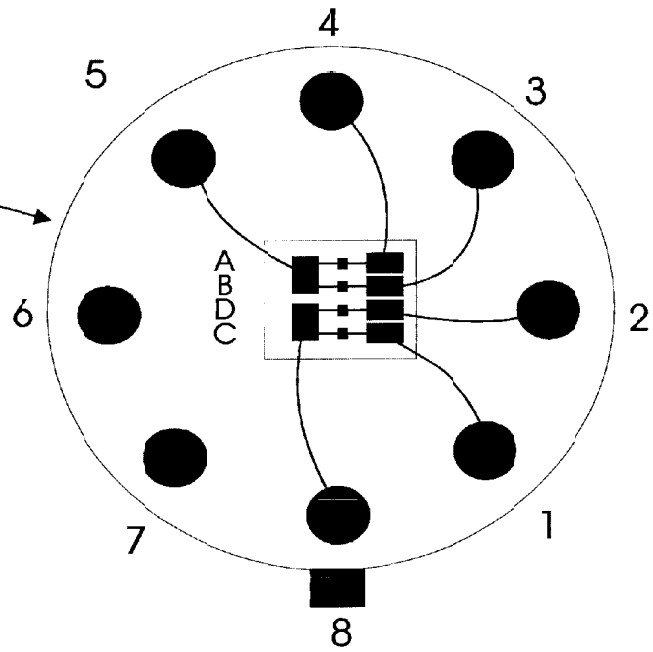

Connectors

- 1x79 way - for detector arrays
- 1x32 way - for illuminators
- 1x26 way - for housekeeping
- All connectors are box flange mount conforming to MIL-C-38999/21
- All connectors are now in the possession of the array groups.

Proposed BACUS Filtration Scheme

29cm^{-1} Bandpass
$\lambda / \Delta\lambda \approx 3$
PLUS
52cm^{-1} edge
(polyprop. or supported)
Both size 5 (56mm OD)

300mK Filter
35-40cm^{-1} edge
Polypropylene
Size 5 (56mm OD)

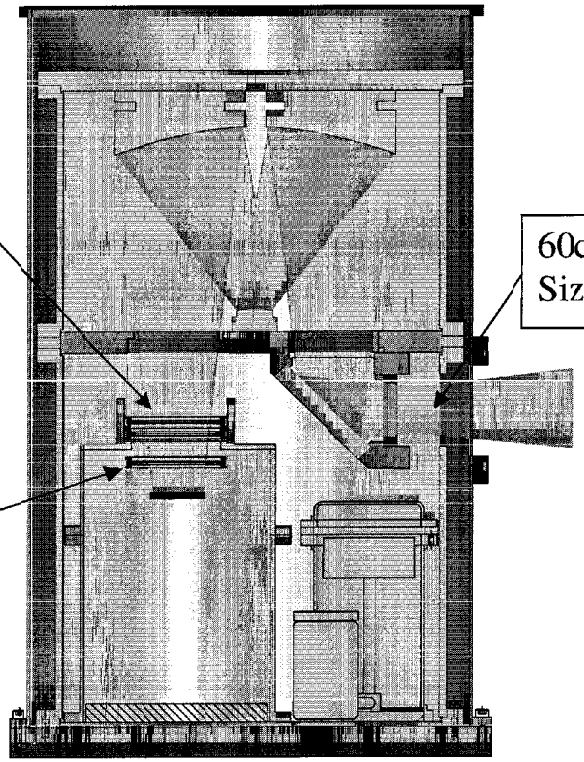

60cm^{-1} edge
Size 5 (56mm OD)

BACUS filters

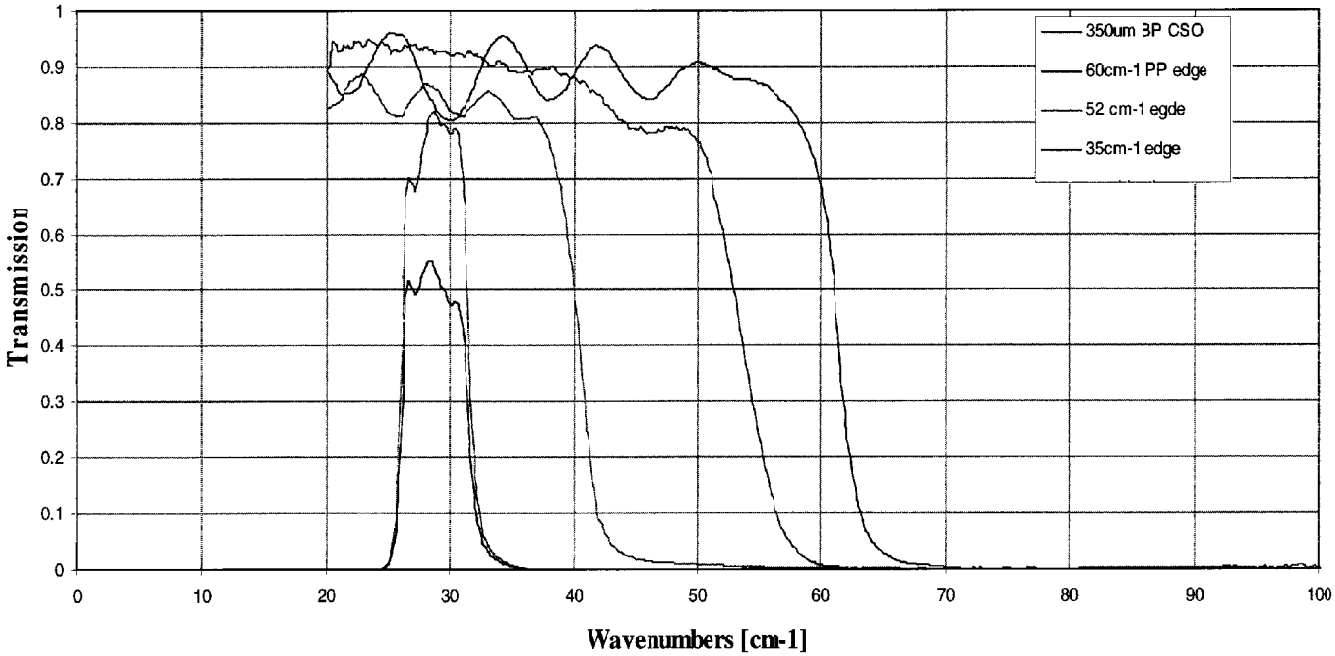

BACUS Capabilities

- V-Is - blanked or with uniform background
- Speed of response
- Flat fielding / array uniformity
- Cross talk
- Sensitivity
- Dynamic Range
- Linearity
- Optical NEP
- Spectral response
- Fringing between optical elements
- Calibration of detector responsivity (external black body)
- Connection to telescope simulator

Test Plan

- Three identical cryostats and BACUS modules are being built
- US detectors to be built into their own dewars & pre-tested before shipment to QMW
- Final definitive tests to be carried out at QMW using the "master" BACUS module
- All CEA/Sap detector integration and testing to be conducted in the QMW lab
- All detector groups will supply staff effort at QMW to assist with/oversee tests.

- CEA/Sap test plan
  - Prototype single pixel device being tested in QMW lab
  - Iterative tests on successive generation devices through 1999 with final device delivery at the end of October 1999
- JPL/CALTECH test plan
  - Will provide NTD Ge pixel for characterisation of BACUS stray light
  - Initial array tests to be conducted in JPL lab
  - Final array expected at QMW Sept./Oct. 1999
- GSFC test plan
  - Initial array tests to be conducted in GSFC lab
  - Final array expected at QMW Sept./Oct. 1999

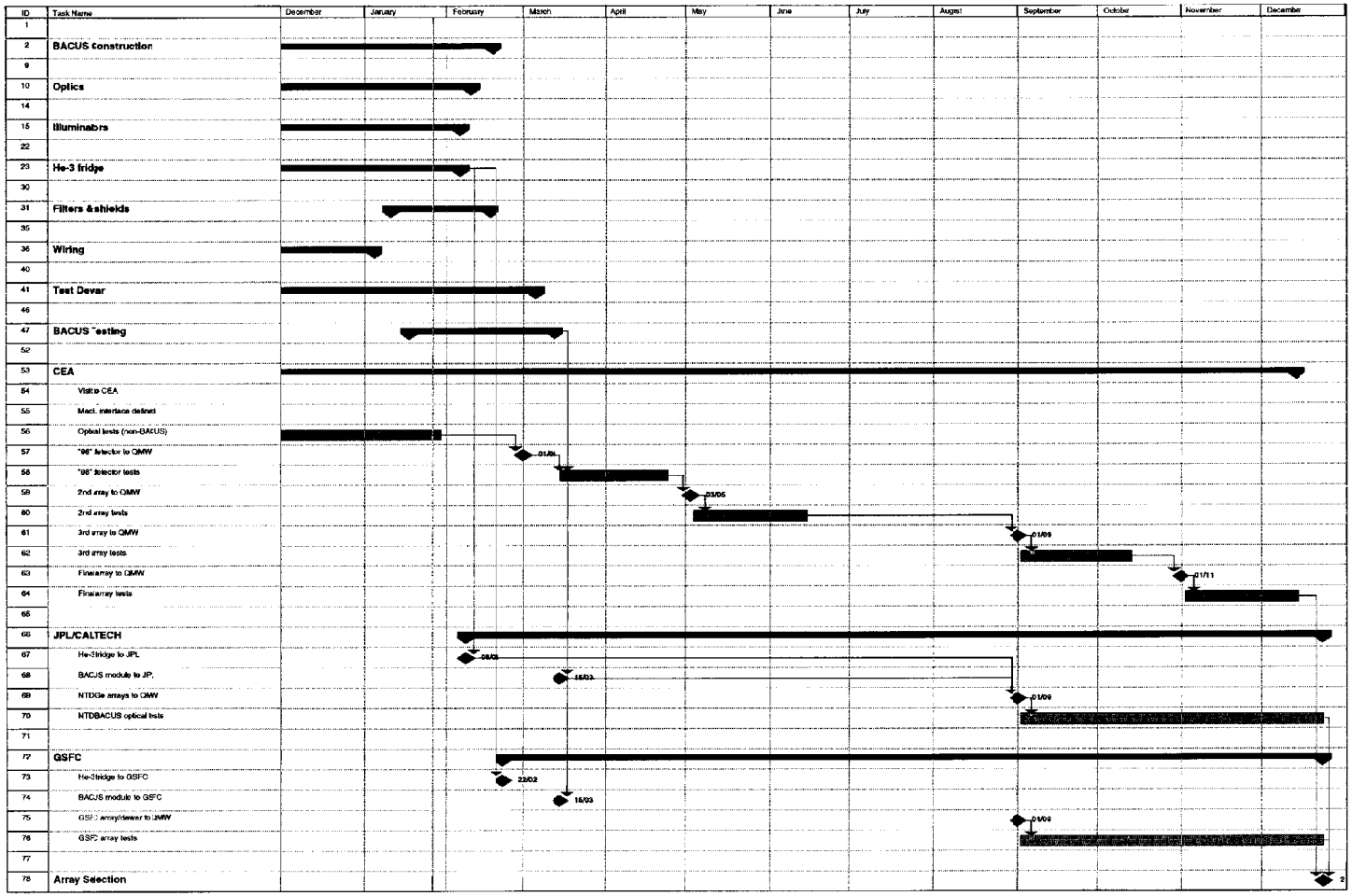
ID
Task Name
December
January
Feorusry
March
April
May
June
July
August
September
October
November
December
1
2 BACUS construction
9
10 Optics
14
15 Illuminabrs
22
23 He-3 fridge
30
31 Filters & shields
35
36 Wiring
40
41 Test Devar
46
47 BACUS "esting
52
53 CEA
54 Visits CEA
55 Mech. interface defined
56 Optical tests (non-BACUS)
57 "95" Selector to QMW
58 "95" Selector tests
59 2nd array to QMW
60 2nd array tests
61 3rd array to QMW
62 3rd array tests
63 Fina array to QMW
64 Fina array tests
65
66 JPL/CALTECH
67 He-3 bridge to JPL
68 BACJS module to JP.
69 NTDGe arrays to QMW
70 NTDBACUS optical tests
71
72 GSFC
73 He-3 bridge to GSFC
74 BACJS module to GSFC
75 GSF: array/dewar to JMW
76 GSFC array tests
77
78 Array Selection
01/05
03/05
01/09
01/11
08/01
15/03
01/09
22/02
15/03
01/09
2

Current Status

- QMW mirrors arrived late October - US mirrors due 2nd Feb.
- RAL progressing with stray light analysis
- Illuminator work progressing - fall back option is to use IR Labs TRS devices (as used on ISO)
- Two of the three He-3 fridges are in the QMW lab - testing should be complete early Feb. Shields are also complete.
- RAL drawings have been submitted for manufacture - completion early Feb.
- Filtration scheme now defined - manufacture at QMW.
- Connector acquisition complete.
- Wiring scheme defined.
- Cryostats - components have been sent from Precision Cryogenics to CALTECH for gold plating. Delivery has been quoted as 2 weeks after parts are returned to Precision Cryo.

Array evaluation and selection criteria

- We must have absolute confidence at time of selection that the chosen option will work
- A full system design document shall be produced by each array group, compliant with SPIRE design, spacecraft resources and IID-A requirements.
- A detailed array fabrication, test and delivery schedule shall be provided (at least up to CQM)
  - Including relevant warm electronics
  - Consistent with the SPIRE schedule
  - Realistic
- Credible space qualification programme and schedule shall be provided
- Performance and comparison of array options in SPIRE shall be evaluated by simulating the complete system

9

SELECTION CRITERIA AND PLAN

MATT GRIFFIN

Summary

- BACUS schedule has slipped since the last meeting - current completion date is early March
- Two of the three He-3 fridges are now in the QMW lab and should be fully tested by early February
- Preliminary tests can be carried out in another dewar once He-3 fridges are fully tested by QMW (early February)
- Schedule is very tight - we need realistic estimates, with reasonable notice, for when we can expect devices at QMW
- QMW staff should visit US labs for pre-tests for device familiarization to avoid subsequent delays and to be prepared for any specific requirements of the technology
- Illuminators need serious consideration - if new GSFC modules can't be developed within our timescale, we have to use eg. IR Labs TRS devices (slow!) and conduct speed tests at QMW using an external chopped source.

Potential Delays

- Delivery of test dewars
- Delivery of GSFC/JPL optical components
- Construction & testing of illuminator arrays
- Delivery of externally manufactured parts

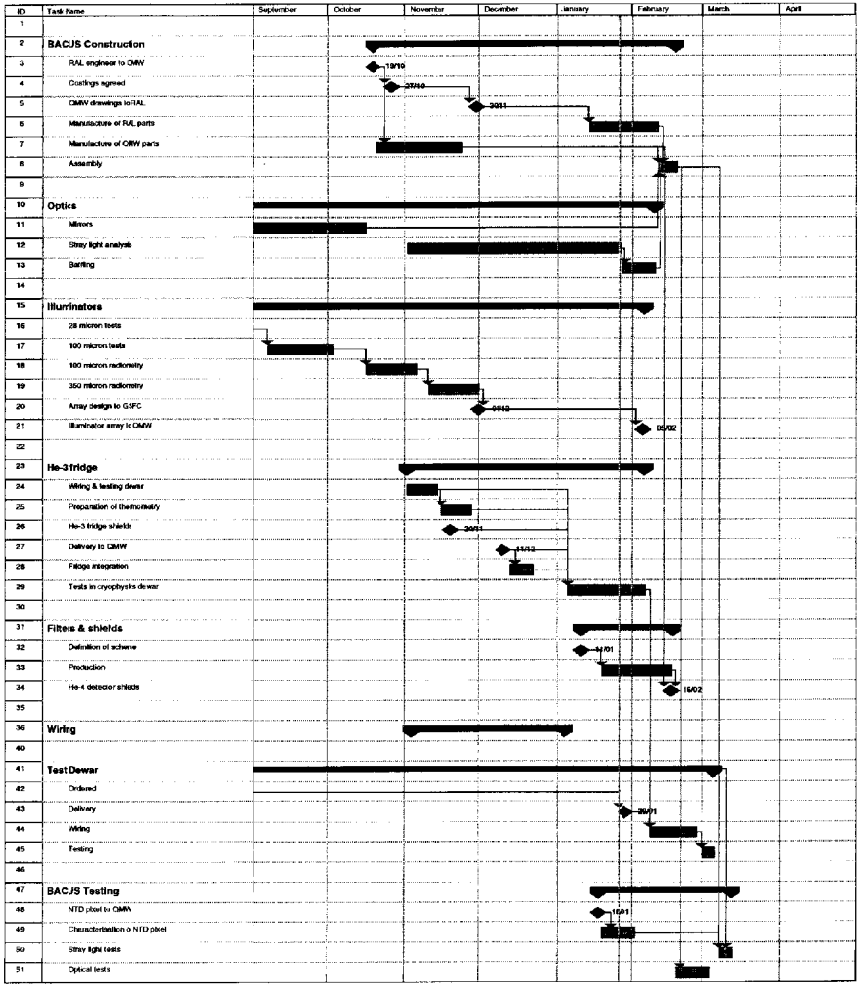
ID
Task Name
September
October
November
December
January
February
March
April
BACJS Construction
RAL engineer to OMW
Coatings agreed
OMW drawings to RAL
Manufacture of RAL parts
Manufacture of OMW parts
Assembly
Optics
Mirrors
Stray light analysis
Baffling
Illuminators
28 micron tests
100 micron tests
100 micron radiometry
350 micron radiometry
Array design to GSFC
Illuminator array to OMW
He-3fridge
Wiring & testing dewar
Preparation of thermometry
He-3 fridge shields
Delivery to OMW
Fridge integration
Tests in cryophysics dewar
Filters & shields
Definition of scheme
Production
He-4 detector shields
Wiring
Test Dewar
Ordered
Delivery
Wiring
Testing
BACJS Testing
NTD pixel to OMW
Characterisation o NTD pixel
Stray light tests
Optical tests

10

SIMULATIONS

LAURENT VIGROUX

See Annex 3

11

SUMMARY AND ACTIONS

MATT GRIFFIN

See minutes

E

Attachments

1. ***The CEA Filled Detector Arrays***
   L Rodriguez

2. ***SPIRE Detector Test Programme – Description and Status***
   P Hargrave *et al.*

3. ***Confusion Noise in SPIRE Surveys, V0.2***
   Aussel et al.

The CEA Filled Detector Arrays

SAp-SPIRE-LR-12-99

Issue: 1.0

Jan. 21, 1999

L.Rodriguez

THE CEA FILLED DETECTOR ARRAYS

I-INTRODUCTION.

SPIRE is a spectro-imaging mid-resolution camera dedicated to the observation of the universe in the submillimetric spectral band. The exact wavelength range and ultimate resolution are not already totally frozen: they depend mainly on available mature technology and scientific needs. Today, goal values are 200-650 μm for the spectral coverage and R= 3->500 for the spectral resolution.

This instrument will be built during a very exciting time period. Ground based instruments on large telescopes are now in operation and drive the instrument technology. The final processing of ISO data is in progress. It gives access to the most sophisticated image analysis available. In effect, unfortunately, because the wavelength shift, in spite of an almost 4 meter mirror, the image resolution of SPIRE will be less than those from the ISO camera. This drawback could be partially bovercome by sampling the optical Airy disk, and using deconvolution techniques. High complexity sensitive detector arrays and low optical distortion are two goals driving the instrument.

II-DESCRIPTION.

THE DETECTOR ARRAY CONCEPT.

The CEA detector concept is an attempt to develop monolithic bolometer detector arrays, similar to usual quantum technology ones: filled focal planes without light concentrators and collective manufacture, including portion of the integrated readout circuits.

Large and thin mono crystalline silicon grids, self-suspended to a frame by microscopic silicon "beams" are the sensitive part of the detectors. The temperature sensor, in the grid centre, is an implanted silicon structure. The conversion of radiant energy to temperature is done by metal deposition on the silicon grid.

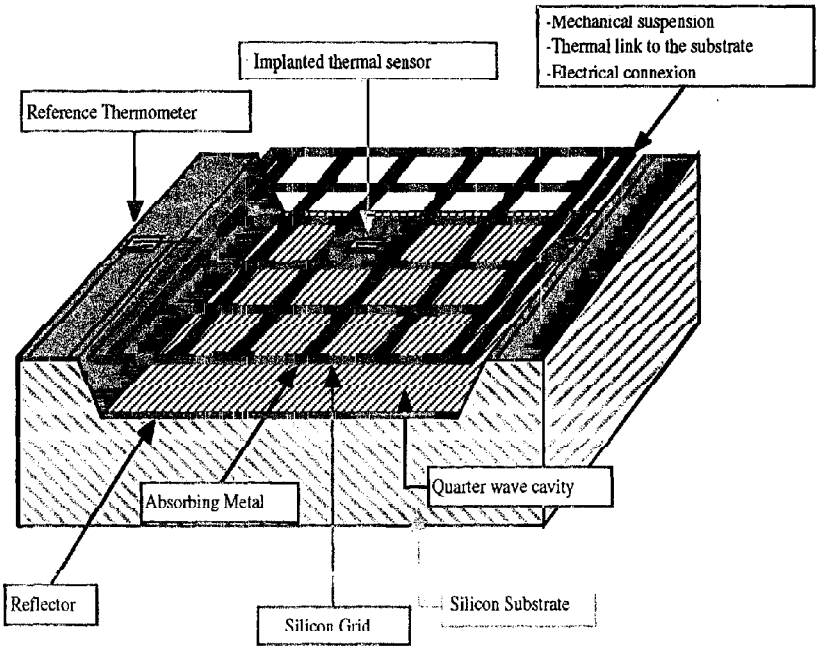

To achieve detectors efficiency close to one. we use the resonant absorption effect by making a quarter wave reflective cavity under the detection grids (Fig 1).

Figure 1: The detector principle. A suspended grid with defined pattern absorber , on a quarter wave reflective cavity, defines the pixel. At the detector centre an implanted thermometer measure the temperature variations of the pixel. On the detector edge, a second thermometer acts as a charge resistor. The signal is the bias variations at the R-R bridge middle point. Heat is extracted towards the surrounding substrate by microscopic silicon beams.

THE ARRAY COLLECTIVE MANUFACTURE.

The structure of the 2D detector arrays is obtained by micro machining silicon techniques, originally developed at CEA/LETI for micro sensors production. These standard techniques are used to produce, at an industrial level, airbags accelerometers, methane sensors, or integrated pressure gauges.

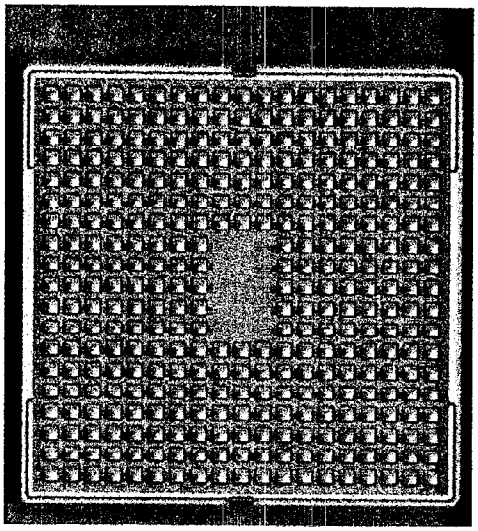

These techniques are used for etching the 450 µm mono crystalline silicon wafer to produce a honeycombed structure ended on one side with thin square grids. Each grid is 5 µm thick including a thermometric structure. The pixel size here is 900 µm. The thermometric structure and implanted *vias* are then passivated and the metallic layer deposited on the silicon grid. Figure 2 shows a typical suspended grid of the prototype array. The grids are linked mechanically and thermally to the substrate by tiny silicon beams (700 µm long, and 2 x 5 μm^2 section). Many grids aspects were tested during the prototyping phase 97-98. See on the figure 3, a detail of the beam showing the geometry of the silicon cut, which does not follow the crystalline edges of the mono crystal.

Fig. 2 Detail of the suspended grid which defines the bolometer array pixel. The thermometer is implanted in the grid centre. Heat is transferred towards the substrate by the four microscopic suspension beams.

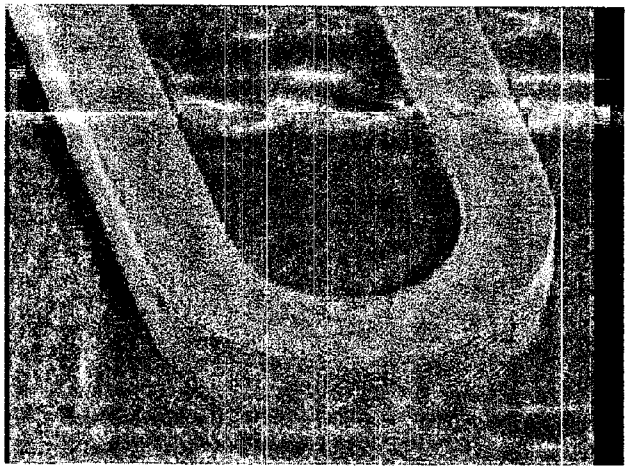

Fig. 3: Micro photography of a detail of the microscopic beam geometry.

The resonant cavity structure is obtained by indium bump hybridisation of the bolometric array on a network circuit (NC) with metallic reflectors. The indium bumps ensure two functions:

We measured a slight noise excess with regard to a MOS amplifier. As bias is increased, as the detector impedance drops with temperature, the noise is reduced to the MOS level. The noise equivalent temperature is close to 1μK/√Hz (Fig. 11).

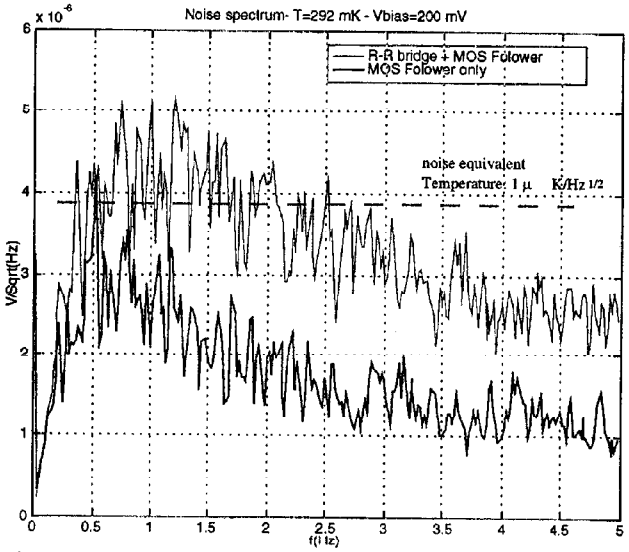

Fig 11 Low frequency noise spectrum.

THERMODYNAMIC PARAMETERS.

The determination of the thermodynamic properties of the bolometers, was made thanks to the thermal tests vehicles implanted in the prototype detector arrays. We can see on the figure below the geometry of one of these test vehicles. In the central part **two thermometers** are implanted, one used as heat source the second to measure the dynamic temperature elevation.

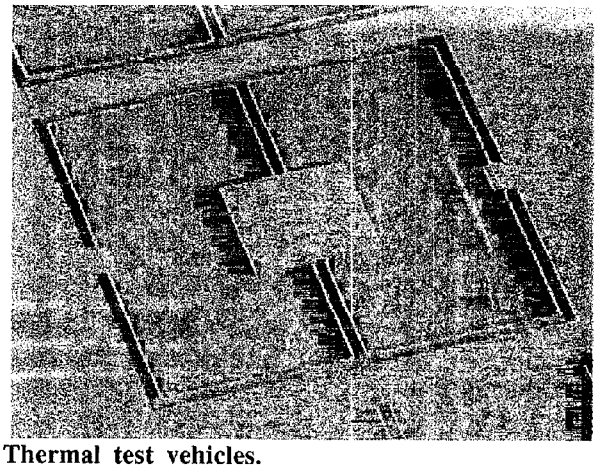

Figure 12: The Thermal test vehicles.

The experimental results are in good agreement with theoretical calculations. Figure 8 shows the T_0 obtained with our thermometers in the low field limit compared to our numerical hopping model and other experimental works. The typical responsivity is 10V/°K. Non ohmic behaviour is consistent with a field effect model where the mean hopping length L varies quadratically with T (Fig. 10).

The relative dispersion on the arrays is less than 0.8, while the close R-R bridges are only a few percent. This is an important result for the bolometer array application.

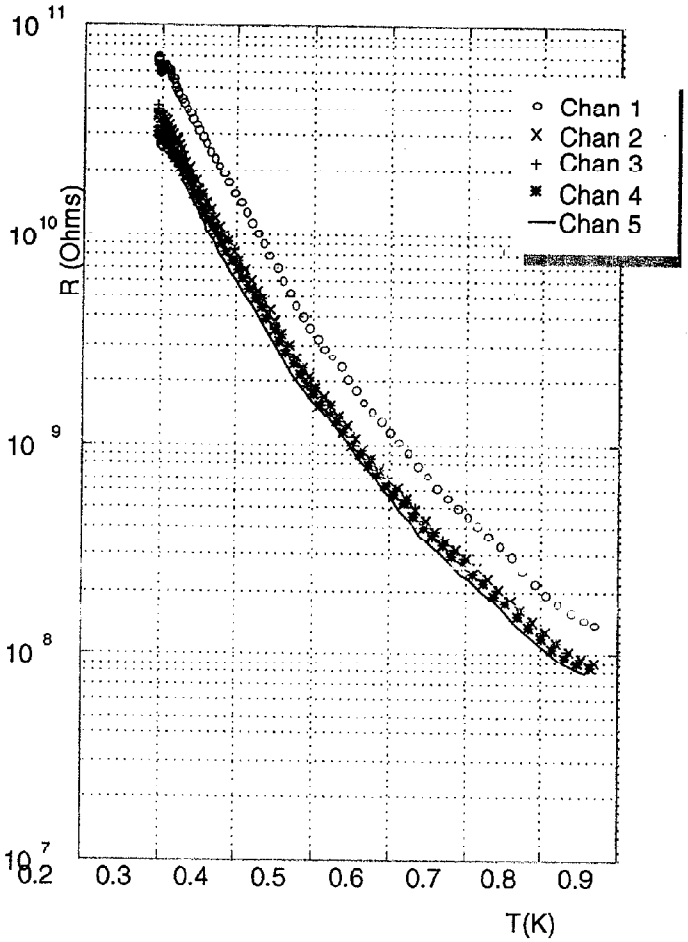

Fig. 10 Bolometers resistance variation dependence with temperature

Measurement of absolute values of detector efficiency is not a trivial test: as bolometer are wide band detectors, all the parasitic sources must be controlled, and calibrations must be done with well known adapted blackbodies

The dynamic response, is not only the measurement of the detector frequency dependence, but also the knowledge of the thermalisation process. In this case the impulsional response will be measured to determine possible interaction between the different elements of the pixel.

THERMOMETER PERFORMANCES.

Theoretical studies of charge transport in doped semiconductors at low temperature have shown that thermally activated tunnelling between doping sites is the dominant conduction mechanism on the insulator side of the metal insulator transition. In an effort to have quantitative tools, we developed a numerical model of conduction in the doping band. The resistivity has a temperature dependence which is highly correlated to the shape of the Density Of States in the silicon impurity band. The first step of the calculation was to determine the DOS for different doping and compensation levels. The results show clearly the appearance of the Coulomb gap as compensation ratio (**k**) is increased.

The second step was to establish a model of Variable Range Hopping carrier transport. The calculated responsivity is consistent with the Coulomb Gap Model [2]:

$R(T)=R_0 \exp((T_0/T)^{1/2})$.

The sizes of manufactured thermometers ranged from 10 x 10 μm^2 to 100 x100 μm^2 with width ratios between 0.2 and 5.

$$\rho = \rho_0 \exp\sqrt{\frac{T_0}{T}}$$

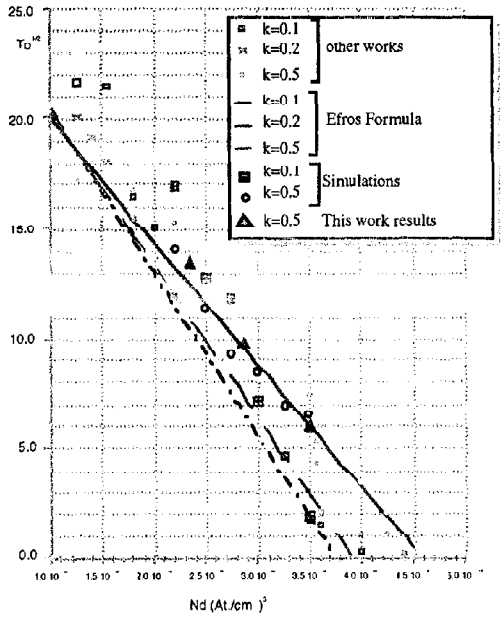

Comparison of current results with Efros Model and Monte Carlo calculations

Fig. 9: see figure captions.

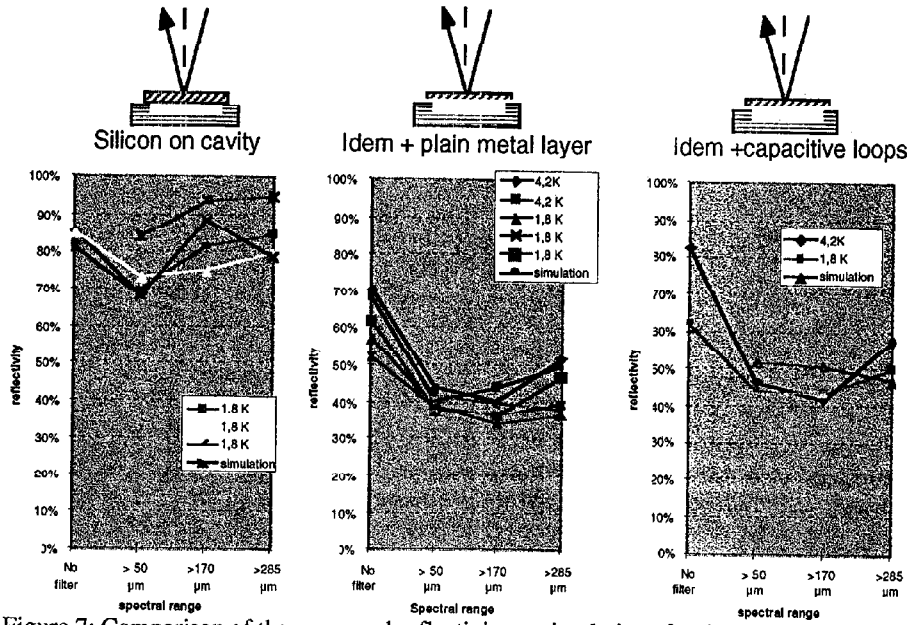

Figure 7: Comparison of the measured reflectivity to simulations for three configurations.

This measurement permitted also to confirm that the two metal alloys layers are well below the superconductive transition at 300 mK (fig. 8).

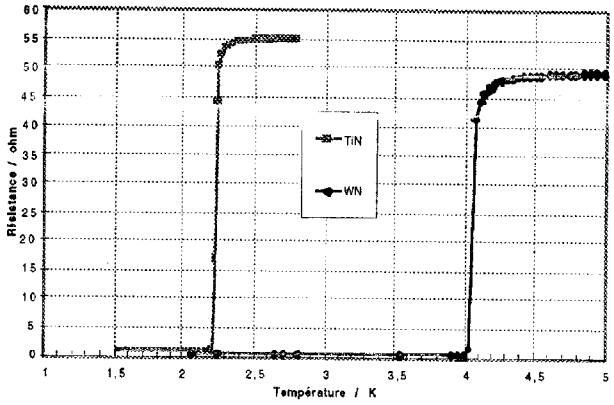

Fig 8 DC resistance of the metallic absorber layers

At the end of 1998, we started with the QMW group a development program to test different aspects of the detectors electro-optical behaviour. Two different test are planned: detector efficiency and dynamic response.

absorber layers, and test some resonant absorbing patterns, in comparison with a well known reflector.

The radiation produced by a small blackbody developed for ISOCAM, was wavelength filtered and routed by an off axis parabolic mirror, a flat mirror , and an oversized waveguide to the sample mounted on a moving platform on top of the 300 mK fridge. The reflected radiation amplitude was measured by three InSb hot electrons bolometers from IRlab company. The electromagnetic input beam was modulated by a fork type. 1.5 K chopper at the oversized guide output._

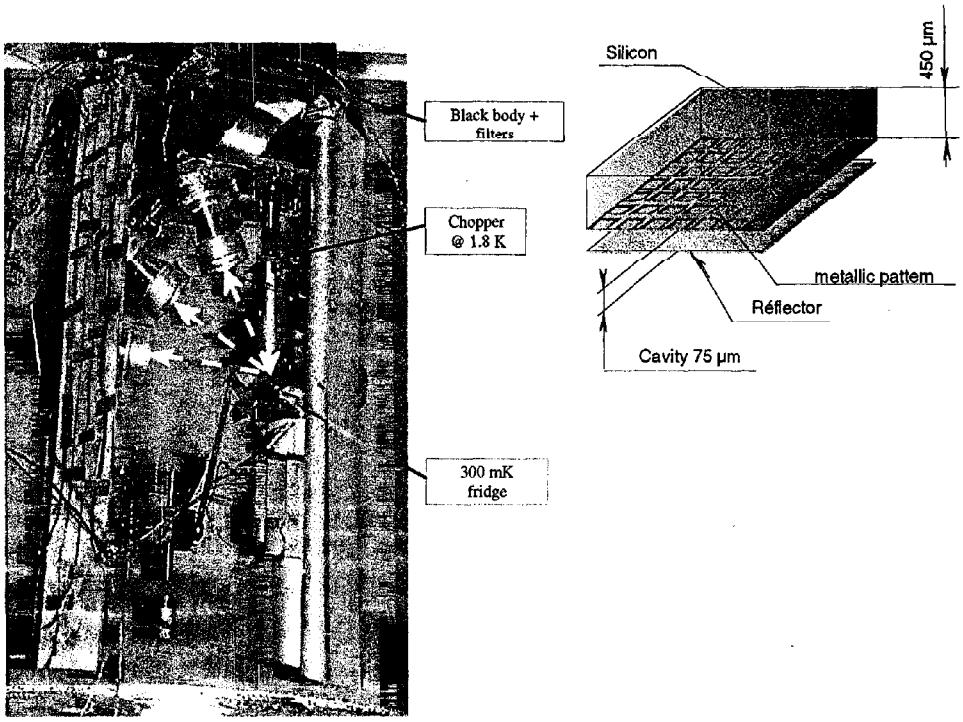

Fig. 6 : Absorption test set up and scheme of the sample.

The strongest difficulty was to build a sample representative of the final detector design. We overcame this difficulty by deposition of the absorber metal (with or without pattern) on a silicon film over a 75 µm copper cavity.

Two metallic alloys were tested: WN and TiN, known to be compatible with IC manufacture technology.

Comparisons were made for different filter ranges to the code results. All the code prediction were confirmed within experimental errors as shown in Fig 7.

Once we have identified the technical method to build the detector arrays, we have to define the different parameters necessary for the detectors design. A bolometer being mainly a thermal machinery, we had, in a first step, to determine the main thermodynamic properties in the temperature range foreseen for our application : heat capacitance of the different elements which constitute the pixel structure (silicon crystal, passivation layer, [P:B] thermometer & metallic absorber), and the thermal conductivity of the microscopic beam which links the pixel to the silicon substrate.

AVAILABLE PHYSICAL PROPERTIES.

ABSORPSION OF THE ELECTROMAGNETIC RADIATION.

The absorption of the submillimetric radiant energy by the metallic layer deposited on the silicon grids is the first element to determine the detectors efficiency. A 3D integral Maxwell code, developed for military applications, was adapted to our problem. Many simulations were then done to optimise the pixel drawings. We determined the influence of the silicon grid and pattern geometry to achieve a broad absorption profile. One solution is to combine the vertical resonance made by the quarter wave cavity (which gives a well known bell shaped profile), with horizontal resonance(s) induced by the metallic pattern deposited on the grids. Many pattern types were tested. The best result, we have found, is obtained by capacitive loops with main resonances located at wavelengths of 200 and 400 µm. A typical calculated absorption profile is shown in figure 5.

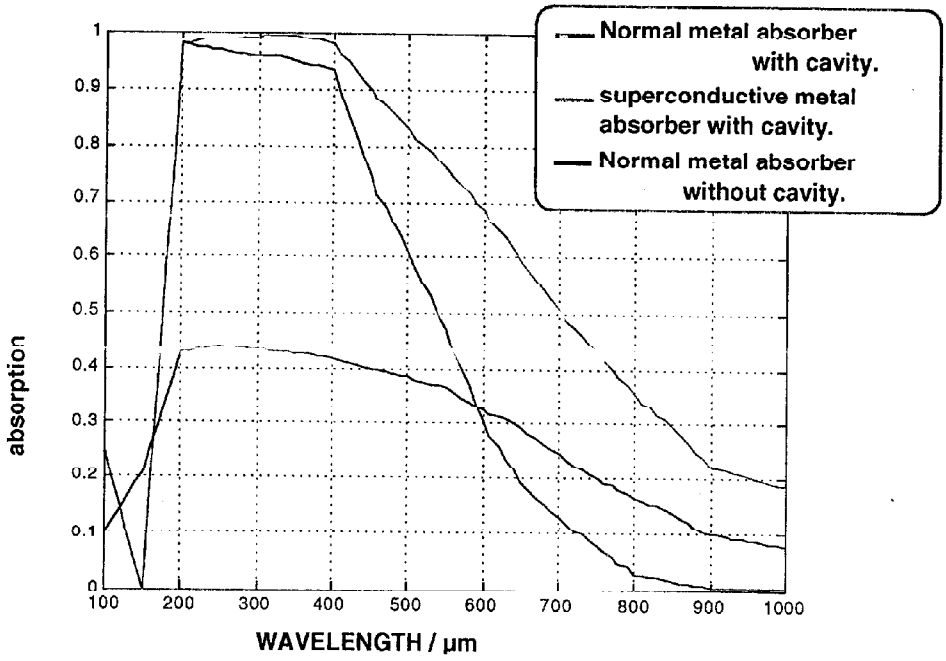

Figure 5: Detector calculated absorption

Well before the prototype array manufacture, we have built a cryogenic test set up to validate the code results. The principle was to measure the relative reflectivity of different metallic

adjust the cavity size, and connect each thermometer to a multiplexer (MUX) and to the readout chip (R/O IC) located on one side of the network circuit (fig.4). A kapton harness extracts the detector signals towards the warm electronics.

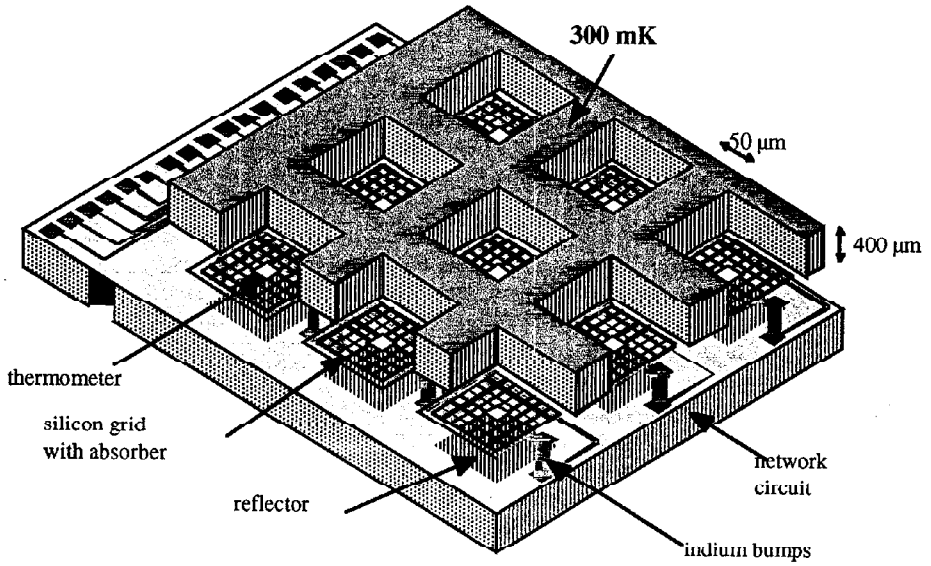

Fig. 4: Scheme of the detector assembly. The bolometer circuit and the network circuit are hybridised by Indium bumps, which ensure the λ/4 cavity separation and electrical contact.

One of the technological constraints to build large filled detector arrays is to be able to access to each individual pixel using a reasonable number of wires. This imply the necessity to multiplex signals from the array towards the readout circuit. As demonstrated on ISOCAM LW detectors, MOS preamplifiers can operate at very low temperature: 1.5 K and below, and enables the read out circuit to be close to the detector array to reduce electrical capacity, EMI pollution and microphony. The MOS transistors are also used as gates for the multiplexing function of the detectors (fig. 15).

A reference thermometer (used as charge resistor) is implanted on the pixel edge (on the inter pixel separation wall). As detector warms up under the effect of radiant power converted by the absorbing metallic layer, the thermometer resistance decreases modifying the middle point bias of the resistor bridge. Bias variations are then injected at the MOS preamplifier input. The preamplifier output impedance is now of the order of few kΩ, and signals can be extracted a few meters away without significant losses

The MOS preamplifier readout requires high impedance sources (R>10 GΩ) for proper operation. We then explored new ranges of thermometer impedance, offering the possibility to have more sensitive sensors.

Thermometric structures are obtained by Phosphorus silicon doping compensated with 50% boron.

The doping ions are implanted at several different energies to control as precisely as possible the shape of the thermometric doped channel, in order to get a flat topped profile.

THE PIXEL GEOMETRY.

The Pixel geometry was modified in different ways. The pixel step is a little reduced now: 750 μm. The inter pixel wall is 50 μm and the suspension beams length are reduced to 600 μm. A large fraction of the silicon in the grid is climinated to reduce the bolometer heat capacity. The mechanical rigidity is obtained by the wide cross shaped structure. The thermometer is implanted in a platform at the grid centre. The three metallic patterns (grids, loops and crosses) will be deposited for processing different arrays types, in TiN or WN alloys.

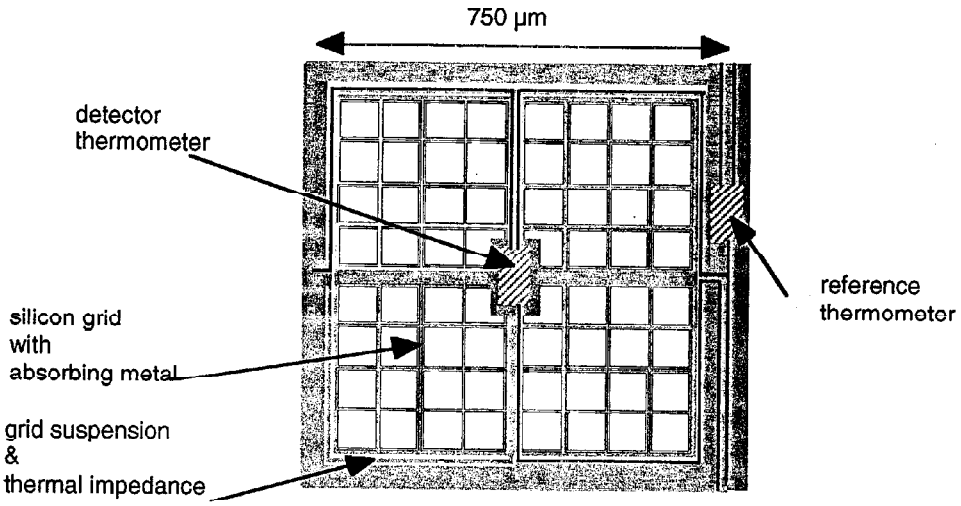

Fig. 18 The new array geometry: pixel.

THE THERMAL SENSORS.

One of the major technologic exploration this year will be made on the thermometer design. Two thermometer options are foreseen: the traditional deep implantation, and mesa thermometer technology.

In the first option, we will have to explore the effect of bias on the thermistor gate. An increasing bias could affect the effective conduction channel and recover the detector performances in case of unexpected high backgrounnd level.

In the second option, a double SOI wafer is used, and the doping ions are implanted in the 1 μm upper silicon layer. This layer is separated from the grid structure by a thin oxide barrier; the doping profile is then flattened by high temperature baking without diffusion in the grid structure. The aim of this development is to increase the thermal response homogeneity of the arrays and test the thermometer shape influence. The only way to avoid the non-ohmic thermometer behaviour, is to increase the doped channel length, reducing then the local electric field. This can be done easily if we give a "S" shape to the thermometers avoiding a large extension of the sensor. Unfortunately with implanted thermometers the effect is not seen, probably because a current leakage appears between close circuit portions at different electrical potential.

III-PRESENT STATUS.

THE NEW DETECTOR ARRAY DESCRIPTION.

New detector arrays were designed and manufactured in 1998. Design parameters were deduced from all the physical properties found during the different characterisations made these past years and described before. One of these new arrays will be used for the evaluation process at QMW by the end of this year.

Main changes from the prototype detector arrays are discussed below.

THE ARRAY GEOMETRY.

New arrays are 16 x 16 pixels with a cavity of 75 μm. The central absorption wavelength is close to 320 μm.. They include the MUX and readout chips on the detector side. The readout chip which is the most power consuming element of this assembly can be isolated from the 300 mK stage by a silicon membrane and linked to the 2 K structure. Fig 17 shows a picture of the detector with MUX and readout circuit.

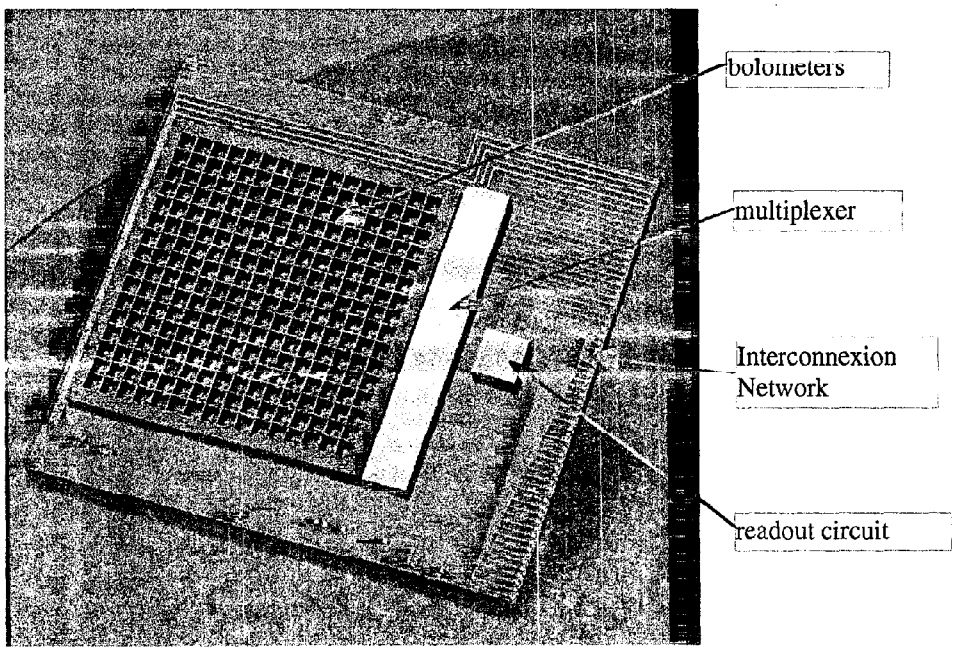

Fig. 17: The new 16 x 16 pixels detector array.

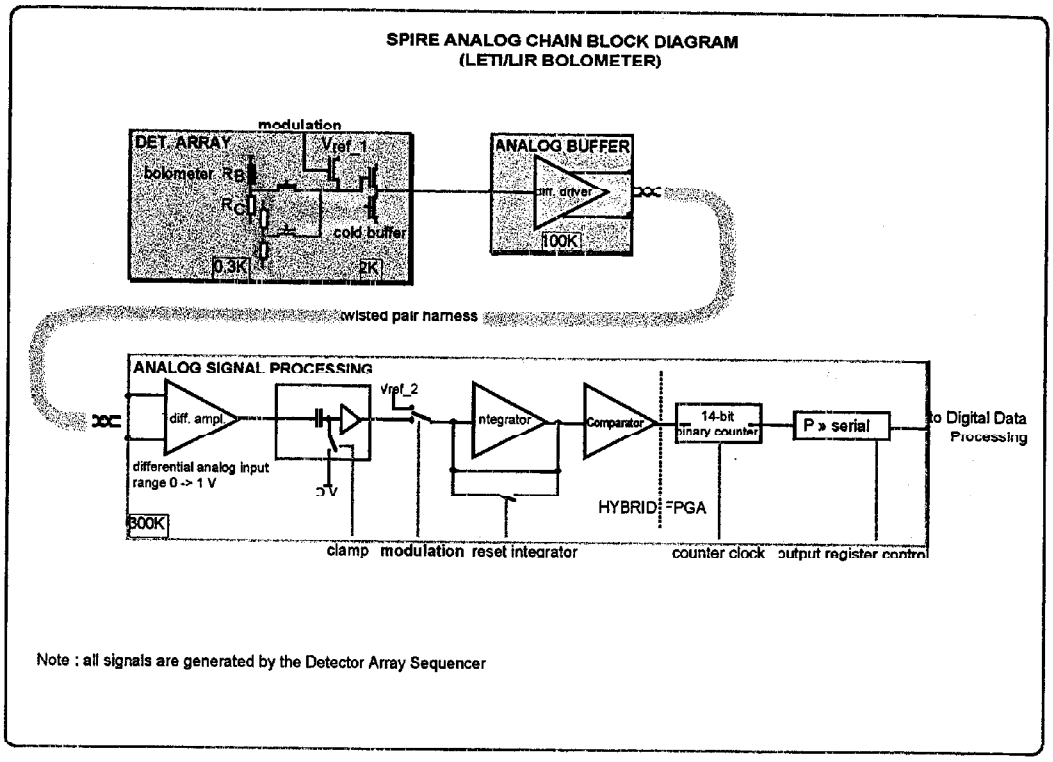

Fig 16. :Analogue Electronics Diagram

The resistances of the thermometer and the charge can be adjusted independently by the voltage applied to the thermistor gates (Gb & Gc).

ANALOG SIGNAL PROCESSING ELECTRONICS.

This electronics will be in charge of processing the analogue signal before conversion into digital signal. It receives preamplified differential signals from the BUFFER AMPLIFIER UNIT. Its concept is based on a dual slope integrator system running at the bolometer signal modulation frequency. The integrator input is switched between the bolometer optical signal (signal dependant positive slope) and an internal reference signal (fixed negative slope). This integrator discharge occurs up to its output cross 0 volt. The system features also analogue to digital conversion by measuring the total duration of this discharge phases. This measurement is performed by implementing a gated binary counter running at a frequency given by the pixel rate and the digital signal resolution (typically 1 MHz). A more sophisticated design may be considered to reduce the counter frequency or to increase the dynamic range : the conversion time is divided into two steps : a coarse for the lower resolution bits and a fine for the higher resolution bits. The analogue signal processing also includes a clamp functionality between the input differential receiver and the integrator. At the end of the conversion period the digital data is stored in a register for acquisition. Since all bolometer array output are processing in parallel for both the photometer and the spectrometer instruments 282 identical analogue chains are required (232 for the photometer and 50 for the spectrometer – bolometer output multiplexing ratio : 8->1).

In order to keep low power consumption for the overall analogue electronics special care must be taken for the choice of components, only CMOS parts must be considered.

The command pulses required to operate this electronics are generated by the Detector Array Sequencer synchronously with the detector array operation. The following figure shows the diagram of a complete analogue chain including the cold buffer, the analogue buffer electronics and the analogue signal processing electronics.

This concept takes advantage of the bolometer signal modulation (i.e. 1 kHz) to limit the signal bandwidth efficiently (especially for 1/f readout noise reduction). Its operation is equivalent to a double correlated sampling (high pass filter) followed by a low pass filter without requiring many high precision capacitors. Its also takes into account the low pixel readout frequency which allow to design low speed and low power analogue chain.

Implementation

Due to the large number of detector array outputs this electronics will take advantage of hybrid or surface mounted components technologies. In the case of hybridization 8 analogue chains are implemented in one package.

The major result with respect to our application is the thermometer heat capacity, which was uncertain at the project start. The total heat capacity is dominated by the Si3N4 passivation layer. It can be removed without impact on future bolometers.

All these results were used as inputs for the design of the new bolometers arrays produced by end 1998. Rather fast thermal operations are expected: 50 -> 70 Hz thermal bandwidth.

ELECTRONICS.

COLD READOUT ELECTRONICS

The CEA array incorporate cold electronics at the detector level. The cold readout electronics scheme is shown in figure 15.

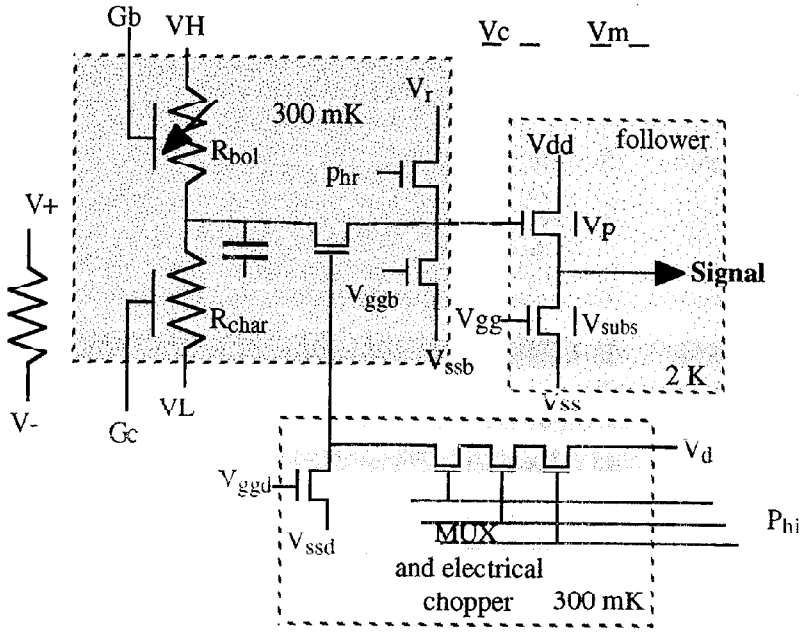

Fig 15 Cold readout electronics scheme.

On the left side of this scheme we can see the bolometer and charge resistance bridge. The middle point of the R-R bridge is linked to the gate of the MOS preamplifier at 2 K. An integrated MOS transistor at 300 mK inserted in this link connect one bolometer amongst 8 to the preamplifier thanks to the MUX circuit electrical configuration (Phi). As detector resistance is high, large voltage can be applied to the detection circuit (VH-VL), and large signal is expected at the follower output.

The major noise source in this circuit is the follower preamplifier. Introduction of a modulation between the detector and the preamplifier permit to recover the detector performances : the follower is periodically connected to the bolometer and to a stable voltage source **Vr** by the MUX circuit switch Vggd and the gate connected to Phr.

DETECTOR THERMAL IMPEDANCE.

The determination of the bolometers thermal impedance is relatively easy. The first step is the thermometer calibration. This calibration is done on a "substrate" thermometer close to the test vehicle by varying of the ^{3}He fridge temperature. Then we "switch on" the "heater" at the test vehicle centre, and measure the equilibrium temperature. The knowledge of dissipated power and temperatures gives access to the thermal conduction. The measurement was done for different configurations: straight beams, wiggled beams (fig. 13), with, or without passivation layer or metallic track.

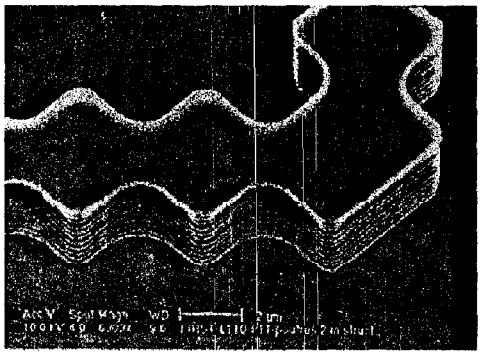

Figure 13: Wiggled suspension beam.

For straight beams, the conduction measured is close to calculated values. No effect was seen for wiggled beams, except for the SiN passivation layer conduction (see fig. 14b SiN texturé). We explain the conduction decrease in this case by an effect on 2D phonon propagation. In the case of the wiggled beams , the phonon specular reflection is affected by the inhomogeneous geometry. This effect is not seen on the silicon beams because wiggles are only present on the vertical edges.

PIXEL HEAT CAPACITY.

Heat capacity was measured on the same test vehicles. From one test vehicle to the other only one parameter was modified: the thermometer size, the silicon pad size, the passivation layer, or the metallic absorber layer. An ohmic impulse was then injected, and the temperature variation recorded. Knowing the beams thermal conductance, the total heat capacity was deduced from the temperature slope. Then the peculiar heat capacity for each element was obtained by subtraction.
The figures hereafter give a summary of all the thermodynamic measurements.

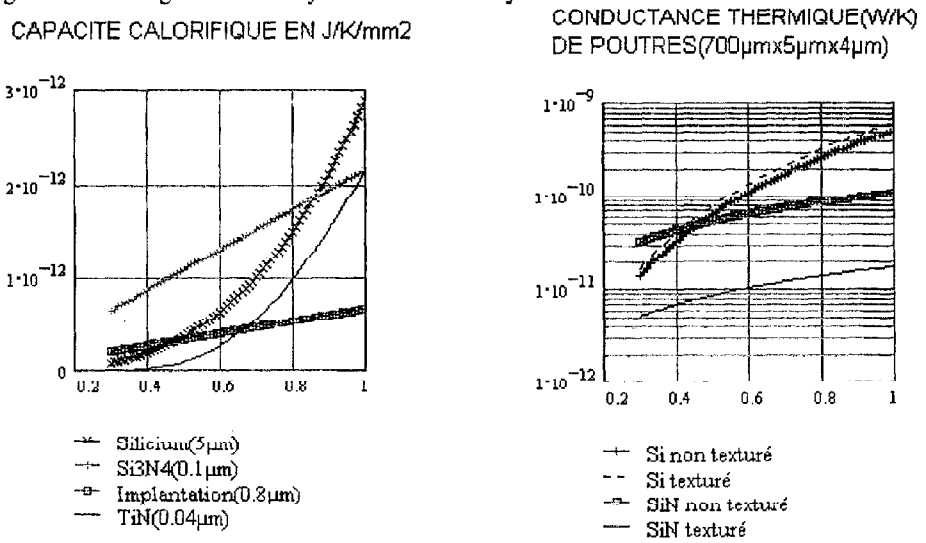

Fig 14: Summary of detectors thermodynamic properties: a-heat capacitance for pixel components. b-thermal conductance to the substrate.

IV-FUTURE: 1999 DEVELOPEMENT PROGRAM.

In 1999 many aspects of the program will be developed.

The first one will be, of course, an intense test activity to sort out the best technology amongst thermometers types, metal absorbers, patterns etc... and once the detector type has been chosen, to sort out the better array (better efficiency, sensitivity, or array homogeneity).

In parallel we will test some other aspects: mechanical resistance to vibrations, chocks tests, acoustic tests, to determine if the solutions retained for manufacture are consistent with the launch constraints.

Recent experience from ISO shows that the radiation susceptibility (gamma ray or charged particles) is an important aspect of the detector development. We plan to test the radiation susceptibility with a gamma ray source in a first step, and then the effect of proton or other charged particles. A modelisation process for all these aspects has already started in our lab.

The detector and readout electronics schedule for this year is presented below.

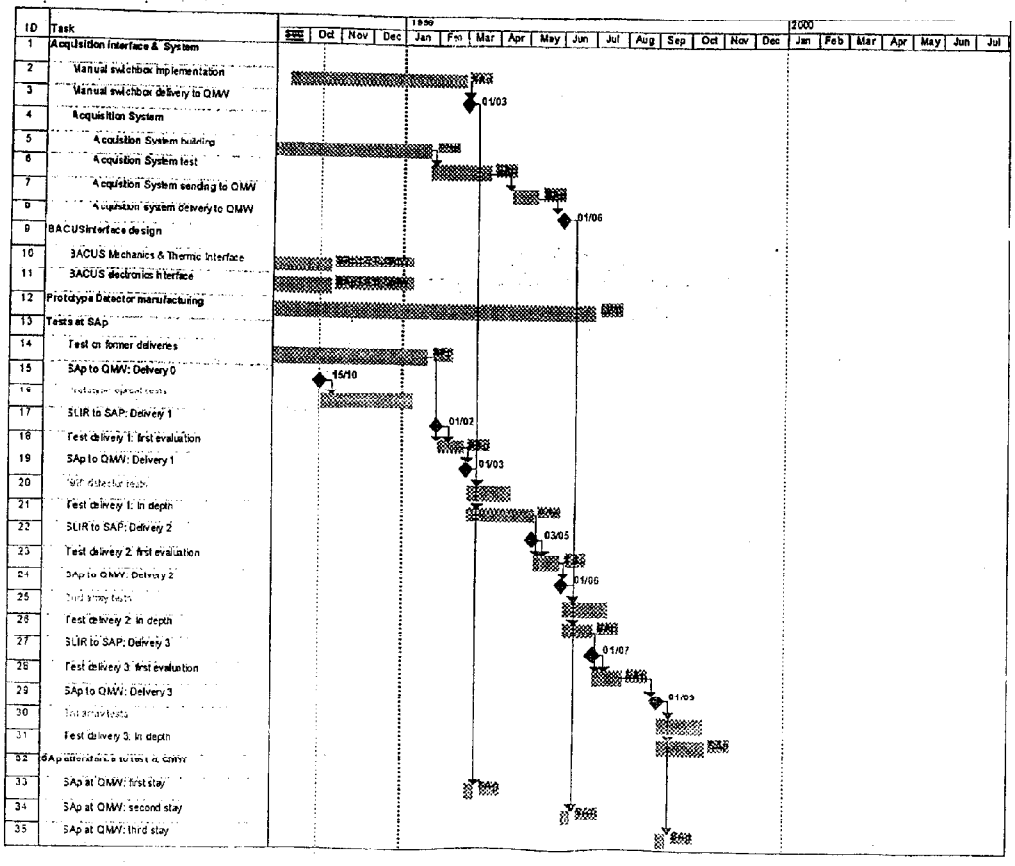

We expect to be able to deliver three detector arrays in the coming months, before the last formal delivery in November 1999 for final evaluation.

CONCLUSIONS.

In a two years period, a large amount of work have been done to produce a new technology bolometer array. Even, if all the technical processes are used in different fields of detector or micro-sensors are already well known. This detector manufacture is a first attempt to combine these technologies.

Many unexpected problems arose during these combinations, some have been overcome, others due to the lack of time have been bypassed. Some interesting problems of fundamental physics, like the effect of wiggles on the heat transport at low temperature, have been seen but unfortunately not studied. By chance, the behaviour of compensated thermometers seem to have awaked some interest for solid state physicists. our student C. Buzzi have the matter for a good thesis. The effect of resonant absorption process in our application have been measured and discussed by an other engineer student with great success. He is now working with us, in Saclay, on another subject relative to SPIRE: the Fourier Transform Spectrometer.

These aspects are highly satisfactory for the people involved in this development. It is not always easy to show, only these aspects of a technological work, to the founding institutions, even if only one step, of a complex process have been done. We have the opportunity today to show a major milestone of the detector array development (fig 19).

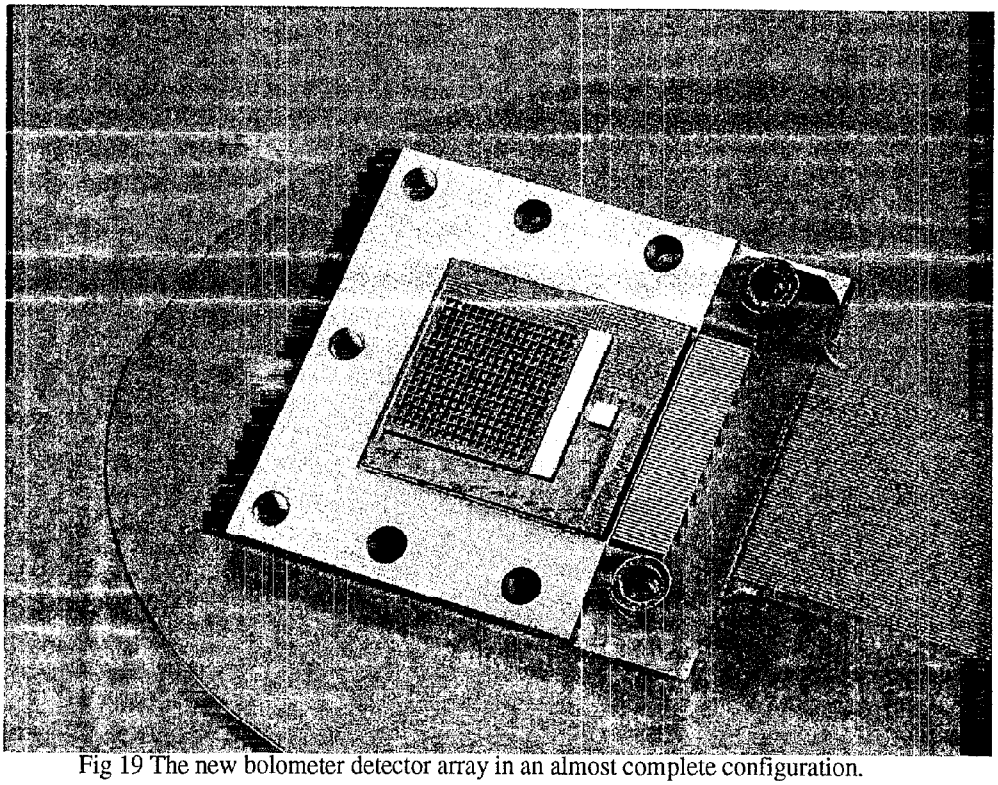

Fig 19 The new bolometer detector array in an almost complete configuration.

SPIRE detector test program – Description and Status

Peter Hargrave, Bruno Maffei, Raul Hermoso & Matt Griffin

This document describes the test and evaluation program for the candidate detector technologies for the SPIRE instrument. The first section describes in some detail the tests to be carried out, while the second part describes the current status of the test program.

1. Detector Tests

The majority of detector tests will be carried out in a dewar with a specially designed test and calibration module called BACUS (Bolometer Array Calibration Unit for Spire). This section will first give a detailed description of the BACUS module, followed by a list of the tests we propose to be performed on each detector array.

1.1 The BACUS test module

A sketch of the BACUS module in relation to the detector position and associated cryogenics is shown in figure 1.

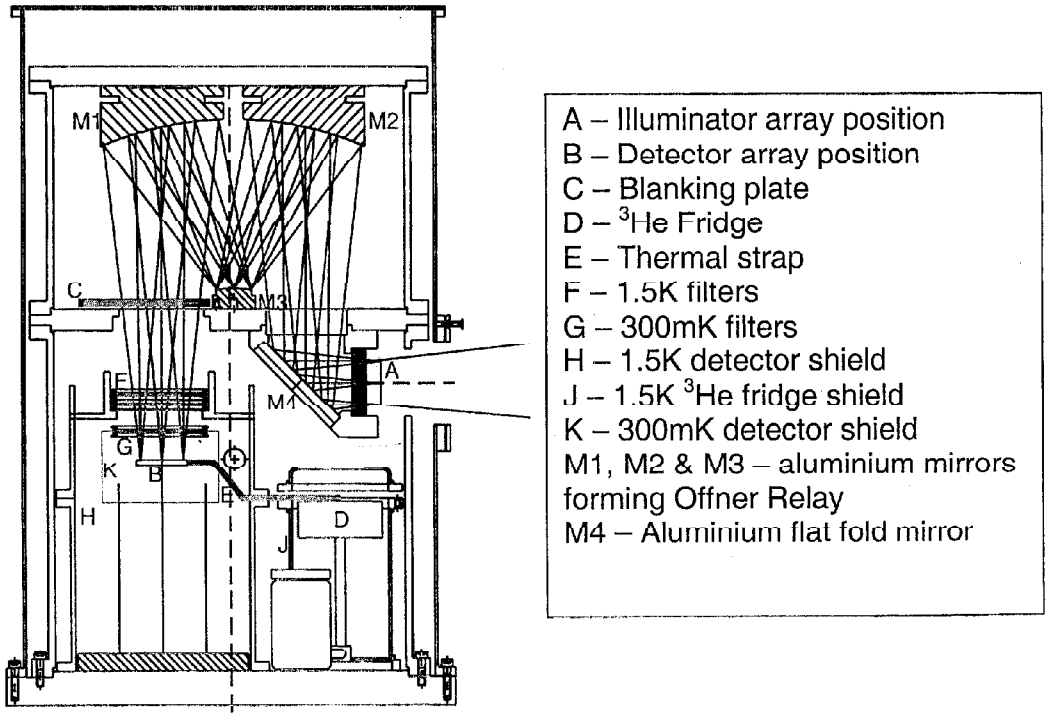

Figure 1 The BACUS module in the test cryostat.

The basic concept of the BACUS module is the employment an F5 Offner Relay to re-image an array of illuminators (or, when removed, the input from an external

telescope simulator) onto the detector array. In addition to this, a variable temperature blanking plate may be moved into position above the array.

1.1.1 Optics

The optics (M1, M2 and M3 on figure 1) form an F5 Offner Relay. This is a 1:1 re-imaging system that gives good image quality over a wide field. An Offner Relay is formed in this case by, in effect, two spherical mirrors. One is convex, radius R, and is placed at the focus of the other concave mirror of radius 2R. In this application, the larger concave mirror has been formed from two smaller mirrors M1 and M3 in order to minimise stray light, as shown in figure 2. In this configuration, M2 forms the system stop.

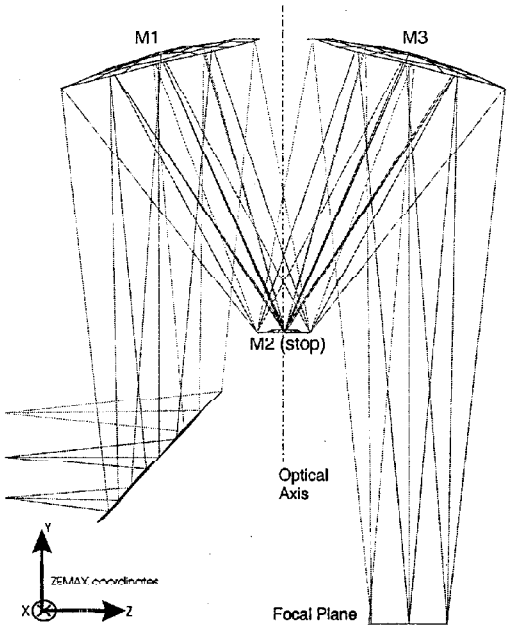

Figure 2 Illustration of BACUS Offner Relay system

The ideal Offner Relay has been slightly "tweaked" using a commercial ray-tracing package (ZEMAX – Focus Software Inc.) to provide optimal image quality on the detector array. The parameters used for the final mirror positions in BACUS are shown in table 1. In this table, the zero in the "Z" direction is taken as the optical axis, while the zero in the "Y" is the focal plane.

Table 1 Parameters for perfectly aligned system.

Mirror	M1	M2	M3
Radius (mm)	35.2	10.1	35.2
Radius of Curvature (mm) (-ve=concave)	-200	100	-200
X-offset (mm)	0	0	0
Y-offset (mm)	200	100	200
Z-Offset (mm)	-42.5	0	42.5
Tilt about X (degrees)	-12	0	12
Tilt about Z (degrees)	0	0	0

This system has been modeled in ZEMAX with the following constraints:-

- In the model, M2 was designated the system stop, and the ray tracing was performed with paraxial real reference ray aiming switched on, i.e. the rays were launched from the system stop. This was to account for pupil aberration.
- The image plane was defined as a 25x25mm square aperture centered on the array.
- All mirrors were defined as apertures equal to their actual radii. Therefore any vignetted rays were not traced.
- The object fields chosen for ray tracing were ±12.5mm, ±11mm, and on axis. This was for the purpose of a misalignment analysis - any misalignment that caused non-tracing of the ±11mm rays was considered to be the tolerance limit (see figure 3).

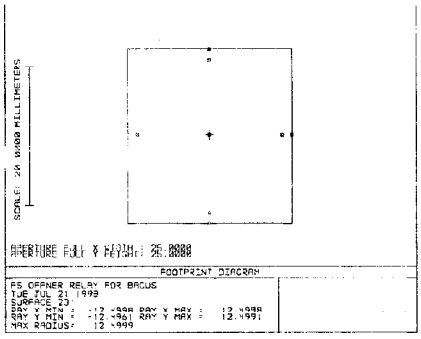

Figure 3 Footprint diagram showing position of fields used in the analysis.

The predicted optical performance of this system is shown in figures 4-7.

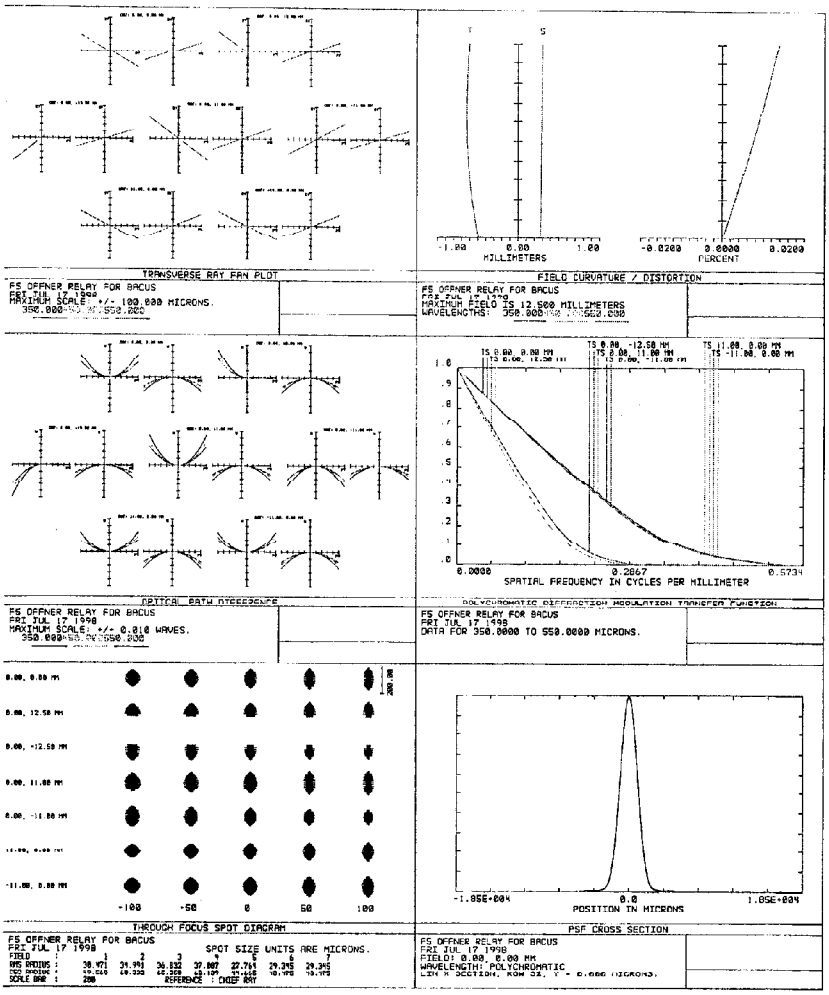

Figure 4 Performance of ideal system

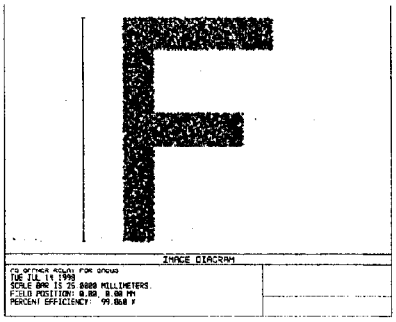

Figure 5 On-axis image quality

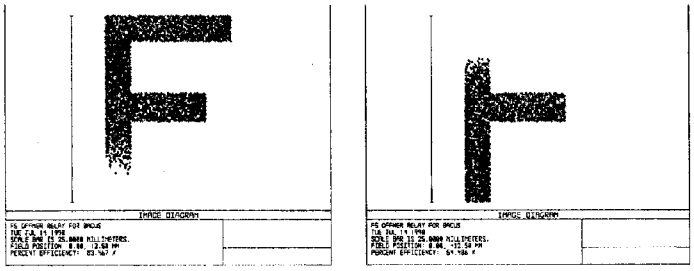

Figure 6 Image quality for 25mm objects at field limits (assuming no image plane aperture).

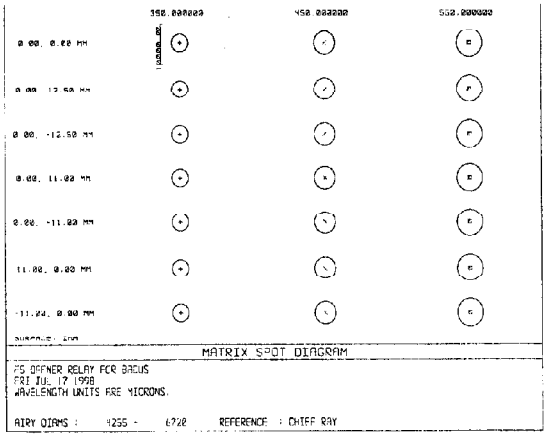

Figure 7 Matrix spot diagram for 350, 450 and 550 μm, using the Airy disc as a scale.

The mirrors for BACUS are manufactured from diamond turned Al-6061 (Symons Mirror Technology)

1.1.2 Cryogenics

The test cryostats are being provided by Precision Cryogenic Systems Inc. (Indiana, USA). These have a 10" Helium cold plate and extension tubes to house the BACUS module. This will enable the optics to be cooled to 4.2K or 1.5K. Bolted onto the cold plate will be a ^{3}He refrigerator supplied by Chase Research. An earlier incarnation of this fridge has been proven to provide 360mK with a 4.2K bath, or 298mK with a pumped ^{4}He bath (1.5K), while the version to be used in BACUS has additional heat exchangers on the support legs which should provide extra cooling power. The detectors will be located on a thermally isolated (from the ^{4}He bath) support which will be connected to the ^{3}He fridge via a thermal strap.

1.1.3 Blanking Plate

In order to make loading measurements, a plate mounted on a motor will be placed near the aperture of the 300mK shield. This will allow the bolometers to be blanked, or enable them to look at the calibration source without having to warm and open the dewar. The temperature of this plate, coated with highly absorbing material, is variable between 1.5K and 50K by means of a heater. This uniform source will allow us to measure device load-curves under varying background levels, as well as allowing measurements of array uniformity.

1.1.4 Calibration Source

Work is progressing to develop an array of illuminators for the BACUS facility. These illuminators should emit well at around 300μm, and have the ability to be modulated at >10Hz. So far, two illuminator types have been tested at QMW to assess their suitability for this application:-

- InfraRed Labs TRS (Thermal Radiation Source) device – This type of illuminator was used as a calibration source on board ISO. These devices emit well at 300μm but are slow, with a maximum modulation frequency of around 1.5Hz.

- Goddard Space Flight Center microlamps – These consist of 4 suspended doped silicon micro beams (4 for redundancy) as shown in figure 8. These are being used as calibration sources on the InfraRed Array Camera (IRAC) on SIRTF. While these devices are approximately 50 times more efficient than the IR Labs TRS at 28μm, dropping to 5 times more efficient at 85μm, there was no detectable emission at 350μm. This is unfortunate as these devices are very fast, with a 2ms time constant. Work is in progress in collaboration with GSFC to redesign the microlamps for optimal emission at around 300μm. This will involve increasing the emitting area of the microlamp, and so will compromise the speed and power consumption.

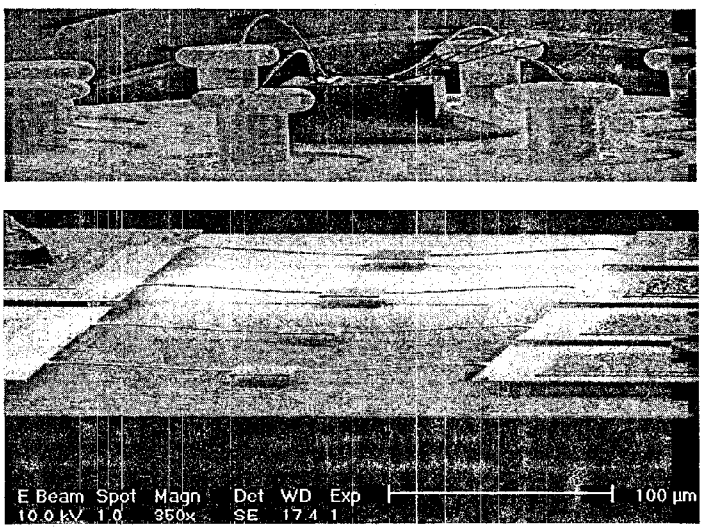

Figure 8 Electron micrographs of GSFC silicon microlamps.

We are also investigating the use of Indium Antimonide chips as potential illumination sources.

The illumination sources will be arranged on a 25x25 plate, divided into a 5x5 grid. A total of 13 illumination sources will be used, arranged as in figure 9.

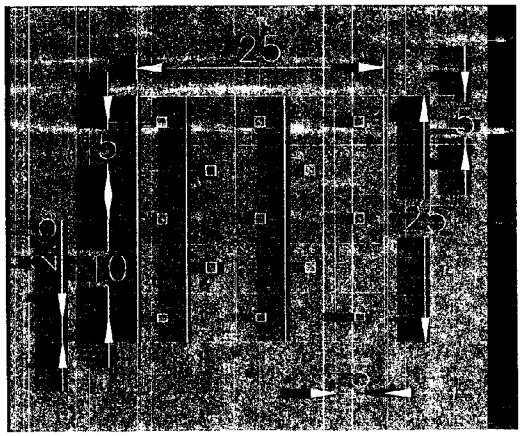

Figure 9 Arrangement of illuminator array (all dimensions in mm).

1.1.5 Wiring and Connectors

Three external hermetic connectors are being used as follows:-

- 1 x 79 pin (shell size 21)– for detector arrays (Ultratech)
- 1 x 32 pin (shell size 19)– for illuminator arrays (Sealtron)
- 1 x 26 pin (shell size 17)– for housekeeping (Ultratech)

All connectors are box flange mount conforming to MIL-C-38999/21 (screw connectors), and will be mounted on the dewar top plate.

The 79 pin connectors for the detectors will be wired according to the individual requirements of the detector array types. However, the illuminator and housekeeping wiring schemes must be standardised for compatibility during the final testing phase. These schemes are defined below in tables 2 and 3.

Table 2 Housekeeping wiring scheme for BACUS cryostat.

Housekeeping			***Junction of cables and devices by micro connectors (MDM) inside the dewar (on He4 stage)***					
26 pin connector (17-26P)			**Fridge MDM15**	**Optics MDM9**	**Illuminator 2 MDM15**		**Detectors MDM**	**He4 stage MDM9**
Male (Plug) on dewar (MIL-C-38999/21)			**15SSB on cable**	**9SSB on cable**	**15SSB on cable**	**15PSB on cable**	**tbd**	**9PSB on cable**
			15PSB on fridge	**9PSB on optics**	**15PSB on illum.**	**15SSB on illum.**		**9SSB on He4 st.**
pin #	Function	Wire (300K to 1.5K)	pin #	pin #	pin #	pin #	pin #	pin #
A	Th. Common	Cu	1	1	1			1
B	Th. He4 stage	Manganin	2					
C	Th. He4 pump	Manganin	3					
S	Th. He3 pump	Manganin	4					
T	Th. Blanking plate	Manganin		2				
U	Th. Bl.Pl. motor	Manganin		3				
V	Th. JFET	Manganin						2
W	Th. Optics	Manganin		4				
X	Ge th. I+	Manganin	5					
Y	Ge th. I-	Manganin	6					
Z	Ge th. V+	Manganin	7					
A	Ge th. V-	Manganin	8					
B	Bl. Plate drive +	Manganin		5				
C	Bl. Plate drive -	Manganin		6				
D	Bl. Plate heater	Manganin		7				
E	Bl. Plate heater rtn	Manganin		8				
F	Th. Illuminators	Manganin			2			
G	Th. Filters	Manganin						3
H	He4 pump heater	Manganin	9					
J	He3 pump heater	Manganin	10					
K	Com. pump heater	Manganin	11					
L								
M								
N								
P								
R								

1.2.2 Speed of response

Detector speed of response may be measured either by modulation of the internal illuminators, or by removing the illuminator module and using a chopped external source. Alternatively, an external gamma-ray source may be used.

1.2.3 Array uniformity

Array uniformity may be tested by use of the variable temperature blanking plate.

1.2.4 Cross talk

1.2.5 Sensitivity

1.2.6 Dynamic range

1.2.7 Linearity

1.2.8 Optical NEP

1.2.9 Spectral response

1.2.10 Fringing between optical elements

1.2.11 Calibration of detector responsivity

1.2.12 Connection to external telescope simulator

2. Test Plan and Current Status

Each detector group will have their own test dewar and BACUS module to enable them to integrate their arrays and run pre-tests (the CEA/SAp dewar to reside at QMW). The complete dewar with integrated array will then be shipped to QMW for testing and evaluation with the one "master" BACUS module.

2.1 Current BACUS status

2.1.1 Optics

- Mirrors arrived late October
- Stray light analysis being carried out by RAL – will also model baffling.

2.1.2 Illuminators

- GSFC illuminators tested with bolometer at 350 μm – seem to give negligible output at this wavelength.
- Working with Goddard to redesign the illuminators for optimisation at 350 μm.
- Array of 13 illuminators needed for each BACUS module – designing array with Dave Robinson (GSFC).
- Following a suggestion by Louis, we are going to try using InSb as a reverse HEB illumination source.

Table 3 Illuminator Wiring scheme

Illuminators				
32 pin connector (19-32P)			Iluminator 2xMDM15	
Male (plug) on dewar (MIL-C038999/21)			**15SSB on cable**	**15PSB on cable**
			15PSB on illum.	**15SSB on illum.**
pin #	**Function**	**Wire (1.5K to 1.5K)**	Pin#	Pin#
1	Element (E) 1+		3	
2	E1-	Cu Twisted Pair	4	
3	E2+		5	
4	E2-	Cu Twisted Pair	6	
5	E3+		7	
6	E3-	Cu Twisted Pair	8	
7	E4+		9	
8	E4-	Cu Twisted Pair	10	
9	E5+		11	
10	E5-	Cu Twisted Pair	12	
11	E6+		13	
12	E6-	Cu Twisted Pair	14	
13	E7+			1
14	E7-	Cu Twisted Pair		2
15	E8+			3
16	E8-	Cu Twisted Pair		4
17	E9+			5
18	E9-	Cu Twisted Pair		6
19	E10+			7
20	E10-	Cu Twisted Pair		8
21	E11+			9
22	E11-	Cu Twisted Pair		10
23	E12+			11
24	E12-	Cu Twisted Pair		12
25	E13+			13
26	E13-	Cu Twisted Pair		14
27				
28				
29				
30				
31				
32				

1.2 Detector tests

This section describes the tests to be carried out on the candidate detector arrays.

1.2.1 Detector load curves

V-Is can be obtained with the detectors blanked or with a uniform background by use of the blanking plate, which can be heated from 1.5K to around 50K. In addition, with the blanking plate out of the way, and with the illuminator module removed, V-Is can be obtained using external loads.

2.2 Testing Status

2.2.1 QMW/SAp

- CEA/SAp have delivered an array to QMW for optical tests (single pixel activated). Test plan for this device has been formulated.
- Cryophysics dewar has been wired and tested in preparation for He-3 fridge tests, and then subsequent use for testing the SAp prototype.
- Initial fridge/array tests in progress at the moment.

2.2.2 JPL (this is a copy of their last progress report dated 12/12/98)

- Operation of BOLOCAM prototype array in the dark successful with expected thermal conductivities and impedances. Noise is 12 nV/rtHz before demodulation. Electronics noise is < 4nV/rtHz. BOLOCAM science array is complete (and has been for some time) up to NTD Ge attachment step. Awaiting new NTD Ge chips.

- Prototype 350um horn array completed. We would like to send it to QMW for testing as soon as possible as we must place the order for the test arrays very soon to be ready for the test dewars.

- Memo describing design of JFET modules completed. Mask design for membrane to support GSFC JFETs completed.

- NJ132L JFET dies for testbed received from Interfet.

- Production of SPIRE test arrays now beginning.

- NTD Ge for arrays completed through implant, metalization of contacts, and In bumps. Should be diced and completed in about a week.

- Transfer of Goddard focal plane support structure completed. We have the focal plane installed in the mount (in Autocad that is) and would like to get some feedback on the mechanical envelope to guide our design.

- Tests of TES bolometers show that 1.2 pW of electrical power heats device to the transition at 450 mK. Implied thermal conductivity is 8 pW/K, and the phonon NEP = 7e-18 W/rtHz. Device shows excess 1/f noise that increases with electrothermal feedback. Excess resistive noise in the film or the contacts should decrease with electrothermal feedback, so the excess noise is better described by energy fluctuations. We will conduct further tests to find out the source of the 1/f noise.

2.2.3 GSFC

2.1.3 He-3 fridge and thermometry

- Two of the 3 fridges are now in the QMW lab and are being tested.

2.1.4 He-3 fridge shields

- These have been completed and are ready for shipment with the tested fridges.
- Design of thermal strap needs to be finalised. Need to consult with US array groups re. their 300mK detector shield design.

2.1.5 He-4 detector shields

- Currently being manufactured by RAL.

2.1.6 General structure (support tubes etc)

- JPL/GSFC will purchase complete, tested BACUS modules. RAL are building structural components for all 3 BACUS modules, which will then be sent to QMW for assembly & testing before shipment to the US. RAL engineer visited QMW in mid October and has put together a cost/delivery estimate. He is overseeing work at RAL. Bruce has ordered mirrors for the 2 additional BACUS modules from Symons Mirror Technology – delivery expected 2nd February.

2.1.7 Filters

- Scheme needs definition, and then QMW to build filter stacks.

2.1.8 Connectors

- Supplier – Ultratech (France) and Sealtron (US). Ultratech have supplied the 79 pin and 26 pin connectors types (in possession of Goddard), while the 32 pin connectors (Sealtron) have been shipped to QMW. There is one spare connector of each type, although JPL has bagged the spare 79-pin connector. All connectors will be distributed at the January meeting at QMW.

2.1.9 Wiring scheme

- This has now been defined and is included with this document.

2.1.10 Cryostat

- Expecting delivery of dewar end-January.
- Components have been sent from Precision Cryogenics to JPL for gold plating. Once gold plating is completed, Precision Cryogenics will deliver within 2 weeks.

2.3 Current test plan and status

Three identical cryostats and BACUS modules are being built for distribution to Goddard, JPL and QMW. The American detector arrays will be built into their own cryostats and pre-tested before shipment to QMW for final testing with the "master" BACUS module, while all SAp detector integration and testing will be conducted in the QMW lab. All detector groups will supply staff effort at QMW to assist with/oversee tests.

2.3.1 CEA/SAp test plan

- Prototype single pixel device is currently being tested in the QMW lab. QMW will perform the following tests:-
  - Test and calibrate the output PMos
  - Dark noise tests and V-Is on detector + PMos
  - Noise and V-Is with known illuminator power on detector + PMos
  - All above tests on detector alone (without PMos)
- Iterative tests on successive generation devices throughout 1999, with final device delivery at the end of October 1999.

2.3.2 JPL/CALTECH test plan

- Will provide NTD germanium pixel for characterisation of BACUS stray light environment.
- Initial array tests to be conducted in JPL lab.
- Final array expected in QMW lab September/October 1999

2.3.3 GSFC test plan

- Will provide illuminator modules pending test results
- Initial array tests to be conducted in GSFC lab
- Final array expected in QMW lab September/October 1999

2.4 Current BACUS production schedule

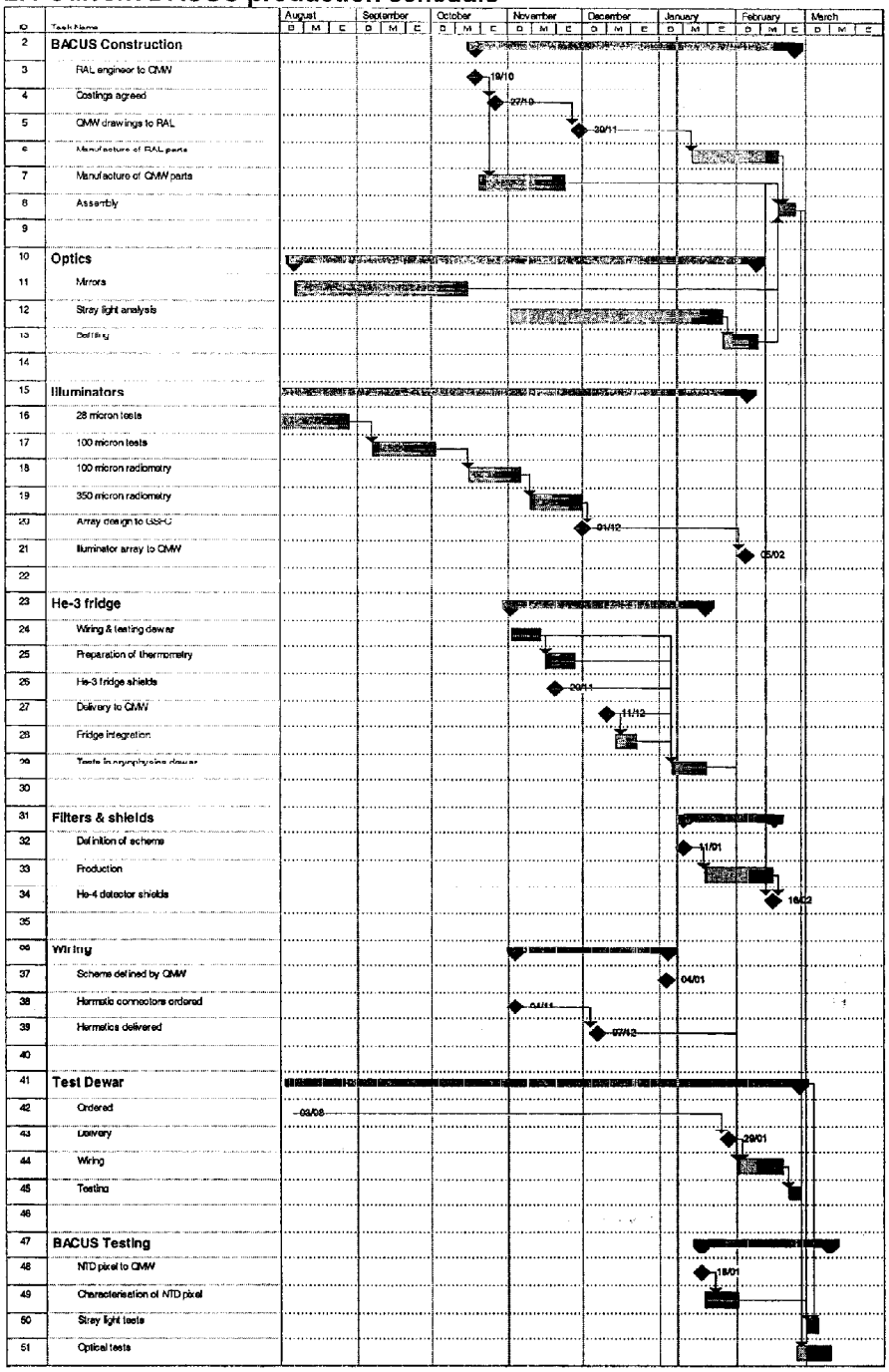

2.5 Current detector test schedule

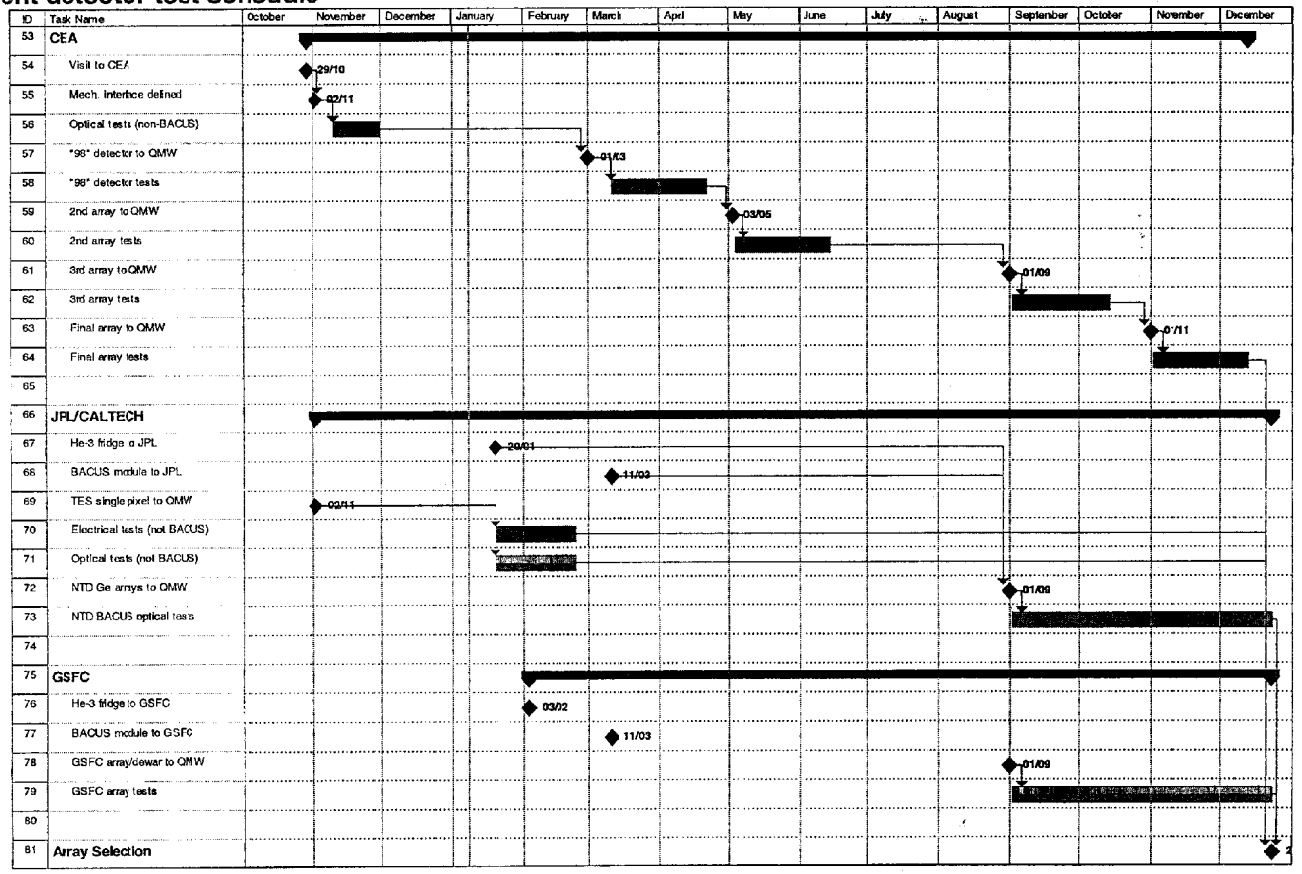

Confusion noise in SPIRE surveys
Version 0.2

H. Aussel, L. Vigroux, P. André
Service d'Astrphysique, CE-Saclay, DSM/DAPNIA,
Bat 709, Orme des Merisiers, CE-Saclay,
F-91191 Gif-sur-Yvette *Cedex*

November 30, 1998

Abstract

We present a simplificated model of extragalactic surveys with SPIRE, the Spectral and Photometric Imaging REceiver on board of FIRST, performed at 250 μm and 500 μm, in order to study the impact of confusion noise. We show on preliminary simulations that confusion is the major issue for dealing with extragalactic source extraction.

Note : Some of the remarks of the note of the 26 October 1998 by Griffin, Oliver and Gear have been taken ino account.

Introduction

This report address the problem of confusion noise for SPIRE, the FIRST bolometer instrument, for its survey mode. Indeed, confusion could be the main limitation of the instrument, due to the high number of extragalactic sources per square arc degree that are predicted by various number counts models. In order to investigate the problem of confusion, we have developped a very simplificated model of a SPIRE survey and we have simulated observations at 250 μm and 500 μm with two kind of detectors : square pixel matrix of bolometers and array of horns (back-up option). We describe in section 1 the model we have used.

1 The model.

1.1 Model for source fluxes and positions

To model the sky as observed in SPIRE surveys, we have used two of number counts models presented in [1], namely the number counts model of Franceschini et al. (1997) [2], and the one of Rowan-Robinson (1998) [4], because they are two extreme models from the point of view of the predicted source density, the counts predicted by the model developped by Guiderdoni et al. (1998) [3] lay between the values predicted by the two others.

Each model result is a function that gives the number N of sources brigther than a given flux S per square degree as a fuction of S. The derivative of this function $N(>S)$ is the number of sources dN with a flux $s \in [S, S+dS]$, multiplied by a factor -1. If one consider only a given flux range, $[S_l, S_u]$, one can build a function f, that gives the number of sources per square degree *dimmer* than a given flux S

and brighter than S_l :

$$f(S) = \int_{S_l}^{S} dN(s)ds \tag{1}$$

If one consider now the function $F(S)$ defined by :

$$F(S) = \begin{cases} 0 & \text{if } S < S_l, \\ \frac{f(S)}{f(S_u)} & \text{if } S_l < S < S_u, \\ 1 & \text{if } S > S_u. \end{cases} \tag{2}$$

The function F grows from 0 to 1 when S varies between $]-\infty, +\infty[$. In this sense, $F(S)$ can be interpreted as the *partition function* of the random variable X_S, the flux of a source. We can therefore build a random flux generator, that follows the number counts model, by computing the function F and using the classical computer implemented uniform generator. The random variable $X = F^{-1}(U)$, where U is a random variable following the uniform law, will have F as partition function.

To simulate a given area of sky A, the models predict that the number of sources brighter than S_l will be $n = A \times N(> S_l)$. We work on an area large enough so that poissonian fluctuations ($\propto 1/\sqrt{n}$) can be neglected.

We choose to simulate an area of 400 square arc minutes, where the number of sources brighter than 15 mJy is roughly of 130, according to the Franceschini model. For our simulations, we choose $S_l = 100\ \mu Jy$ and $S_u = 10\ Jy$. This S_l value gives a number N of sources in our simulation of 16746, with the Franceschini model, $N = 6822$ with the Rowan-Robinson model.

The fluxes of the sources are generated with our random flux generator. The counts obtained from the simulated sets are shown in figure 1 for the various models. The positions in the images are generated by using a uniform generator.

1.2 Simulation of the focal plane

Once the positions and fluxes of the sources are known, we compute a oversampled image of the focal plane of FIRST. The resolution choosed for the computations is 0.5 arcsec, allowing for a good accuracy of the computations, since the smallest pixel size of SPIRE to be considered is 9 arcsec.

We assume an ideal telescope *i.e.* a single circular aperture. Therefore, the intensity of the diffraction limited image of a point source (PSF) is :

$$I = I_0 \left[\frac{J_1(m)}{m}\right]^2 \tag{3}$$

where J_1 is the Bessel function and with :

$$m = \frac{\pi a i}{\lambda} \tag{4}$$

where a is the telescope aperture ($a = 3.5m$), $\lambda = 250\ \mu$m or $\lambda = 509\ \mu$m is the wavelength, and i is the incidence angle (we use the approximation of small angles).

We have computed PSF with a resolution of 0.5 arcsec on the focal plane, on an area of 240 × 240 arcsec. An image of 20 × 20 arcmin with a resolution of 0.5 arcsec is computed by adding one PSF multiplied by the flux for each sources.

Figure 2 presents two simulated fields from each of the two models used.

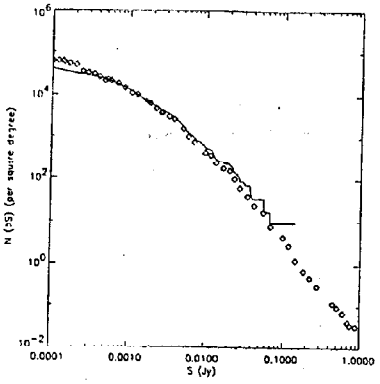

(a) $\lambda = 250$ μm counts model from Rowan-Robinson (1998)[4]

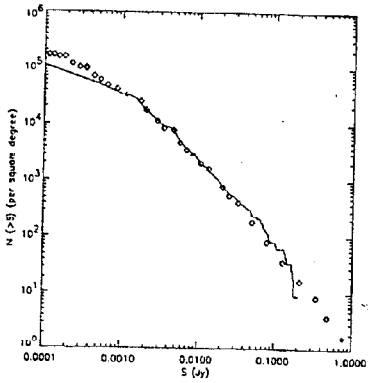

(b) $\lambda = 250$ μm counts model from Franceschini et al. (1997)[2]

Figure 1: Comparaison of the counts obtained with the simulated fluxes with the models.
Line : counts derived from the simulation of a 400 arcmin area.
Diamonds : predictions of the model

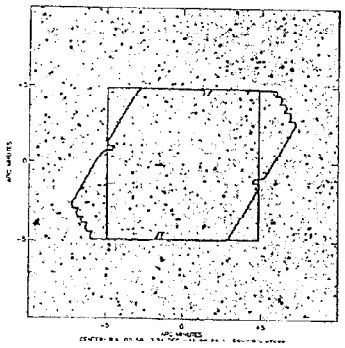

(a) $\lambda = 250$ μm counts model from Franceschini et al. (1997)[2]. Upper cut is 0.2 mJy/arcsec^2.

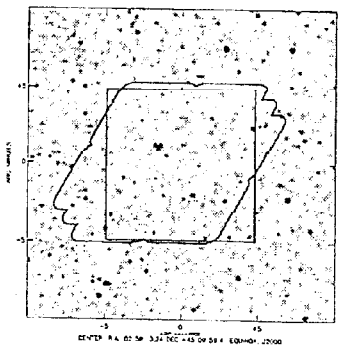

(b) $\lambda = 500$ μm counts model from Franceschini et al. (1997)[2]. Upper cut is 0.1 mJy/arcsec^2.

Figure 2: Simulated images of a 20×20 arcmin area of the sky, as observed at the focus of FIRST telescope at 250 μm with a resolution of 0.5 arcsec. The images are displayed with a resolution of 2×2 arcsec. At 500 μm, confusion is already a problem for faint fluxes with the Franceschini et al. (1997) [2] model (b) at the resolution of the display, that is four times broader than the resolution of the computations. The area surveyed with option 1 and 2 (squares) and option 3 are outlined.

Option	λ_{obs}	Pixel size	Number of pixels
1 ($F\lambda$)	250 μm	18"	16 × 16
	500 μm	36"	8 × 8
2 ($F\lambda/2$)	250 μm	9"	32 × 32
	500 μm	18"	16 × 16
3 ($2F\lambda$)	250 μm	36"	61
	500 μm	72"	19

Table 1: Detailed parameter of the detectors.

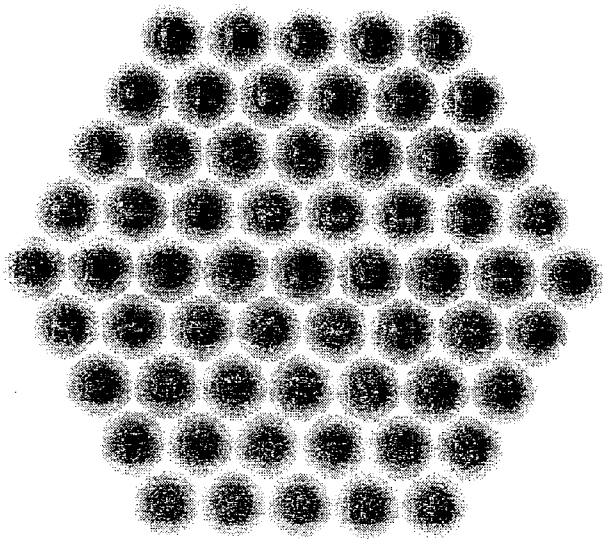

Figure 3: Image of the response of the 61 horns bolometers array

1.3 Simulation of the detectors

We have considered three kind of detectors summarized in table 1 :

1. array of 16×16 square pixels of $F\lambda$ of size, *i. e.* 18 arcsec at 250 μm, and 8×8 pixels of 36 arcsec at 500 μm. The pixels are contigous and their response is constant over the whole pixel.

2. array of 32×32 square pixels of $F\lambda/2$ of size, *i. e.* 9 arcsec at 250 μm, and 16×16 pixels of 18 arcsec at 500 μm. The pixels are contigous and their response is constant over the whole pixel.

3. array of 61 bolometers horns (backup option). The horns hexagonaly placed and separated by $2F\lambda$. Their response is a gaussian of $F\lambda$ FWHM. Figure 3 present a image of the array response.

The calculated image of the survey is projected on the detector, to simulate each pointing of the raster for cases 1 and 2, or of a jiggling map for case 3.

In SPIRE, we have taken two sources of noise into account :

1. detector noise with Noise Equivalent Power (NEP) equal to [1] : $NEP_{det} = 3 \times 10^{-17} W.Hz^{-1/2}$

2. photon noise NEP_{ph}, that is dominated by the telescope itself.

The photon Noise Equivalent Power is computed from the RMS fluctuation $(\Delta n)^2$ of the number n of photon of a black body that arrive on the detector [5]. Thus we have:

$$(\Delta n)^2 = n(n+1) \tag{5}$$

The photon emission is dominated by the telescope, with emissivity ϵ and temperature $T = 80$ K [1]. Last, this energy is received by a bolometer with quantum efficiency η_{bol}, with a telescope of collecting collecting area A_t seeing the pupil under the solid angle Ω, in the frequency range $\Delta\nu$, through an optic with efficiency η_{opt}.The fluctuation of the number N of photon arriving on the detector is therefore :

$$(\Delta N)^2 = \epsilon\eta_{bol}\eta_{opt}N(1+\epsilon\eta_{bol}\eta_{opt}N) = \frac{\epsilon\eta_{bol}\eta_{opt}}{e^{\frac{h\nu}{kT}}-1}\left(\frac{\epsilon\eta_{bol}\eta_{opt}}{e^{\frac{h\nu}{kT}}-1}+1\right) \tag{6}$$

Each photon has an energy $h\nu$ and the density of states it can occupy is :

$$d = 2 \times \frac{2h\nu^3}{c^2} \tag{7}$$

Therefore we have :

$$NEP_{ph}^2(\lambda) = A_t\Omega\int_{\Delta\nu} 2 \times \frac{2h\nu^3}{c^2}(h\nu)\frac{\epsilon\eta_{bol}\eta_{opt}}{e^{\frac{h\nu}{kT}}-1}\left(\frac{\epsilon\eta_{bol}\eta_{opt}}{e^{\frac{h\nu}{kT}}-1}+1\right)d\nu \tag{8}$$

We have for SPIRE [1] :

$$A_t\Omega = \alpha\lambda^2 \qquad T_{tel} = 80K \qquad \epsilon_{tel} = 0.04 \tag{9}$$

$$\eta_{opt} = 0.3 \qquad \eta_{bol} = 0.8 \qquad \Delta\lambda = \frac{\lambda}{3} \tag{10}$$

The value of α depends on the configuration, taking into account Lyot spot and area of the bolometer. Following [6], we take for option 3 $\alpha = 0.8$ so that $A_3\Omega_3 = 0.8\lambda^2$. For square pixels, $\Omega = \pi/4F^2$ [6] is the same (the telescope has the same optical configuration) and the collecting area are $A_1 = (F\lambda)^2$ and $A_2 = (F\lambda)^2/4$, where F is the focal length of the telescope.

The total noise equivalent power of the bolometer NEP_{tot} is then :

$$NEP_{tot} = \sqrt{NEP_{ph}^2 + NEP_{det}^2} \tag{11}$$

If one observes a point source radiating with the flux density $S_{\nu,s}$, assumed to be constant over $\Delta\nu$, the bolometer receives the power :

$$P_b = S_{\nu,s}\, A_t\, \Delta\nu\, \eta_{tel+det}\, \eta_{pix} \tag{12}$$

where η_{pix} is the portion of the PSF intercepted by the bolometer, $\eta_{tel+det}$ is the overall efficiency of the instrument and telescope. We have :

$$\eta_{tel+det} = \eta_{opt}\,\eta_{bol}\,\eta_{chop} \tag{13}$$

		option 1 $\alpha = \pi/4 = 0.785$	option 2 $\alpha = \pi/16 = 0.196$	option 3 $\alpha = 0.8$
Wavelength	Noise	NEP $(10^{-17} W.Hz^{-1/2})$	NEP $(10^{-17} W.Hz^{-1/2})$	NEP $(10^{-17} W.Hz^{-1/2})$
250 μm	photon	9.06	4.53	9.14
	detector	3.00	3.00	3.0
	total	9.54	5.43	9.62
500 μm	photon	5.05	2.53	5.10
	detector	3.00	3.00	3.00
	total	5.88	3.92	5.92
Wavelength	Noise	r.m.s. (mJy)	r.m.s. (mJy)	r.m.s. (mJy)
250 μm	total	0.63	0.36	0.63
500 μm	total	0.77	0.52	0.78

Table 2: Noise equivalent power and noise level (1 σ/pixel) for simulation of 15 min exposures.

where $\eta_{chop} = 0.45$ is the chopping efficiency and $A_t = \pi 3.29^2/4$ [1].

If this sources is observed during the time t, the noise reduces as $\sqrt{t}$ and the signal over noise ratio is therefore :

$$S/N = \frac{S_{\nu,s}\, A_t\, \Delta\nu\, \eta_{tel+det}\, \eta_{pix}}{\frac{NEP_{tot}}{\sqrt{2\eta_{obs}\, t}}} \tag{14}$$

Note that the observing time has been multiplied by a factor η_{obs}, the observation efficiency, to take into account the overheads *i. e.* that not all the time dedicated to the observation is used to take data.

The equation 14 allow to compute the signal over noise for the detection of a point source. In our case, we are interested in computing the noise level in one pixel. Thus, we have to consider for this purpose the observatiom of a constant extended source and use the following equation :

$$S/N = \frac{S_{\nu,s}\, A_t\, \Delta\nu\, \eta_{tel+det}}{\frac{NEP_{tot}}{\sqrt{2\eta_{obs}\, t}}} \tag{15}$$

where η_{pix}, the pixel efficiency, that is the average flux recieved by a pixel when observing a source, is no longer taken into account.

Setting S/N to 1 in equation 15 gives us the flux density r.m.s. of the noise, which, in this case is equal to $S_{\nu,s}$.

Values of α and NEPs are summarized in table 2. Note that we assume that the noise is independant of the simulated sources, because we assume that photon noise due to the sources is neglictible against those of the background and telescope.

Once the projection of one pointing (raster step or jiggling step) has been computed, a gaussian noise with r.m.s. corresponding to the option and wavelength is added to the image.

1.4 Map reconstruction

Once each image (*i.e.* the flux collected by each bolometer for a given pointing) has been computed, they are coadded in a "raster" or "jiggle" map. We follow for this

the prescriptions of the IRAM reduction package NIC [7]. Each pointing is added to the raster map with a weight W :

$$W = \left(\frac{\sin(ud)}{ud}\right)^2 T \quad (16)$$

$$u = \frac{2\pi D}{\lambda} \quad (17)$$

where d is the distance between the poition of the final map and the center of the bolometer and T is the value of the transfert function of the bolometer at this point. A noise map is also produced, using W^2 as weight.

The map of the observation is then interpolated on a regular RA-DEC oriented grid using bilinear interpolation. In option 3, where directions of the "jiggling" are not perpendicular, care has been taken to have a flux conservative reprojection.

2 Results

The model described in the previous section has been used to simulate survey observations with the three kind of detectors. Due to SPIRE design the three (of which two are simulated) are observed at the same time. This means that the same pointings and same integration time are used for the two channels. To fully sample the PSF at the longuest wavelength, one has to scan the sky by steps of $\lambda/2$ in both axis. These leads to a scan in only λ for the shortest wavelength thus leading to an undersampled map. Thus the minimal sampling rate is $\lambda/2$ at 250 μm that gives $\lambda/4$ at 500 μm. Together with this minimal sampling, we have simulated oversampled maps at $\lambda/4$ at 250 μm and $\lambda/8$ at 500 μm.

While the shortest wavelength commands the raster or jiggle step size, the longuest wavelength commands the number of steps : the bolometer size has to be fully covered in order to obtain an homogeneous map. If a $\lambda/2$ step at 250 μm requires 4 × steps to obtain a full coverage of the PSF at 250 μm, this translate to $\lambda/4$ at 500 μm. Thus, a 8 ×8 map is in fact required

2.1 Observations

In order to ensure a proper comparaison of the three detector, we have simulated observations of an area of *fixed surface* within a *fixed total observation time* at a *fixed resolution*. The area for each configuration is 100 $arcmin^2$, except for option 3 (2 Fλ horns) at 500 μm where the 27 horns cover a slightly larger surface giving a total area of 113 $arcmin^2$. To cover at $\lambda/4$ and 250 μm this area, 4 "jiggle" maps of 64 pointings each are required. We set the observing time to 64 minutes, giving an exposure time of 15 seconds per pointings in this configuration. The exposure time per pointing for each other options where computed to fill the same total observing time. For exemple, an array of 16×16 square pixels of 18" can map the same area in the same time and stay 60" at each pointing, with 4 raster maps with half a pixel steps.

The detectors are detailed in table 1 and the observations are detailed in table 3

2.2 Images

Figures 4, 5 and 6 present the images obtained at 250 μm and 500 μm with the low resolution and high resolution mode, on the field simulated with Franceschini et al. number counts [2]. Figures 4, 5 and 6 present the same results for Rowan-Robinson number counts [4]. Note that we had to modify the lower cut of option 3 results

Option	Resolution at 250 μm	Number of pointings	Exposure time	Covered area	Total time
1(Fλ)	$\lambda/2$	4×4×4	1 min	100	1.07
	$\lambda/4$	8×8×4	0.25 min	100	1.07
2 (Fλ/2)	$\lambda/2$	2×2×4	4 min	100	1.07
	$\lambda/4$	4×4×4	1 min	100	1.07
3 (2Fλ)	$\lambda/2$	8×8×4	0.25 min	100	1.07
	$\lambda/4$	16×16×4	0.0625 min	100	1.07

Table 3: Details of the simulated observations. For each option, the step size (resolution) at 250 μm is given, as well as the number of pointing required for a complete coverage at 500 μm. The number of pointings is given in the following way : $N_{step_1} \times N_{step_2} \times N_{raster}$ where N_{raster} is the number of independant raster or jiggle maps needed to cover the area.

to leave some dynamics in the image. Indeed, lower cut is 10 σ while it is 1 σ for options 1 and 2.

It is clear from the output images that confusion dominates all the maps for source extraction. With option 3 (2Fλ horns), only a few pixels are below the 1 σ level, at the edge of the map where redundancy is small, and most of the pixel are *above* the usual 3 σ level used for source détection. Moreover, many sources appear blended together, whatever the detector being used.

Depending on the kind of observations and the detector, the effects of confusion are more or less severe :

- The mapped obtained at a better resolution are less affected.
- The smaller the pixels, the less prominent is confusion at high flux level.

When dealing with exposures as long as the ones simulated, the detector and photon noise originating from the telescope mirror become neglictibles, especially for large pixels.

Two ways can be though to overcome the confusion problem :

- use pixels as small as possible to fight this effect, but big enough to avoid to be dominated by instrument noise.
- observe with scan maps rather than pointed "jiggle" maps, in order to obtain a high resolution on the final map. This is only possible if the relative pointing accuracy and control of the satellite is good.

Two techniques are usually used detect sources against confusion : the deconvolution and the P(D) analysis. Both require a good understanding of the instrumental noise, as well as accurate measures of the beam profile, that are difficult to obtain, especially when the the intrument is very sensitive.

3 Conclusion

We have presented a simplificated model of extragalactic surveys with SPIRE, the Spectral and Photometric Imaging REceiver on board of FIRST, performed at 250 μm and 500 μm, in order to study the impact of confusion noise. We show on preliminary simulations that confusion is the major issue for dealing with extragalactic source extraction. We show that a detector made of small pixel (Fλ/2) is

less sensitive to this problem. Observations obtained with very small steps between pointings or scan technique are also preferred.

Beyond the scope of extragalactic surveys, the problem rises the question of finding a good "empty" place when using chopping techniques. The probability of finding a source bright enough to be above the noise level for in any part of the sky is large, even for short exposures.

This study will be extended to take into detectors closer to reality : non homogenous response of the pixels, pixels with filling factor lower than one, *etc...* Moreover, tests of P(D) and deconvolution will be done to analyse the outputs of the simulations.

References

[1] Griffin M., and the SPIRE consortium, 1998, "SPIRE, a bolometer instrument for FIRST", A proposal to the European Space Agency

[2] Franceschini A., Aussel H., Bressan A. *et al.*, 1997, "Sources counts and background radiation", in *The Far Infrared and Submillimeter Universe*, ESA SP-401

[3] Guiderdoni B., Hivon E., Bouchet F., Maffei B., 1998, MNRAS, 295,877

[4] Rowan-Robinson M., 1998, MNRAS *in press*

[5] Rohlfs K., Wilson L. T., 1996, "Tools of Radio Astronomy", second edition, Springer

[6] Griffin M., Bock J., Gear W., "Comparison of sensitivities of 0.5Fλ, 1.0Fλ and 2.0Fλ arrays for the BOL", Note no. BOL/QMW/N/0026.10

[7] D.Broguière, R.Neri, A.Sievers, NIC Bolometer Users Guide, Version 1.4-01, *http://iraux2.iram.fr/GS/nic/nic.html*

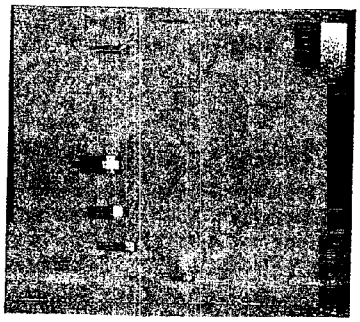

(a) $\lambda = 250\ \mu$m, resolution of $\lambda/2$. Display is Log(f mJy/pixel). Lower cut is 1σ, upper cut is 20 σ.

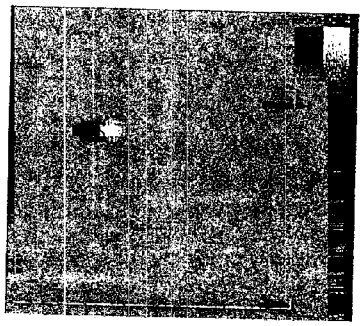

(b) $\lambda = 500\ \mu$m, resolution of $\lambda/4$. Display is Log(f mJy/pixel). Lower cut is 1σ, upper cut is 40 σ.

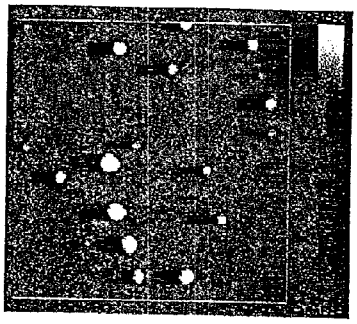

(c) $\lambda = 250\ \mu$m, resolution of $\lambda/4$. Display is Log(f mJy/pixel). Lower cut is 1σ, upper cut is 20 σ.

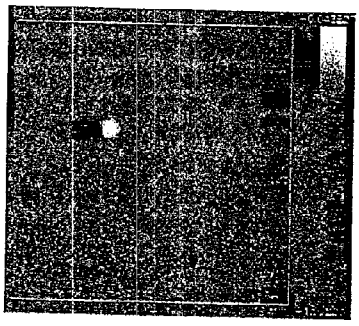

(d) $\lambda = 500\ \mu$m, resolution of $\lambda/8$. Display is Log(f mJy/pixel). Lower cut is 1σ, upper cut is 40 σ.

Figure 4: Observation with option 1 (Fλ square pixels), with a final resolution of $\lambda/2$ at 250 μm (panels a and b), and with a final resolution of $\lambda/4$ at 250 μm (panels c and d)

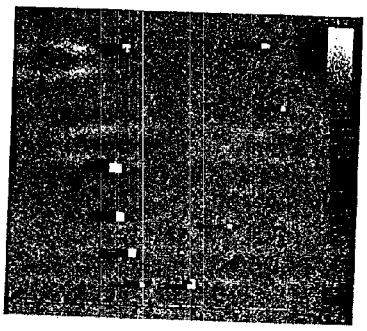

(a) $\lambda = 250\ \mu$m, resolution of $\lambda/2$. Display is Log(f mJy/pixel). Lower cut is 1σ, upper cut is 40 σ.

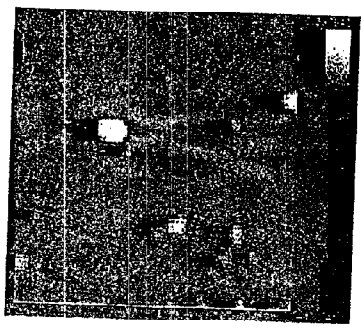

(b) $\lambda = 500\ \mu$m, resolution of $\lambda/4$. Display is Log(f mJy/pixel). Lower cut is 1σ, upper cut is 80 σ.

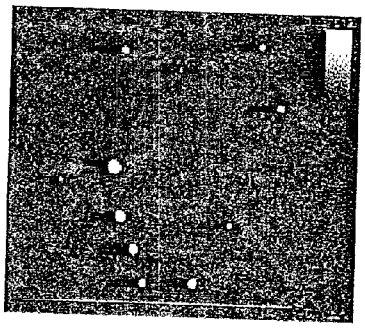

(c) $\lambda = 250\ \mu$m, resolution of $\lambda/4$. Display is Log(f mJy/pixel). Lower cut is 1σ, upper cut is 40 σ.

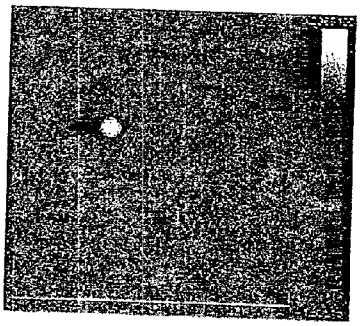

(d) $\lambda = 500\ \mu$m, resolution of $\lambda/8$. Display is Log(f mJy/pixel). Lower cut is 1σ, upper cut is 80 σ.

Figure 5: Observation with option 2 (F$\lambda/2$ square pixels), with a final resolution of $\lambda/2$ at 250 μm (panels a and b), and with a final resolution of $\lambda/4$ at 250 μm (panels c and d)

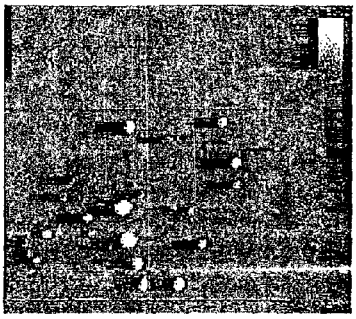

(a) $\lambda = 250$ μm, resolution of $\lambda/2$. Display is Log(f mJy/pixel). Lower cut is 10σ, upper cut is 400 σ.

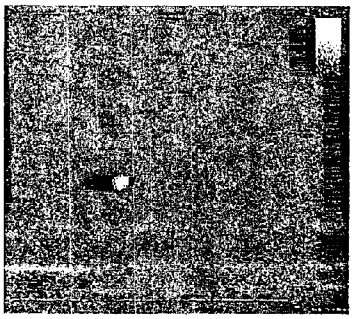

(b) $\lambda = 500$ μm, resolution of $\lambda/4$. Display is Log(f mJy/pixel). Lower cut is 10σ, upper cut is 800 σ.

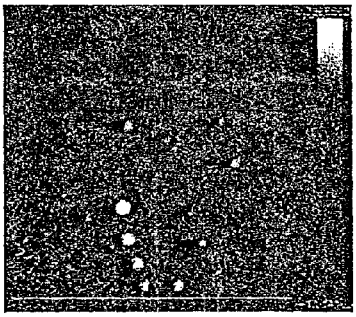

(c) $\lambda = 250$ μm, resolution of $\lambda/4$. Display is Log(f mJy/pixel). Lower cut is 10σ, upper cut is 400 σ.

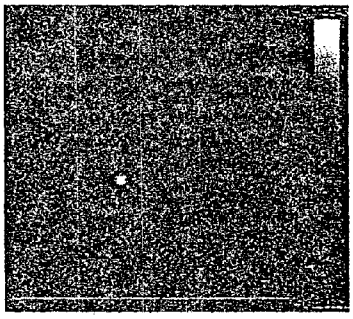

(d) $\lambda = 500$ μm, resolution of $\lambda/8$. Display is Log(f mJy/pixel). Lower cut is 10σ, upper cut is 800 σ.

Figure 6: Observation with option 3 (2Fλ horns), with a final resolution of $\lambda/2$ at 250 μm (panels a and b), and with a final resolution of $\lambda/4$ at 250 μm (panels c and d)